

Biologics *In Vitro* Characterization Advancements to Streamline Development and Approval Timelines

by

Jill L. Kinzer

A dissertation submitted in partial fulfillment
of the requirements for the degree of
Doctor of Philosophy
(Pharmaceutical Sciences)
in The University of Michigan
2023

Doctoral Committee:

Professor Anna Schwendeman, Chair
Dr. Michael Ford, MS Bioworks
Professor James Moon
Professor Brandon Ruotolo
Professor Steven Schwendeman

Jill L. Kinzer

jcoghlan@med.umich.edu

ORCID iD: 0000-0003-3169-1046

© Jill L. Kinzer 2023

All Rights Reserved

To my children, while I may not know you yet, I love you already to the moon and back. Let this PhD inspire you to work hard, dream big and believe in yourself no matter what challenges may arise. Your Dad and I are so grateful to everyone who supported us through this degree and we can't wait to return the favor to you. Always remember, you are amazing kiddos!

ACKNOWLEDGEMENTS

I would like to acknowledge various collaborators that helped make this thesis possible. Within the Schwendeman labs, I would like to acknowledge our lab managers, Karl Olsen, Brian Shay and Rose Ackermann for their dedication towards teaching me not only how to run analytical instruments, but also how to be a confident and considerate researcher. I would like to also thank previous students in the Schwendeman lab, namely Jay Kang and Sang Kim, for guiding me through the early years of my PhD work. Similarly, I would like to acknowledge lab-mates who have worked with me on various projects including Troy Halseth, Alex Benet, Visha Krisnan, Alyssa Marconi, Preethi Kumaran, Daria Salamevich, Youngseo Na, Nick Econom, Mark Vander Roest and Jen Nguyen. The biggest acknowledgement goes to Anna Schwendeman for mentoring me these last years in research, leadership, career development and personal life.

Outside of the Schwendeman lab, I would like to acknowledge our industrial collaborators for their time, efforts and resources. I would like to thank everyone at MS Bioworks, especially Michael Ford and Ravi Amunugama, for teaching me invaluable mass spectrometry skills. I would like to thank folks at Protein Metrics, including St. John Skilton, Lawrie Veale and Mark Bennett, for allowing us access to their software packages and sharing best practices in mass spectrometry processing. I would like to thank Promega for their support in providing us resources for bioassays. In particular, I would like to thank Sergei Saveliev at Promega for his help in optimizing protein digestion.

Additionally, I would like to acknowledge the various funding sources that made this research possible. Throughout my PhD I was funded by the Cellular Biotechnology Train-

ing Program at the University of Michigan, National Institutes of Health T32-GM1415304, a NIIMBL and NIPTE award, UDR0000066 PC5.1-005, and Food and Drug Administration grants, U18-FD007054 (Center for Research on Complex Generics) and U01-FD007763 (Biosimilar User Fee Amendments).

Now onto the non-science acknowledgements, for the folks who shaped me and truly made the last five years some of the best of my life.

To my husband, Bryan – for making me laugh, smile, dance, follow my faith, ponder strange concepts, and for acting as a space heater when you steal the sheets. To my parents, Kathy and Kevin – for encouraging me to dream big, supporting me through life’s adventures, and making the best lobster rolls since day one. To my siblings, Katelyn – for paving the way and letting the hamsters sleep in our room, Kevin – for just “getting it” in this stage of life as PhD athletes, and Lissie – for reminding me to let me loose and sing Katy Perry to my heart’s content. To my in-laws, Tom and Stacey – for accepting me as your daughter and showing me love (even when I catch the biggest fish), Michael – for being excited to spill the tea without your brothers, Daniel and Anna – for always entertaining us with calls during road trips or pranks on vacation, Mike – for showing me the beauty of listening to Stairway to Heaven while driving through Zion. To my bonus parents, Sue and Mark – for visiting all of the parks with us, even if it means getting muddy.

To the rest of my “Michigan family” who experienced a lot of life with me and Bryan. In particular, to the girls – Mery, Kristen, Meg and Corrine – for spending countless hours watching The Bachelor while simultaneously planning weddings, birthday parties, vacations, etc. and reassuring me that we will truly be friends for life. To Khoi – for making LaTeX look easy. To the rest of the Hill House/Harbor House/Din Den crew – there are too many to count – for bringing game days to life and proving that grad students can have fun. To friends from St. Mary’s – especially Ruby, Cecilia, Katie, Mike, Andrew (both M and Z), Ellie, Brian, Ted, Megan, Karina and Fr. Joe – for sharing their faith with me and

teaching me how to grow closer to God through my thoughts and actions. To NCRB pool crew/Team Zoot/Force Multisport – Arielle, George, Rob, Eric and Kelsey – for sweating with me day in and day out while coaching me through triathlons, marathons and open water swims. To AAPS and CBTP – for helping me gain confidence as a leader and willingly participating in professional development events I have curated.

While I would love to write every single person a heartfelt note describing how they have impacted my life and shaped who I am today and will be in the future, I only have limited space in this document and heard that Word crashes after 100 pages. Therefore, for those not explicitly listed, you are still loved by me and I genuinely cherish our relationship.

TABLE OF CONTENTS

DEDICATION	ii
ACKNOWLEDGEMENTS	iii
LIST OF FIGURES	ix
LIST OF TABLES	xii
LIST OF ABBREVIATIONS	xiii
ABSTRACT	xv
CHAPTER	
I. Introduction	1
II. Anti-TNFα mAb Structure and Function Characterization	25
2.1 Introduction	25
2.2 Materials and Methods	31
2.2.1 Reagents and Kits	31
2.2.2 mAb Sample Information	31
2.2.3 Glycosylation Analysis	31
2.2.4 TNF α Binding ELISA	33
2.2.5 AlphaLISA for Fc γ RIIIa (V158 Variant) Binding Affinity	34
2.2.6 ADCC for Effector Function	34
2.2.7 Statistical Analysis	35
2.3 Results	35
2.3.1 Glycan Profiling	35
2.3.2 TNF α Binding Affinity	37
2.3.3 Fc γ RIIIa binding	38
2.3.4 Antibody-Dependent Cellular Cytotoxicity (ADCC)	39
2.4 Discussion	40
2.5 Conclusion	43

III. Disulfide Shuffling Analysis in mAb Innovators and Biosimilars . . .	45
3.1 Introduction	45
3.2 Materials and Methods	50
3.2.1 mAb Sample Information	50
3.2.2 Digestion Reagents	50
3.2.3 Incubation of Proteins	50
3.2.4 Protein Digestion and Data Analysis	51
3.2.5 Protein Degradation Analysis	53
3.3 Results	54
3.3.1 Disulfide Bond Quantification and Qualification by LC-MS/MS	54
3.3.2 Detection of Trisulfide Formation by LC-MS/MS	57
3.3.3 Protein Degradation Measurement by SEC	58
3.3.4 Protein Degradation Characterization by SDS-PAGE	61
3.4 Discussion	63
IV. Comparison of Glycan Profiling Methods for mAbs	67
4.1 Introduction	67
4.2 Materials and Methods	74
4.2.1 mAb Sample Information	74
4.2.2 Released Glycan Commercial Kits	74
4.2.3 Intact MS	76
4.2.4 Peptide Mapping	77
4.3 Results	78
4.3.1 Released Glycan Kits with NIST mAb	78
4.3.2 Peptide Mapping LC-MS/MS of NIST mAb	81
4.3.3 Intact MS of NIST mAb	84
4.3.4 NIST mAb Glycan Profile Summary	84
4.3.5 Glycan Characterization of Trastuzumabs	84
4.4 Discussion	88
V. Research Summary and Future Directions	96
5.1 Introduction of Concluding Thoughts	96
5.2 Chapter Summaries	97
5.2.1 Chapter II: Anti-TNF α mAb Structure and Function Characterization	97
5.2.2 Chapter III: Disulfide Shuffling Analysis in mAb Innovators and Biosimilars	97
5.2.3 Chapter IV: Comparison of Glycan Profiling Methods for mAbs	98
5.3 Broader Future Directions	99

BIBLIOGRAPHY 107

LIST OF FIGURES

Figure

1.1	Schematic representation of the factors affecting the efficacy of therapeutic mAbs in IBD patients. High levels of afucosylated glycans at Asn-297 leads to higher FcγRIIIa binding affinity, resulting in higher ADCC and efficacy in IBD patients. Patients with the FcγRIIIa 158 V/V polymorphism (15% of the population) have increased binding affinity and ADCC in comparison to those with FcγRIIIa 158 F/V and F/F polymorphisms. Image adapted from Kang et al., 2018. [1]	3
1.2	Remicade [®] and Remsima [®] glycan profile and Fc binding comparison.(A) Relative contribution of afucosylated glycoforms; (B) Average KD values for binding of Remicade [®] and Remsima [®] to FcγRIIIa as measured by biolayer interferometry (n = 4 lots; mean ± SEM; asterisks denote a p < 0.05 level of significance). Image adapted from Pisupati et al, 2017. [2]	4
1.3	Schematic of the ThermoFisher Fusion Lumos Tribid Orbitrap.	6
1.4	Schematic of IgG1 glycan position with examples of sugar moieties commonly found on human glycans.	14
1.5	Concentration vs. time post-injection of 300 mg of Mab1 administered in a single patient. Shown are the M5 glycoform and all non-M5 glycoforms. Half lives for the glycoforms were approximated by fitting the experimental data points to a first-order rate equation (dashed lines). Plot adapted from Goetze et al., 2011. [3]	17
1.6	Specific lysis from an <i>in vitro</i> ADCC assay. A) Comparison of natural variants of AB1 using Ag1-expressing target cells; Ab1-29 has higher levels of Fc sialylation and required 7-fold higher concentrations to trigger same levels of cell lysis compared to Ab20; B) Comparison of natural variants of AB2 Ag2-expressing target cells; Ab2-26 required 6-fold higher concentrations to achieve same effect as Ab2-0 variant with no detectable sialic acid. Plots adapted from Scallon et al., 2007. [4]	18
1.7	Schematic representation of various analysis methods commonly used to characterize N-glycans on mAbs. Image adapted from Carillo et al., 2020. [5]	20
1.8	Schematic of IgG1 mAb highlighting the 12 intrachain disulfide bonds (red) and 4 interchain disulfide bonds (orange).	21

1.9	Examples of shuffled disulfide bond patterns, either intermolecularly or intramolecularly, that can occur in antibodies. Image adapted from Zhang et al., 2011. [6]	22
1.10	Schematic depicting the insertion of a third sulfur group into an existing disulfide bond to form a trisulfide bond. Image adapted from Shion et al., 2019. [7]	22
2.1	Glycan data collected for each mAb using two methods is presented for some of the most abundant glycans. (A) depicts the top 10 glycans identified for the mAbs by LC-MS/MS and (B) separates the LC-MS/MS detected glycans into their percent contribution based on glycan type. (C) Characteristic LC-FLR chromatograms for each mAb and (D) separates the LC-FLR detected glycans into their percent contribution based on glycan type. Error bars are SEM. ns: not significant, *p < 0.05, **p < 0.01, ***p < 0.001, ****p < 0.0001.	36
2.2	TNF α ELISA data for all three mAbs are shown as (A) an absorbance vs. mAb concentration curve and (B) EC50 values derived from the ELISA curve in (A). Error bars are SEM. ****p < 0.0001.	38
2.3	AlphaLISA V variant data for all three mAbs are shown as (A) a normalized luminescence signal vs. mAb concentration curve and; (B) IC50 values derived from the AlphaLISA curve in (A). Error bars are SEM. ***p < 0.001, ****p < 0.0001.	39
2.4	AlphaLISA V variant data for all three mAbs are shown as (A) a normalized luminescence signal vs. mAb concentration curve and; (B) IC50 values derived from the AlphaLISA curve in (A). Error bars are SEM. ***p < 0.001, ****p < 0.0001.	40
3.1	Schematic of expected disulfide bond locations for rituximab and bevacizumab. Fc region is shown in black and Fv region is shown in red. 12 intrachain (red) and 4 inter-chain (orange) bonds are typical for IgG1. . .	47
3.2	(A) Schematic of the Byos disulfide bond workflow. (B) Highlighted bevacizumab shuffled disulfide bond used for representation of LC-MS/MS data plots. Generated data depicted as a (C) MS1 plot; (D) MSMS plot; (E) Mass error plot; and (F) XIC intensity plot.	54
3.3	(A) Schematic of the Byos disulfide bond workflow. (B) Highlighted bevacizumab shuffled disulfide bond used for representation of LC-MS/MS data plots. Generated data depicted as a (C) MS1 plot; (D) MSMS plot; (E) Mass error plot; and (F) XIC intensity plot.	56
3.4	Trisulfide bonds detected for bevacizumab samples by LC-MS/MS. (A) Total trisulfide bond contribution relative to the XIC sum of all identified disulfide bonds for bevacizumab OR (0 week—peach, 2 weeks—orange, 4 weeks—red orange) and BS (0 week—teal, 2 weeks—green, 4 weeks—dark green). (B) Prevalence of the shuffled bond locations normalized to the total number of shuffled bonds for bevacizumab OR (0 week—peach, 2 weeks—orange, 4 weeks—red orange) and BS (0 week—teal, 2 weeks—green, 4 weeks—dark green) (N = 3, mean \pm SD, 2-way ANOVA, *p < 0.05, **p < 0.01, ***p < 0.001, ****p < 0.0001).	58

3.5	Representative SEC chromatograms at 214 nm for 15 µg of antibody. (A) Rituximab OR at 0 (pink), 2 (red) and 4 (purple) weeks; (B) Rituximab BS at 0 (light blue), 2 (blue) and 4 (navy) weeks; (C) Bevacizumab OR at 0 (peach), 2 (orange), and 4 (brown) weeks; (D) Bevacizumab BS at 0 (teal), 2 (green) and 4 (dark green) weeks. Stressed samples were shaking at 240 RPM, incubating at 37°C for 2 or 4 weeks. Chromatograms are zoomed in to depict the increase in aggregates and/or fragments detected in each sample across each timepoint.	59
3.6	SDS-PAGE of representative 0.25 mg/ml samples for bevacizumab OR and BS and rituximab OR and BS depicting the fragmentation and aggregation of the samples at each timepoint. Samples were incubated 0, 2 or 4 weeks at 37°C, shaking at 240 RPM.	62
4.1	Example NIST mAb fluorescence chromatogram with glycans labeled with the 2AB express kit. Glycans were identified using a UNIFI algorithm based on a Dextran calibration ladder. Highlighted at a retention time of 16 minutes is the F(6)A2 glycan, or G0F, which is expected to have the highest signal for NIST mAb.	79
4.2	Example NIST mAb fluorescence chromatogram with glycans labeled with the 2AB express kit. Glycans were identified using a UNIFI algorithm based on a Dextran calibration ladder. Highlighted at a retention time of 16 minutes is the F(6)A2 glycan, or G0F, which is expected to have the highest signal for NIST mAb.	82
4.3	Relative % contribution of each glycan type for NIST mAb as identified by LC-MS/MS after protein digestion. Glycans were identified using the Protein Metrics PTM workflow. N=3; Error bars are standard deviation.	83
4.4	Relative percent contribution of glycans as detected by intact MS. (A) Deconvoluted spectra from Protein Metrics Intact workflow; (B) Visual representation of the Relative % contribution of the detected glycans detailed in table (C). N = 3; shown is mean ± standard deviation. Note: glycans shown as pairs in the spectra were subsequently normalized to depict individual glycan contribution.	85
4.5	Relative % contribution of each glycan type for NIST mAb as identified by LC-MS/MS after protein digestion. Glycans were identified using the Protein Metrics PTM workflow. N=3; Error bars are standard deviation.	87
5.1	Proposed workflow for designing a broadly applicable PTM toolkit.	100
5.2	Schematic of relevant stakeholders involved in biologics research, development, approval and administration.	105

LIST OF TABLES

Table

1.1	Examples of bioactivity assays conducted by the sponsoring company comparing Humira® vs biosimilars. Note: Imraldi™ data shown here is the average of a data range given for each assay in the product quality review summary table. ^a Approximated values from a graph.	8
1.2	Comparison of Clinical Trials Results in Rheumatoid Arthritis Patients Based on Full-Analysis Set (FAS) Results, Except for Imraldi™ Where Per Protocol Set (PPS) Data was Reported for the Primary Outcomes. ^a Note: Amsparity data for ACR20 response rate was taken from the 12-week main phase. ADA positive data was taken from week 26 samples to give a closer comparison to other biosimilars with ADA measured at week 24.	10
1.3	Percentage of charge variants/glycans for each biosimilar relative to Humira® given as a range (average). Each biosimilar is compared to a reference Humira® (left of biosimilar column) that was tested simultaneously during analysis.	14
2.1	General product administration and dosing information for the three anti-TNF α mAbs.	28
2.2	Binding stoichiometry, pharmacokinetic properties and immunogenicity characteristics.	29
3.1	SEC data depicted as average % concentration contributions of monomer, aggregate, fragment peaks (N = 3, mean \pm SD). Aggregates and fragments include summations of multiple peaks, where applicable. Stressed samples were shaking at 240 RPM, incubating at 37°C for 2 or 4 weeks. All samples were diluted to 1.5 mg/ml to load 15 μ g of antibody on the column. N = 3, mean \pm SD, 2-way ANOVA, *p < 0.05, **p < 0.01, ***p < 0.001, ****p < 0.0001. *Denotes statistical significance of BS, compared to OR, at same timepoint for the same protein type.	60
4.1	List of glycan sugar types and their influence on therapeutic mAb efficacy and safety.	70
4.2	Comparison of the total number of glycans, broken down by glycan type, detected on NIST mAb via the five methods. N = 3; shown is mean \pm standard deviation.	80
4.3	Comparison of the total number of glycans, broken down by glycan type, detected on trastuzumabs via the five methods. N = 3; shown is the average value.	86

LIST OF ABBREVIATIONS

2AB	2-aminobenzamide
ACN	acetonitrile
ADA	anti-drug antibodies
ADC	antibody drug conjugates
ADCC	antibody-dependent cellular cytotoxicity
ADCP	antibody-dependent cellular phagocytosis
AlphaLISA	amplified luminescent proximity homogenous assay
AI	artificial intelligence
ANOVA	analysis of variance
BLA	biologics license application
BS	biosimilar
BsUFA	biosimilars user fee act
CD	Crohn's disease
CDC	complement-dependent cytotoxicity
CH	constant heavy chain
CHO	Chinese hamster ovary cells
CL	constant light chain
CQA	critical quality attribute
EC50	half maximal effective concentration
ELISA	enzyme-linked immunosorbent assay
EMA	European Medicines Agency
Fab	antigen binding fragment
Fc	cystallizable fragment
FcγR	crystallizable fragment receptor
FDA	United States Food and Drug Administration
FLR	fluorescence
FRET	fluorescence resonance energy transfer
FWHM	full width at half maximum
GlcNAc	N-acetylglucosamine
H/DX-MS	hydrogen deuterium exchange mass spectrometry
HCD	higher energy collisional dissociation
HER2	human epidermal growth factor receptor 2
HLA	human leukocyte antigen
HPLC	high performance liquid chromatography
IBD	irritable bowel disease
IC50	half maximal inhibitory concentration

ICH	International Council for Harmonization of Pharmaceuticals
IgG	immunoglobulin
InstantPC	Instant procainamide
IV	intravenous
LC-FLR	liquid chromatography-fluorescence
LC-MS	liquid chromatography-mass spectrometry
Lys-C	lysine-C
mAb	monoclonal antibody
MS	mass spectrometry
MWCO	molecular weight cut off
NEM	N-ethylmaleimide
NIIMBL	National Institute for Innovation in Manufacturing Biopharmaceuticals
NIST	National Institute of Standards and Technologies
OR	originator
PK	pharmacokinetics
PTM	post-translational modification
QTOF	quadrupole time of flight mass spectrometer
RF	RapiFluor-MS
SC	subcutaneous
SDS-PAGE	sodium dodecyl-sulfate polyacrylamide gel electrophoresis
SEC	size exclusion chromatography
SPR	surface plasmon resonance
SS	disulfide bond
TCEP	tris(2-carboxyethyl)phosphine
TFA	trifluoroacetic acid
TNF	tumor necrosis factor
UC	ulcerative colitis
UPLC	ultra performance liquid chromatography
VEGF	vascular endothelial growth factor
VH	variable heavy chain
VL	variable light chain
XIC	extracted ion chromatogram

ABSTRACT

Monoclonal antibodies (mAbs) account for over 120 FDA approved products and are frequently used to treat patients with chronic autoimmune diseases or cancer. Despite being approved for similar indications, not all mAbs share the same structure-function motifs. Given complexities in sizes, structures and manufacturing processes, there are known differences between mAbs of similar classes. One notable difference between mAbs is their post-translational modification (PTM) profile. PTMs are comprised of features native to amino acids such as oxidation, deamidation, methylation, etc. Two PTMs in particular – glycans and shuffled disulfide bonds – are of great interest to the pharmaceutical field given their impact on drug safety and efficacy. Characterizing these two PTMs on mAbs *in vitro* in order to predict safety/efficacy implications is what drove my research.

Chapter II encompasses my work studying anti-TNF α mAbs: Humira[®], Remicade[®] and Simponi Aria[®]. For this project we determined glycosylation profiles using LC-MS/MS and LC-FLR. Then we performed *in vitro* functional assays, TNF α binding ELISA, Fc γ RIIIa AlphaLISA and ADCC, to correlate structure and function. Humira[®] had the fewest unique glycans, 12.1 \pm 0.7% of which were afucosylated and mannosylated, and, perhaps consequently, had the highest Fc binding affinity. Humira[®] had a 7.2-fold higher binding affinity to Fc γ RIIIa than Remicade[®] and 3.3-fold higher than Simponi Aria[®]. Since Humira[®] had significantly higher Fc and Fab binding affinities, it was 15.1% or 19.7% more potent in the ADCC assay when compared with Remicade[®] and Simponi Aria[®], respectively. Our results confirmed significant differences between the three mAbs, yet recognized that *in vivo* efficacy may differ due to confounding variables.

Chapter III follows my research on shuffled disulfide bonds found in rituximab and bevacizumab innovator/biosimilar pairs. We studied the formation of shuffled disulfide bonds and subsequent degradation via non-reduced digestion followed by LC-MS/MS, SEC and SDS-PAGE. After a 4-week incubation, innovator bevacizumab had an upward trend in shuffled disulfide bonds ($0.58 \pm 0.08\%$ to $1.46 \pm 1.10\%$) whereas innovator rituximab maintained its shuffled disulfide bond level ($0.24 \pm 0.21\%$ to $0.51 \pm 0.11\%$). Bevacizumabs started with an average of 70% more shuffled bonds than rituximabs, leading to a higher propensity for aggregation. The bevacizumabs had approximately 6% monomer loss primarily due to aggregation compared to a 1.5% monomer loss due to fragmentation for rituximabs. Our results showcased the importance of monitoring lower abundance PTMs and degradants.

Chapter IV covers my research comparing glycosylation analysis methods using NIST mAb as a standard. We performed five glycan analysis techniques – three FLR released glycans kits, protein digestion followed by LC-MS/MS and intact MS. The LC-MS/MS method identified 25.2% more glycans than the FLR kits and 5.5 times more glycans than intact-MS. When applying these methods to Herceptin[®] and its biosimilars, Kanjinti[®] and Ogivri[®], we observed that Kanjinti[®] had a relative % mannosylated contribution of $1.01 \pm 0.38\%$ while Ogivri[®] was $5.95 \pm 0.97\%$. This translates to a 142.0% difference between mannosylated glycans identified in Kanjinti[®] compared to Ogivri. When comparing mannosylated glycan contributions between biosimilars and innovator, there was only a 100.5% difference between Kanjinti[®] and Herceptin[®] and a 64.4% difference between Ogivri[®] and Herceptin[®]. This work emphasizes the need for method standardization to consistently identify glycan species.

Chapter V summarizes each project and shares potential future directions for this research. Overall, this dissertation highlights techniques for glycan and disulfide shuffling analysis, emphasizes the need to standardized methods and reporting, and discusses potential collaborations to streamline PTM impact analyses.

CHAPTER I

Introduction

Biologics have taken the pharmaceutical field by storm in recent years. Excluding COVID-19 vaccines and treatments, more than half of the ten top-selling drug products in 2022 were biologics. Most of the 2022 top-selling biologics, such as Humira[®] (\$21.2B in sales) or Keytruda[®] (\$20.9B in sales), are monoclonal antibodies (mAbs), but Eylea[®], a recombinant fusion protein with \$12.7B in sales, continued to gain traction. [8] As if the lucrative sales were not enough evidence of biologics' popularity, over 120 mAb products, a number that continues to appreciably rise every year, have been FDA approved. [9] We anticipate that this number will drastically increase as more mAbs lose patent exclusivity and biosimilars, biological products that are highly similar to and have no clinically meaningful differences from an existing FDA-approved reference product, enter into the market. [10] Therefore, now is the time to jump into biologics research and contribute to the ever-growing knowledgebase.

To seize this opportunity, multiple groups began elucidating the structural differences between innovators and biosimilars and relating them back to known functional differences. [1, 2, 11–18] Frequently, labs assess structural features such as primary, secondary and higher order structures, size heterogeneity, charge heterogeneity and post-translational modifications (PTMs) including glycosylation, oxidation, deamidation, methylation, and disulfide bond shuffling. [12, 19] By doing so, each group is identifying poten-

tially significant structural differences that could impact the mAb's efficacy and/or immunogenicity.

Certain PTMs, like glycans, have been linked to either enhanced or subdued Fc binding affinity. This, in turn, can influence how well the mAb binds to the Fc receptors involved in effector function signaling cascades. Since ADCC is dependent on Fab target antigen binding and Fc natural killer cell binding, its potency can be influenced by the glycan structure located in the Fc region of an antibody. As ADCC is a proposed mechanism of action for anti-TNF α therapeutics, especially in irritable bowel disease (IBD), it is critical to understand how the level of specific glycans, such as afucosylated glycans, impacts drug potency. Figure 1.1 illustrates such phenomenon and depicts how if there are more afucosylated glycans present on an antibody, there is likely to be higher efficacy in IBD patients. [1] Remicade[®] is known to have higher relative ADCC activity (99.8%) compared to its biosimilar Remsima[®]/Inflectra[®] (50.3%). [1] Therefore, it is unsurprising that significantly higher levels of afucosylated glycans, which confer better Fc binding affinity and, thus, ADCC, were observed for Remicade[®] than for Remsima[®]. (Figure 1.2) [2]

PTMs are just one of many factors that can influence a mAb's normal target binding and its circulation *in vivo*. Another factor that influence's a mAb safety, efficacy and/or pharmacokinetics are aggregates. Aggregates can reduce a drug's functionality by preventing normal target binding while also inducing immunogenicity and increase clearance rates. [20] Increased clearance rates result in reduced therapeutic efficacy as the drug is eliminated from the body faster. Immunogenicity in the form of anti-drug antibodies (ADA) leads to adverse events and patient safety concerns.

To contextualize the influence of structural features on a therapeutic's efficacy, labs perform functional activity assays (Fab binding, Fc binding, antibody-dependent cellular cytotoxicity, complement dependent cytotoxicity). Performing functional assays in tandem with structural analysis not only paints the whole picture of the mAb *in vitro*, but also proposes anticipated *in vivo* outcomes. Therefore, to gain a broad understanding of

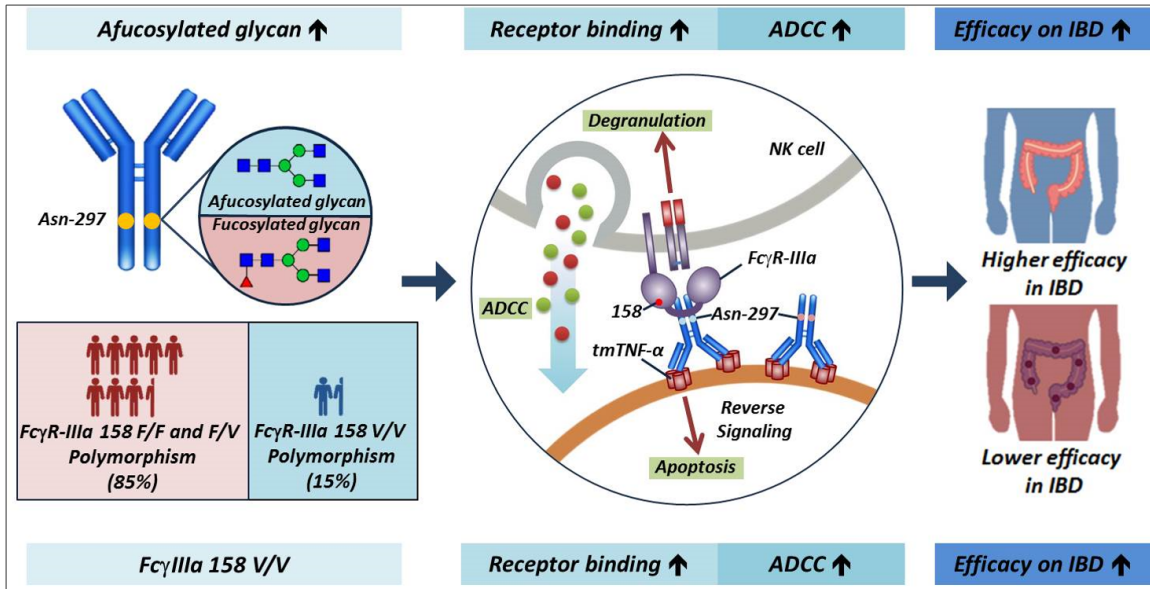


Figure 1.1: Schematic representation of the factors affecting the efficacy of therapeutic mAbs in IBD patients. High levels of afucosylated glycans at Asn-297 leads to higher FcγRIIIa binding affinity, resulting in higher ADCC and efficacy in IBD patients. Patients with the FcγRIIIa 158 V/V polymorphism (15% of the population) have increased binding affinity and ADCC in comparison to those with FcγRIIIa 158 F/V and F/F polymorphisms. Image adapted from Kang et al., 2018. [1]

various mAb products, we conducted both structural and functional assays in house, with future plans to translate our findings into *in vivo* animal studies. For my thesis, we have expanded upon current innovator/biosimilar research by simultaneously comparing multiple competitive innovators or innovator/biosimilar pairs and lots in our sample sets. In these sample sets, we monitored post-translational modifications (PTMs) and degradants using semi-automated sample preparation and mass spectrometry methods, along the way highlighting best-practice methods in hopes of improving current standards and acceptance criteria.

In particular, we have analyzed three anti-TNF α mAbs, Humira[®] (adalimumab), Remicade[®] (infliximab) and Simponi Aria[®] (golimumab), during our first project. These are all full-length mAbs indicated for autoimmune diseases such as rheumatoid arthritis, psoriasis, ulcerative colitis and Crohn's disease. Humira[®] and Simponi Aria[®] are fully humanized mAbs whereas Remicade[®] is chimeric, containing some mouse portions in the variable

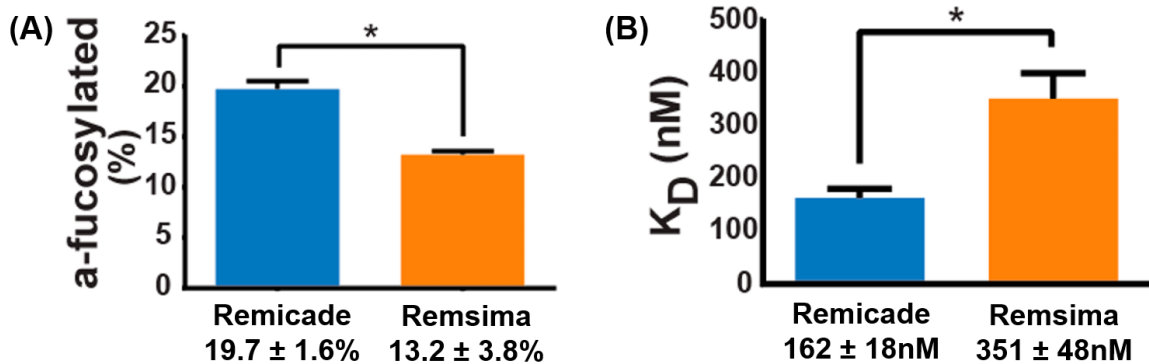


Figure 1.2: Remicade® and Remsima® glycan profile and Fc binding comparison. (A) Relative contribution of afucosylated glycoforms; (B) Average KD values for binding of Remicade® and Remsima® to FcγIIIa as measured by biolayer interferometry (n = 4 lots; mean ± SEM; asterisks denote a p < 0.05 level of significance). Image adapted from Pisupati et al, 2017. [2]

region. In our second project we studied Avastin® (bevacizumab) and Rituxan® (rituximab) and their Russian biosimilars from Biocad. Avastin® is a fully humanized anti-VEGF antibody used to treat cancers including metastatic colorectal cancer, non-squamous non-small cell lung cancer and metastatic breast cancer. Rituxan® is a chimeric anti-CD20 antibody indicated for diseases such as Non-Hodgkin's lymphoma, chronic lymphocytic leukemia and rheumatoid arthritis. For our third project, we used the NIST mAb, which is the closest thing to a standard antibody, to conduct an initial glycan analysis method comparison. Then we applied our methods to Herceptin® (trastuzumab) and its biosimilars Kanjinti® and Ogivri®. All these trastuzumabs are fully humanized, anti-HER2 mAbs indicated for overexpressing HER2 breast cancer. Every antibody described and tested in this thesis is an immunoglobulin, more specifically IgG1.

As alluded to above, in order to broadly characterize these mAbs we have to conduct multiple methods ranging from functional binding assays – ELISA, AlphaLISA, ADCC – to aggregation detection – SEC, SDS-PAGE – to structural characterization – LC-MS/MS, intact MS. The details of each method are described further in the methods section of the applicable chapters. One method commonly used across all chapters is LC-MS/MS. Given its broad applicability in this thesis, we thought it would behoove us to describe this

method in greater detail upfront.

LC-MS/MS, or liquid chromatography tandem mass spectrometry, is a widely used method for analyzing everything from the identification of peptides in a sample to the quantitation of an impurity to the interaction between targets and proteins. [21–24] Its high sensitivity, resolution, reliability and robustness makes LC-MS/MS a desirable analytical tool. For our purposes, we used it mainly for the identification of PTMs on multiple innovator and biosimilar mAbs. Prior to running samples on the LC-MS/MS, we cleaved the proteins with trypsin and Lys-c during a protein digestion process. For chapter II and IV, we performed a reduced digestion procedure while in chapter III we performed a non-reduced digestion in order to maintain the disulfide bonds within the protein for shuffled disulfide bond analysis. Once the samples were digested, samples were purified using C18 solid phase extraction tips. After preparing the samples, we ran 500 ng of each sample using a 30-minute gradient on an LC-MS/MS system (Waters Acquity M Class HPLC interfaced with a ThermoFisher Orbitrap Fusion Lumos Tribrid mass spectrometer) to identify the peptides and PTMs present in the digested mAb solutions (Figure 1.3).

The LC-MS/MS system works as follows: first peptides are separated based on hydrophobicity using a reversed phase C18 column in the LC portion. Then the peptides are ionized using electrospray at the ion source. They are further focused and accelerated to mass analyzers via ion optics, the curved linear trap, and the ion routing multipole. Various applied voltages continue to transmit the ions throughout the instrument. Within the Lumos Tribrid, there are three mass analyzers. The first is the quadrupole, which separates the ions by applying RF and DC voltages across the metal rods to generate an electric field. In doing so, the electric field allows only certain m/z values to pass through the quadrupole, thus filtering out ions not within the target range. The second is a linear ion trap, which contains three transfer lenses and two pressurized cells (one high, one low). Within the linear ion trap, ions can be stored, isolated and/or collisionally dissociated. Again, carefully selected voltages are applied and ions not within the target m/z

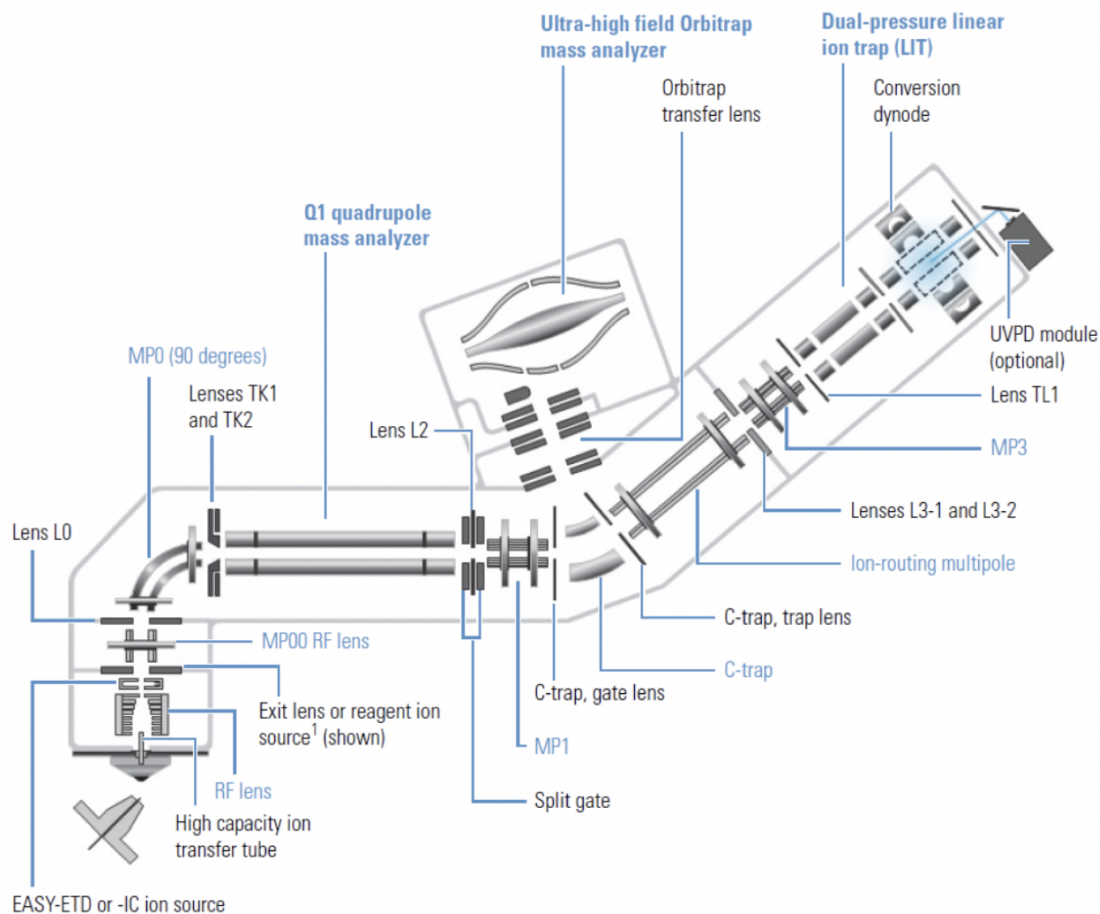


Figure 1.3: Schematic of the ThermoFisher Fusion Lumos Tribrid Orbitrap.

window are removed from the ion trap. The third mass analyzer is the Orbitrap. Orbitraps have a central electrode and two bell-shaped outer electrodes. Moving ions delivered from the C-trap into the Orbitrap fly in spiral patterns due to the presence of variable voltages and their electrostatic field. The oscillations resulting from this phenomenon are then transformed into a mass spectrum readout.

Depending on how sensitive the data needs to be and the structural features one is looking for, the number of collision/fragmentation steps during the MS run can be adjusted. For our research, we did MS² or MS/MS. During this analysis, the ions were selected in the quadrupole then transmitted to the ion routing multipole for higher energy collisional dissociation (HCD). The fragmented product ions resulting from the HCD were

then moved into the Orbitrap for analysis. The data output generated from LC-MS/MS is a raw file mass spectrum that can be analyzed using Protein Metrics' software. For chapters II and IV, we used the PTM workflow in Protein Metrics and for chapter III we used the SS workflow. After using the automated processing, we manually combed the data looking at the MS1, MS2, XIC and sequence coverage maps to ensure that there were no false positives or missing data. As is discussed in more depth in the latter chapters, the LC-MS/MS data, as expected, yielded the most sensitive and highest resolution of all PTM analysis methods. Therefore, for us it acted as our "gold standard" for data acquisition. [25]

By analyzing multiple IgG1 mAbs, for their structural and, in the case of anti-TNF α mAbs, functional properties, we aimed to enhance our expertise in the biologics space. This thesis research has the potential to drive forward progress in the field of post-translational modifications analysis on mAbs, especially with regards to method automation, optimization, standardization and implementation. Additionally, we believe that this work can set the foundation for developing PTM method "toolkits" in collaboration with other academic, industrial and governmental laboratories.

Although the punch line is great, it is important to take a step back and preface what mAbs are and why automation, optimization, standardization and implementation of certain methods has proven challenging. As a subset of biological products, or biologics, mAbs are protein therapeutics manufactured using living organisms with an active ingredient that is biological in nature. They are generally larger and more complex than small molecule products. Between their size, complexity, and living-organism dependent manufacturing processes, mAbs are inherently variable. [10] While a protein's primary sequence can usually be readily reproduced, higher order structures and post-translational modifications can differ due to seemingly minute variations in manufacturing processes such as pH, temperature, buffer composition, change in excipient vendors, etc. [26, 27] They can also be altered if there are changes to other processing/handling stages or storage conditions. [28, 29] These variations in structural features can result in altered ther-

Table 1.1: Examples of bioactivity assays conducted by the sponsoring company comparing Humira® vs biosimilars. Note: Imraldi™ data shown here is the average of a data range given for each assay in the product quality review summary table. ^a Approximated values from a graph.

Humira® vs Amgevita™			
Attribute tested for biosimilarity	Method of analysis	Average (relative activity, %)	
		Humira® (US)	Amgevita™
sTNF-α binding	ELISA	110	108
mTNF-α binding*	Cell-based competition assay: mTNFα expressed on CHO cells, quantified by image cytometer measuring AlexaFluor	105	103
TNF-α neutralization	Apoptosis inhibition: U-937 cells used to measure NFκβ pathway (methods for NFκβ-dependent and independent apoptosis)	107	104
C1q binding	ELISA	n/a	n/a
CDC	Cell-based: TNF expressing CHO cells (target) labeled with calcein, quantified by fluorescence	96	102
ADCC	Cell-based: Fluorescence labeled CHO cells expressing mTNFα (target) with NK92-M1 cells (effector), quantified by fluorescence	85	87
Apoptosis induction	Apoptosis potency assay using genetically modified Jurkat T cells expressing mTNFα, quantified by Caspase-Glo assay and plate reader	n/a	n/a
Humira® vs Imraldi™			
Attribute tested for biosimilarity	Method of analysis	Average (relative activity, %)	
		Humira® (US)	Imraldi™
sTNF-α binding	FRET	101	99
mTNF-α binding	Cell-based flow cytometry	91	93
TNF-α neutralization	Cell-based: HEK293 cells transfected with NFκβ luciferase reporter gene	104	100
C1q binding	ELISA	96	91
CDC	Cell-based CDC assay	99	94
ADCC	Cell-based: NK cell ADCC assay	108	98
Apoptosis induction	Apoptosis potency assay: stimulation of mTNFα induced apoptosis	102	105
Humira® vs Hyrimoz™			
Attribute tested for biosimilarity	Method of analysis	Average (relative activity, %)	
		Humira® (US)	Hyrimoz™
sTNF-α binding	SPR	102	105
mTNF-α binding	Cell-based competition assay: mTNFα expressed on HEK293 T-cells, quantified by flow cytometry	97	100
TNF-α neutralization	Cell-based: HEK293 cells transfected with NFκβ luciferase reporter gene	96	98
C1q binding	ELISA	92	98
CDC	Cell-based: Jurkat T cells expressing mTNFα	103	93
ADCC	Cell-based: Fluorescence labeled HEK293 expressing mTNFα (target) with NK3.3 cells (effector), quantified by fluorescence	103	99
Apoptosis induction	Apoptosis potency assay using genetically modified Jurkat T cells expressing mTNFα, quantified by flow cytometry	94	93

apeutic immunogenicity, efficacy, activity, and pharmacokinetics. [27] Therefore, post-translational modifications and higher order structures are considered to be critical quality attributes (CQAs) defined by the FDA as “physical, chemical, biological or microbiological propert[ies] or characteristic[s] that should be within an appropriate limit, range or distribution to ensure the desired product quality”. [30]

Companies monitor mAb batches for proper protein folding and PTM profiles not only during development, but also during production of marketed product, to confirm that all batches are meeting their specifications prior to administration in patients. [31] After all, it has been shown time and time again that lot-to-lot variability exists and has potentially negative consequences if too great. [32, 33] Plus, in the case of biosimilars, regulators consider PTMs such as glycosylation to be an important CQA when comparing the “similarity” of biosimilars with their innovator counterparts. [29, 34]

While monitoring batches of mAbs throughout their development and post-market manufacturing many experiments have to be conducted by the sponsoring pharmaceutical company. These extensive experiments are detailed in biologics license applications (BLAs) and cover everything from structural and functional analysis *in vitro* to pharmacokinetics and immunogenicity in humans during clinical trials. Shown in table 1.1 are just some of the *in vitro* experiments conducted by sponsoring companies as they were developing Humira[®] (adalimumab) biosimilars. [35] Clinical data such as clearance rate, anti-drug antibody formation and clinical endpoints can be found in the prescribing information documents. Table 1.2 provides a snapshot of the clinical data for adalimumabs that was presented to regulatory agencies for review and is now available in package inserts. [35]

Table 1.1 tells a number of different stories. First, it shows that not only do many experiments have to be conducted, but many features of the mAb are analyzed in order to paint a full picture of the therapeutic. As therapeutic mAbs are immunoglobulins, typically IgG1, they are composed of two heavy chains and a two light chains, each with a

Table 1.2: Comparison of Clinical Trials Results in Rheumatoid Arthritis Patients Based on Full-Analysis Set (FAS) Results, Except for Imraldi™ Where Per Protocol Set (PPS) Data was Reported for the Primary Outcomes. ^aNote: Amsparity data for ACR20 response rate was taken from the 12-week main phase. ADA positive data was taken from week 26 samples to give a closer comparison to other biosimilars with ADA measured at week 24.

Product	Study Name	Study Population	Treatment Duration	ACR20 Response Rate (Week 24)	ADA Positive (Week 24)
Amgevita™	20120262	ABP501: N = 264 Humira®: N = 262	Main phase: 24 w Total: 28 w	ABP 501: 74.6% Humira®:72.4%	ABP 501: 38.3% Humira®: 38.2%
Imraldi™	SB5-G31-RA	SB5: N = 239 Humira®: N = 237	Main phase: 24 w Total: 52 w	SB5: 72.4% Humira®: 72.2%	SB5: 33.1% Humira®: 32.0%
Hulio™	FKB327-002	FKB327: N = 367 Humira®: N = 363	Main phase: 24–26 w Total: 76 w	FKB327: 74.4% Humira®: 75.7%	FKB327: 57.9% Humira®: 55.5%
Cyltezo®	1297.2	BI695501: N = 324 Humira®: N = 321	Main phase: 24 w Total: 48 w	BI695501: 69% Humira®: 64.6%	BI695501: 39.6% Humira®: 45.3%
^a Amsparity™	B538-02	PF-06410293: N = 297 Humira®: N = 299	Main phase: 12 w Total: 78 w	PF-06410293: 68.5% Humira®: 72.7%	PF-06410293: 37.7% Humira®: 43.5%

variable domain (VH or VL, respectively) and a constant domain (CH or CL, respectively). The variable region, made up of VH and VL, gives the antibody its ability to bind specific antigens. The constant region is comprised of three CH domains (1-3) and a CL domain in each arm. Disulfide bridges connect the two heavy chain arms together give antibodies their characteristic Y shape [36,37]. The upper part of the “Y” structure contains the fragment antigen binding, Fab, portion of the antibody, which is usually involved in the primary mechanism of action for the therapeutic. The Fab region binds to the target antigen of interest, inhibiting its functionality and/or preventing cell signaling, thereby reducing symptoms or halting further progression of a patient’s disease. The tail part of the “Y” structure, comprised of CH2 and CH3 domains from each arm, is known as the fragment crystallizable, Fc, region. The Fc region can also play a part in the primary or secondary mechanisms of actions for mAbs. After binding to the target antigen via the Fab region, the Fc region is available to binding to effector cells including macrophages, natural killer cells or C1q. Once bound to effector cells, cell signaling induces effector functions such as antibody-dependent cellular cytotoxicity (ADCC), complement dependent cytotoxicity (CDC) or antibody-dependent cellular phagocytosis (ADCP). Effector functions result in cell death often through apoptosis or phagocytosis. [38] For patients, it is beneficial to kill cells that are causing the chronic disease symptoms and/or are malignant.

The second story that table 1.1 tells is that there is acceptable variability between

innovators and biosimilars. For example, CDC relative activity for Humira[®] was 103% and for Hyrimoz[™], 93%. Similarly, ADCC relative activity for Humira[®] was 108% and Imraldi[™], 98%. These products are both approved by the EMA and FDA, so clearly these values fall within the acceptance criteria despite being 10% different. Along those lines, table 1 also shows that there is going to be variability across biosimilars. Using ADCC as our example, Amgevita[™] reported a relative % activity of 87%, Imraldi[™], 98%, and Hyrimoz[™], 99%. [35] We are unable to fully compare these values because the experiments were conducted at different sites, by different personnel, using different cell assay conditions. Nevertheless, it provides context for the last story that table 1 tells and bolsters our reasoning to conduct my thesis research.

The third story coming from table 1.1 is that method standardization is lacking for mAbs. To assess sTNF α binding, a primary mechanism of action for Humira[®] and its biosimilars, three different methods were employed. For Amgevita[™], ELISA was used; for Imraldi[™] FRET was used; and for Hyrimoz[™] SPR was used. [35] Therefore, we expect to observe differences in the reported relative activities as each method has its own expected outcomes and limitations. This lack of standardization makes head-to-head comparison impossible. Yet, based on our work described in Chapter IV and the work of others, it is important to understand not only how much a biosimilar varies from its reference product but also how much it varies from competitor biosimilars. Without such knowledge, the idea of interchangeability, where a biosimilar can be substituted for its reference at the pharmacy without a physician's consent, remains stagnant. Perhaps these biosimilars can be approved as interchangeable because they are close enough to the reference, but further switching studies between biosimilars may prove detrimental if there are unknown significant differences between the two biosimilars.

Clinical data such as clearance rate, anti-drug antibody (ADA) formation and clinical endpoints can also be found in the prescribing information documents. Table 1.2 provides a snapshot of the clinical data for adalimumabs that was presented to regulatory agencies

for review and is now available in package inserts. [35] One glaring takeaway from Table 1.2 is that the ADA levels, while similar between concomitantly tested biosimilar/innovator pairs, do vary greatly between the different adalimumab innovator/biosimilar pairs. ADA levels, especially neutralizing ADA levels, are important to study because they are linked to immunogenicity. Immunogenicity is detrimental in patients as it can reduce a therapeutic's overall efficacy and/or exacerbate its safety implications. [39] Hyrimoz™ reported the lowest ADA formation in 25% of patients, but most were identified as neutralizing ADAs. Neutralizing ADAs are undesirable as they completely block the adalimumab from binding with TNF α , thus reducing its activity and efficacy. Idacio® had the highest ADA formation at 90%, but in looking at clinical data not included in Table 1.2, it appears as if only half of those are neutralizing ADAs. Although many of the ADAs were reported to be non-neutralizing, it is important to still monitor for these ADAs because they can increase the clearance rate of the drug, reducing its therapeutic efficacy. [40] Of course, it is still important to keep in mind the role that ADAs have on inducing immunogenicity and subsequent patient safety concerns and adverse events.

Additionally, there were significantly different response rates reported for the biosimilar/innovator pairs. The response rate was measured using a Psoriasis Area and Severity Index score (PASI 75) at which there was a 75% improvement from the baseline score 16 weeks post initial treatment. [41] For all three biosimilars tested in plaque psoriasis patients, the clinical trials were carried out beyond the 16-week primary endpoint to 51 - 54 weeks. Mirroring the ADA level trends, the PASI 75 scores were relatively similar between the biosimilar and concurrently tested Humira® but varied across the biosimilars. Hyrimoz™ had 57% positive PASI 75 response rates whereas Amgevita™ had 78% and Idacio® had over 90%.

What is more important to and supportive of similarity claims is that the PASI75 values and ADA levels for each biosimilar are close to the respective Humira® values tested in the same trial. Frequently, these differences between the innovator/biosimilar pairs can

be explained by other factors such as variations in the reporting or measuring of scores at individual trial sites. [42, 43] Although the PASI metric is considered to be the “gold standard” for psoriasis monitoring, like with any inherently subjective metric, it does have its limitations. [44] These limitations, especially given the fact that these trials were conducted with different patients, and likely handled by different clinicians, could explain why such variability exists between biosimilars. Likewise, different methods of reporting ADAs, such as sorting ADAs into neutralizing and non-neutralizing or not, or using a full-analysis dataset instead of a per protocol dataset, may impact the final results presented. Finally, limited congruity in the assays used to measure ADAs, resulting in different sensitivity, resolution and reproducibility, may also influence public data outcomes. Again, this ties back to how discrepancies in measuring and reporting data can make direct comparisons between similar products nearly impossible to complete. It bolsters the idea that there needs to be more uniformity across the pharmaceutical industry by standardizing optimized, validated methods.

Nevertheless, the varying ADAs and PASI 75 scores should still be a red flag to patients, physicians and pharmaceutical companies. Perhaps the differing values are stemming from something other than method and reporting variability. For example, they could be due to structural differences in glycosylation patterns. Discussed in more depth below are specific types of glycans and how they may influence functionality and/or safety by inhibiting target binding, increasing clearance rates or inducing immunogenicity. In brief, though, it is known that certain glycans can impact the overall immunogenicity of a mAb. Perhaps Idacio[®], which yielded the highest efficacy but had only half of its ADAs categorized as neutralizing, had more mannosylated glycans than other biosimilars. This could explain the relatively high efficacy - mannosylated glycans are known to increase effector function - and the higher number of ADAs, most of which are non-neutralizing - mannosylated glycans are known to increase clearance rates and, thus, increase immunogenicity. Unfortunately, the glycan profiles for Idacio[®] and other adalimumabs are not

Table 1.3: Percentage of charge variants/glycans for each biosimilar relative to Humira® given as a range (average). Each biosimilar is compared to a reference Humira® (left of biosimilar column) that was tested simultaneously during analysis.

Charge Variants/Glycans	Humira®	Amgevita™	Humira®	Imraldi™	Humira®	Hyrimoz™
% basic	19.7–29.3 (24.5)	10.8–16.5 (13.7)	17.5–30.2 (23.9)	8.6–10.9 (9.8)	>20.3	12.9–17.7 (15.3)
% acidic	13.1–18.2 (15.7)	17.6–21.7 (19.7)	11.9–18.7 (15.3)	22.6–25.6 (24.1)	9.2–13.9 (11.6)	6.8–10.7 (8.8)
% afucosylated	7.5–13.3 (10.4)	6.7–10.8 (8.8)	1.6–2.3 (2.0)	2.0–3.6 (2.8)	0.5–0.9 (0.7)	2.4–3.2 (2.8)
% sialylated	0.1–0.3 (0.2)	0.5–1.2 (0.9)	0.0–0.6 (0.3)	2.1–3.5 (2.8)	<LOQ	0.3–0.5 (0.4)
% galactosylated	16.5–23.0 (19.8)	19.9–39.2 (29.6)	18.3–21.4 (19.9)	19.3–28.3 (23.8)	14.7–23.1 (37.8)	23.7–37.4 (30.6)
% high mannose	5.6–10.6 (8.1)	5.0–8.5 (6.8)	4.4–9.3 (6.9)	5.3–9.9 (7.6)	3.9–6.6 (5.3)	0.9–1.3 (1.1)
% C terminal lysine	n/a	n/a	5.7–9.6 (7.7)	1.3–3.1 (2.2)	13.3–18.7 (16.0)	3.1–6.0 (4.6)

publicly shared. Therefore, we just have to make hypotheses.

Higher order structure, post-translational modifications and other structural features, such as those listed in table 1.3, are also critical to an antibody’s safety, efficacy and pharmacokinetics. [35] For the purposes of this thesis research, we are particularly interested in monitoring two post-translational modifications, glycosylation (Chapter II and Chapter IV) and disulfide bond shuffling (Chapter III), and correlating them to functionality assays (Chapter II) or degradation patterns (Chapter III).

A glycan is a sugar moiety located off of asparagine at position 297 near the hinge region of mAbs (Figure 1.4). The presence of a glycan at N297 is conserved across the IgG1 mAbs we have studied here, but the structure of the glycan at this location varies greatly, even for mAbs within the same protein solution.

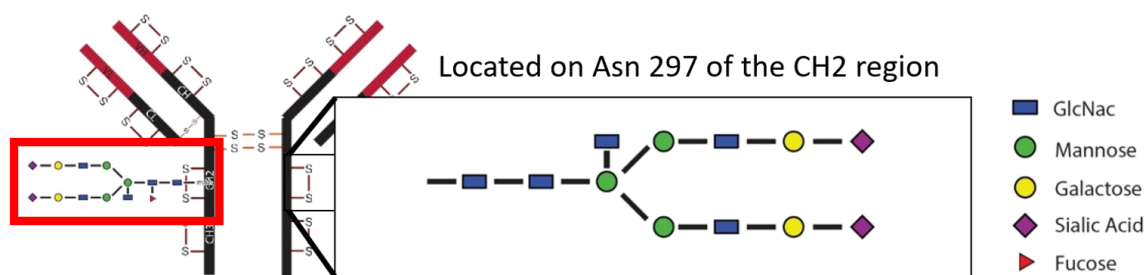


Figure 1.4: Schematic of IgG1 glycan position with examples of sugar moieties commonly found on human glycans.

The location of the glycan on the Fc region also means that it can influence a number of mAb properties such as protein folding, Fc effector function, clearance rate, and anti-drug antibody formation. Depending on the type of glycan, the Fc region can be in an open

conformation, allowing for increased binding to Fc receptors (FcγR), or a closed conformation. Within the realm of FcγR binding, there are a number of possible interactions affected by the type of glycan at N297, including glycan-glycan interactions that occur between the glycan at N297 and the glycans at position 162 on FcγRIIIa and FcγRIIIb. [38] These Fc interactions lead to difference signaling cascades that can not only alter effector functions, but also influence immune responses and/or recognition and uptake by antigen-presenting cells.

There are five main glycan types we are interested in characterizing which include (a)fucosylated, mannosylated, sialic acid, galatosylated and bisecting GlcNAc. These glycan types are of interest because of their known effects on drug safety, efficacy, activity, and/or pharmacokinetics. Below are descriptions for all of the glycans of interest.

Fucosylated glycans can reduce an antibody's Fc binding affinity. This is attributed to the steric hindrance that the presence of fucose provides. Reduced binding affinity results in diminished therapeutic efficacy, primarily through ADCC and CDC. Houde et al confirmed this phenomenon through H/DX-MS where they found that the removal of fucose increased the binding affinity of IgG1 to FcγRIIIa by 49-fold. [45] There was no associated IgG1 conformational change suggesting that the glycan instead directly mediates the IgG1-FcγRIIIa binding interaction. Other analytical methods such as modeling of IgG-FcγRIIIa binding sites in the presence and absence of fucosylation [46], as well as the performance of ADCC assays for IgGs with varying levels of fucosylation [47, 48] have also confirmed differences in binding affinity. Thus, afucosylated glycans are generally preferred as they enhance ADCC and CDC, mechanisms of action for many therapeutics IgG1 mAbs. [34, 49, 50]

Mannosylated, or high mannose, glycans are an example of an afucosylated glycan that can enhance ADCC. However, mannosylated glycans also increase the clearance rate of a drug due to their recognition by endogenous mannose and asialoglycoprotein receptors. [50] Goetze et al proved the correlation between mannosylation levels and clear-

ance through a number of ELISA assays and peptide mapping experiments conducted on IgGs. [3] The glycoforms with high mannose (M5) had noticeably shorter half-lives than those lacking mannose. They also showed that higher levels of mannose, 20% vs. 5% by peptide mapping, and higher pairing ratios between the antibody and mannose receptor yielded faster clearance. [3]

Upon recognition of the high mannose glycan, endogenous receptors bind, uptake, and degrade the high mannose-containing mAb. This results in a decrease in the number of therapeutic mAbs in circulation and, in turn, an overall increase in the therapeutic clearance rate, as exhibited in Figure 1.5. [34, 49, 50] Increased clearance rates are problematic because they require more frequent dosing in order to achieve desired therapeutic levels. Additionally, the formation of anti-drug antibodies, hallmarks of immunogenicity and patient safety concerns, can occur more rapidly if the therapeutic is readily recognized. [50–53]

Sialylated glycans, which contain sialic acid, can be both beneficial and detrimental to patients. They can be beneficial in that they initiate anti-inflammatory effects by upregulating FcγRIIb, an immune checkpoint that suppresses immune responses. [54] Autoimmune diseases such as rheumatoid arthritis, Crohn's disease, and ulcerative colitis are frequently associated with innate IgGs lacking terminal sialic acid and galactose [55]. Therefore, there is increased binding between the IgG and FcγRIII, greater effector function, and a higher pro-inflammatory response. In diseases such as these where symptoms are exacerbated by pro-inflammatory responses, a common goal of therapeutics is to combat the response by inducing anti-inflammatory activity. Therefore, many intravenous IgG (IVIG) therapeutics carry terminal sialic acids to counteract the innate antibody pathogenicity. [56] For patients with cancer though, the inhibition of the immune response in tumor micro-environments may allow the malignancy to survive. In fact, there is a new clinical-stage FcγRIIb antibody being developed by BioInvent targeting FcγRIIb. [57] It aims to improve the outcome of current mAb cancer treatments like trastuzumab or rit-

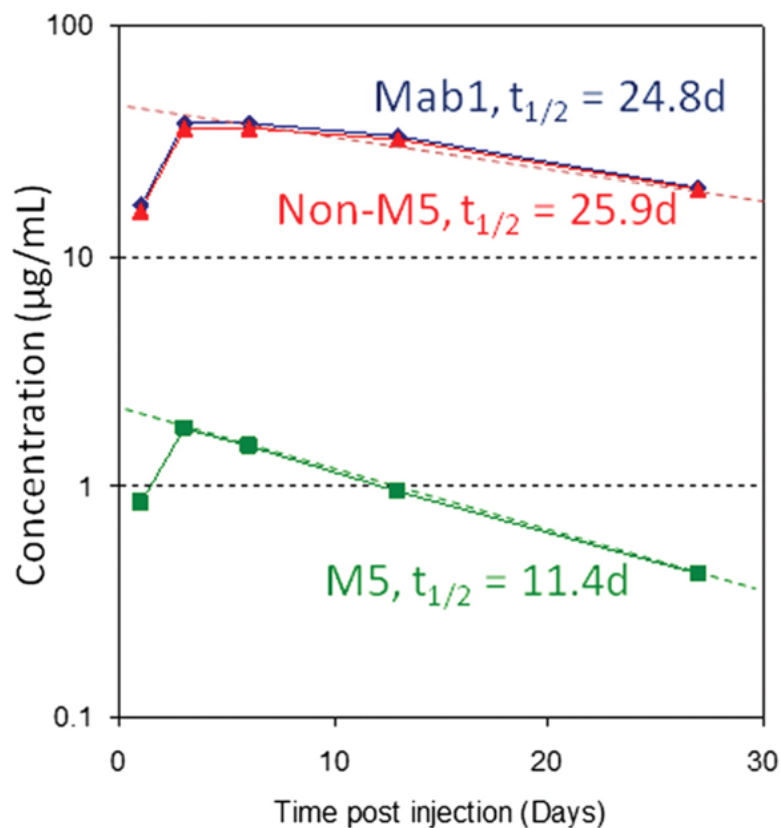


Figure 1.5: Concentration vs. time post-injection of 300 mg of Mab1 administered in a single patient. Shown are the M5 glycoform and all non-M5 glycoforms. Half lives for the glycoforms were approximated by fitting the experimental data points to a first-order rate equation (dashed lines). Plot adapted from Goetze et al., 2011. [3]

uximab by enhancing efficacy and overcoming current resistance challenges.

Additionally, sialic acids have been associated with reduced FcγRIIIa binding and ADCC (Figure 1.6). Terminal sialylation has been linked to decreased binding with FcγRs because it closes the binding site between an IgG and FcγR. [4, 38, 54] Non-human sialic acids, like the murine-derived sialic acid, NGNA, may also potentially increase immunogenicity. [34, 49, 50, 58, 59]

Galactosylated glycans, which have an exposed terminal galactose residue, can elicit more protein binding at FcγRIIIa, enhancing the ADCC and CDC effector function of antibodies. [37] This phenomenon was confirmed by Houde et al in an H/DX-MS experiment where complete IgG1 galactosylation prevented some residues from exchanging. [45] The

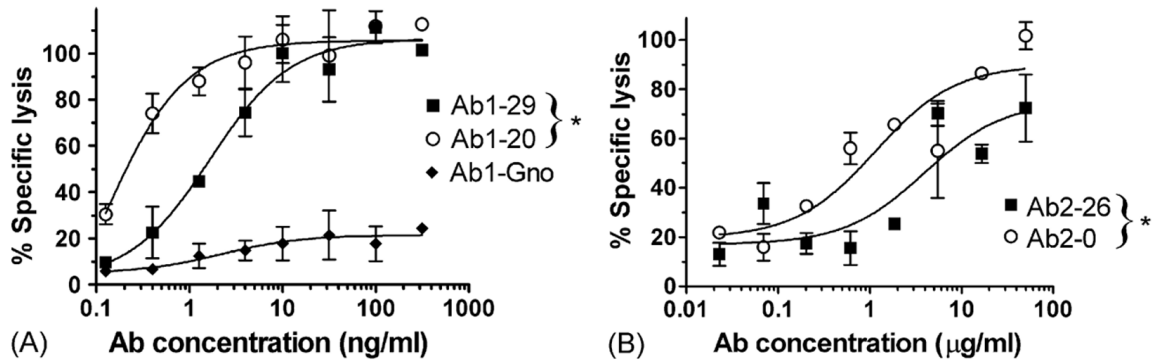


Figure 1.6: Specific lysis from an *in vitro* ADCC assay. A) Comparison of natural variants of AB1 using Ag1-expressing target cells; Ab1-29 has higher levels of Fc sialylation and required 7-fold higher concentrations to trigger same levels of cell lysis compared to Ab20; B) Comparison of natural variants of AB2 Ag2-expressing target cells; Ab2-26 required 6-fold higher concentrations to achieve same effect as Ab2-0 variant with no detectable sialic acid. Plots adapted from Scallon et al., 2007. [4]

lack of exchange was correlated with increased structural rigidity and, consequently, increased receptor binding, due to changing the relative orientation of the CH1 and CH2 domains¹⁸. Galactosylated glycans' role in enhancing CDC is more prominent as they have high affinity for C1q, a critical component of the complement cascade. Galactose has also been affiliated with anti-inflammatory responses by binding to FcγRIIb. In patients with autoimmune diseases there are higher numbers of innate degalactosylated IgG, suggesting either that these are more pathogenic or that galactosylated IgG have anti-inflammatory activity. [38] Terminal galactose may increase the clearance rate of mAbs as well because the asialoglycoprotein receptors can recognize and bind galactose. [34, 49, 50, 59]

Bisecting GlcNAc glycans increase binding affinity to FcγRIIIa and therefore enhance ADCC. It is still unknown whether this phenomenon is due to the presence of the bisecting GlcNAc or due to the lack of fucose. [34, 49, 50, 59] Bisecting GlcNAc has also been classified as a proinflammatory trait in autoimmune diseases such as Crohn's disease. This can perhaps be linked to methylation, which is related to the disease progression and pathogenesis of Crohn's disease. [60]

Given the impact glycans can have on a therapeutics' activity, efficacy, pharmacoki-

netics and immunogenicity, we characterized the glycan profiles of various mAbs using semi-automated technology in my chapter II and chapter IV research projects. For the first project, we analyzed the glycan profile of three innovator anti-TNF α mAbs, Humira[®], Remicade[®] and Simponi Aria[®], using liquid chromatography-tandem mass spectrometry, LC-MS/MS, and liquid chromatography-fluorescence, LC-FLR. We did this in conjunction with functional assays such as Fc binding and ADCC in order to determine if we could predict the binding affinity and effector function outcomes based on the presence of specific glycans. To our knowledge, we were the first group to perform a head-to-head comparison of three innovator mAbs indicated for the same disease states. The reason why this is important is because there is inherent site, user and method variability that prevent treatments from being appropriately compared unless there is a normalizing factor. In our case, the normalizing factor is conducting analyses simultaneously, under the same conditions and with the same methods. Since patients are frequently switched between these three proteins and other treatments in order to maintain therapeutic efficacy, it is important to understand how they vary and what impact that may have on a patient's outcome. [61–64]

For the second project, we also looked at glycosylation in the context of method standardization. As is apparent from table 1.1, different methods used to measure the same endpoint can yield varying data outcomes. Albeit, table 1.1 refers to *in vitro* functionality assays, but the sentiment remains the same for structural analysis methods. Many methods are available for analyzing glycans, ranging from released glycan kits to LC-MS/MS to capillary electrophoresis-MS (Figure 1.7). In fact, multiple studies have been conducted applying various glycan analysis methods to antibodies in order to highlight method similarities and differences. [5, 65–70]

Yet, standardization of glycan analysis methods is still lacking. This may present problems down the line with regards to determining acceptable limits of low abundance glycans. Without a gold standard, companies are performing multiple glycan analysis exper-

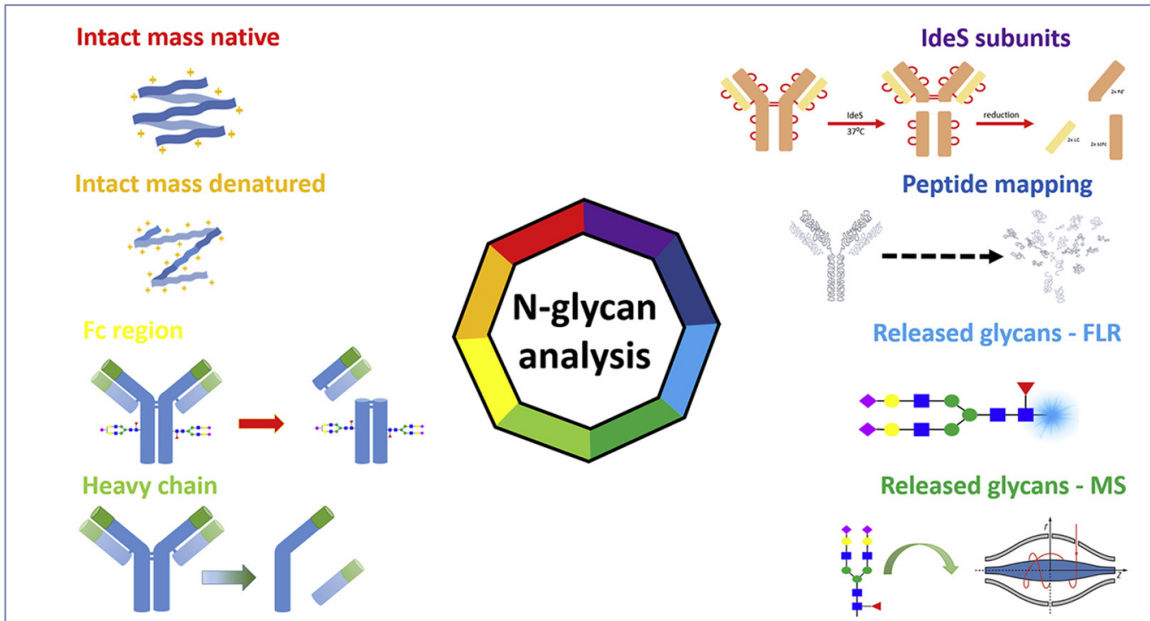


Figure 1.7: Schematic representation of various analysis methods commonly used to characterize N-glycans on mAbs. Image adapted from Carillo et al., 2020. [5]

iments in hopes of presenting a plethora of data to the FDA to prove that their therapeutic should be approved. Therefore, we completed our third project using NIST mAb as our standard to identify the limitations of various glycan analysis methods and provide recommendations and groundwork for future method standardization.

Glycosylation characterization was a focus for this thesis research, but it is not the only PTM worth studying. Another PTM that falls into the CQA category is disulfide shuffling. In IgG1s, there are 12 intrachain disulfide bonds and 4 interchain disulfide bonds (Figure 1.8). These covalent bonds are composed of one cysteine that pairs with its normal cysteine partner to form a disulfide bridge. Disulfide bridges are critical for maintaining proper protein folding and stability. [71]

However, there are occasions where a cysteine residue, or thiol group, bonds with an “incorrect” free thiol partner. This phenomenon, illustrated in Figure 1.9, is called disulfide shuffling or scrambling. Disulfide shuffling is problematic as it alters the protein conformation, potentially inducing aggregation and/or reducing target binding affinity. Aggregation is problematic because it is a precursor for immunogenicity. Higher immunogenic

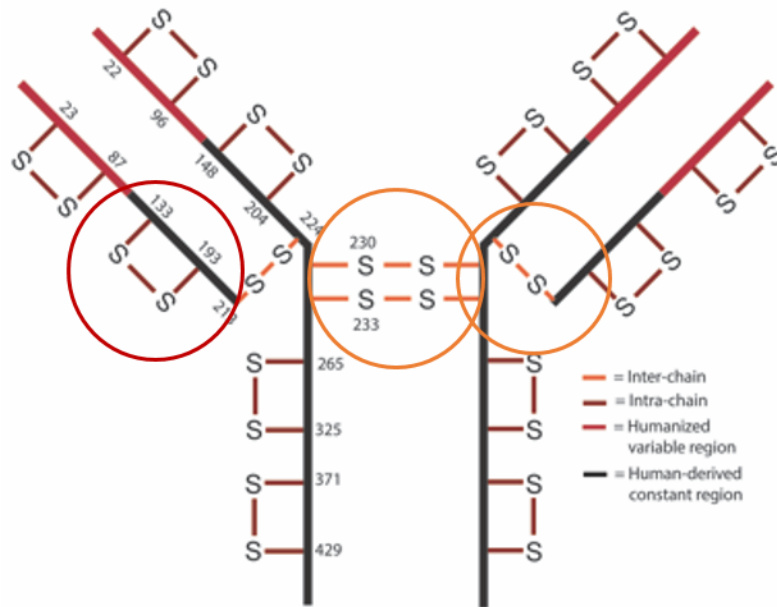


Figure 1.8: Schematic of IgG1 mAb highlighting the 12 intrachain disulfide bonds (red) and 4 interchain disulfide bonds (orange).

responses can lead to patient safety concerns. [71,72] Reduced target binding affinity will decrease the efficacy of a mAb by altering mechanisms of action including Fab neutralization of a target antigen or Fab/Fc binding induced ADCC.

There are also trisulfide bonds, which are rare modifications with a third sulfur group added in the middle of a disulfide bond (Figure 1.10). These modifications have not been directly linked to adverse effects but have been correlated with unhealthy cell cultures. [71,73–75] As healthy cell cultures are critical to producing a reproducible antibody, they are worth monitoring.

Despite being a CQA reported to the FDA through a mAb submission package, there are limited publications describing methods for characterizing shuffled disulfide bonds on IgG1s. Therefore, for my second project detailed in chapter III, I worked on developing a semi-automated platform for disulfide bond analysis. By using an AssayMAP Bravo robot for liquid handling and sample preparation, then processing my samples acquired from LC-MS/MS via Protein Metrics’ disulfide bond workflow, I was able to streamline the characterization of disulfide bonds on rituximabs and bevacizumabs. Although shuffled

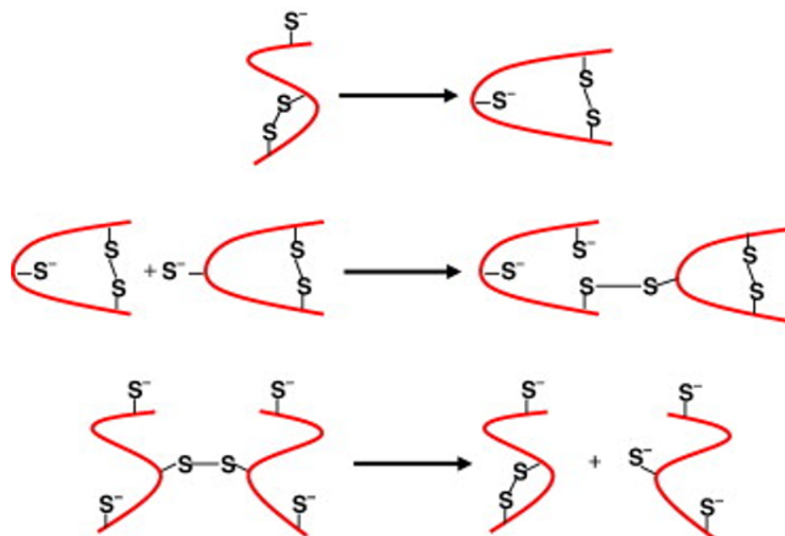


Figure 1.9: Examples of shuffled disulfide bond patterns, either intermolecularly or intramolecularly, that can occur in antibodies. Image adapted from Zhang et al., 2011. [6]

disulfide bonds are rare modifications, we did see shuffled bonds in both the rituximabs and bevacizumabs, with bevacizumabs having higher relative levels of shuffled disulfide bonds. This proved that our method was sensitive enough to detect low abundance PTMs.

We also highlighted the importance of applying PTM characterization methods to innovator/biosimilar pairs in this project. We studied Rituxan[®] and one of its biosimilars along with Avastin[®] and one of its biosimilars for shuffled disulfide bonds. Although we did not see many significant differences, which may be expected given that the biosimi-

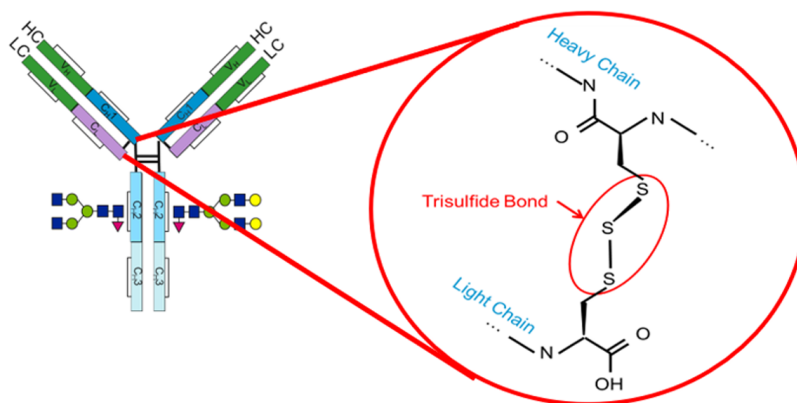


Figure 1.10: Schematic depicting the insertion of a third sulfur group into an existing disulfide bond to form a trisulfide bond. Image adapted from Shion et al., 2019. [7]

lars are approved products, we did find it helpful to show that different trends between biosimilars and innovators, even if not statistically significant, could be teased out with our method.

Another mAb property we studied in the second project was higher order structure, namely in the form degradation formation. We hypothesized that if a protein had more shuffled disulfide bonds, it may have a higher propensity to aggregate. Therefore, we exposed our mAbs to stressed conditions and monitored not only disulfide bond shuffling over an incubation period, but also aggregation. Interestingly, the bevacizumab samples, which had higher initial levels of shuffled bonds that generally increased over the course of an incubation, yielded more aggregates over time as measured by SEC and SDS-PAGE. The rituximabs, which had <1% shuffled disulfide bonds throughout the incubation period, did not aggregate but rather fragmented when under stress. Whether the disulfide bonds are the sole culprit for aggregation in bevacizumabs, but not in rituximabs, remains to be seen. Nevertheless, this work showed that there is potentially a correlation with shuffled disulfide bonds and aggregation and reemphasized the importance of not only PTMs, but also higher order structure, on protein performance.

Taken altogether, this thesis emphasizes the importance of adequately characterizing PTMs on biologics in order to identify potential safety, efficacy, activity, immunogenicity and/or pharmacokinetic concerns prior to administration in patients. To do so, we have broken down the research conducted into three distinct projects. Chapter II discusses the head-to-head-comparison of anti-TNF α mAbs with regards to their glycosylation patterns and affiliated *in vitro* functionality. Chapter III describes disulfide bond shuffling and its potential effect on aggregation/degradation propensities for innovator and biosimilar anti-cancer mAbs. Chapter IV compares the data outcomes and limitations of five glycosylation analysis methods using NIST mAb as a standard and trastuzumabs as a show-and-tell application. Chapter V highlights the broader impacts of each project and discusses future directions both for the lab and for stakeholders in other areas of the

biologics field.

CHAPTER II

Anti-TNF α mAb Structure and Function Characterization

This chapter describes our research comparing structural differences and functional activities of three anti-TNF α mAbs, Humira[®], Remicade[®] and Simponi Aria[®]. We determined glycosylation profiles by LC-MS/MS and LC-FLR, then performed *in vitro* bioassays to determine whether glycan profiles could predict Fc binding activity outcomes. As the first head-to-head comparison of these three anti-TNF α mAbs, we set the precedent for comparing competitor mAbs prior to patient administration and/or prescription switching. This chapter is based on work published in *International Journal of Pharmaceutics*. [76]

2.1 Introduction

In the U.S., there are more than 24 million patients diagnosed with an autoimmune disease. [77] These diseases are not a one-size-fits all, but rather they present in different organs and at different levels of severity depending on the patient. Despite this, numerous autoimmune conditions can be treated with therapies that target an inflammatory cytokine, tissue necrosis factor alpha (TNF α). The primary mechanism of action for these products is through binding and neutralization of TNF α . By binding to soluble and membrane-bound TNF α , these therapies block endogenous p55 and p75 TNF

receptors from binding to $\text{TNF}\alpha$. $\text{TNF}\alpha$ binding by p55 and p75 initiates immune and inflammatory response pathways. By blocking these interactions, the therapeutics are suppressing systemic inflammation and immune responses (i.e. generation of additional pro-inflammatory cytokines like IL-1 and IL-6). [78] Given that patients with autoimmune diseases such as rheumatoid arthritis, psoriasis, and irritable bowel disease (IBD) often suffer from overactive immune systems, the therapeutics' interference in immune responses helps reduce localized symptoms such as inflammation, swelling and joint pain. In addition to the primary mechanism of action there is a secondary mechanism of action, Fc-mediated apoptosis, (i.e. antibody-dependent cellular cytotoxicity (ADCC) and complement-dependent cytotoxicity (CDC)), proposed to evoke treatment response in IBD patients. [1, 79–81] Fc-mediated apoptosis, commonly referred to as effector function, requires both proper $\text{TNF}\alpha$ binding by the Fab region of the anti- $\text{TNF}\alpha$ antibody and Fc binding by natural killer cells or C1q proteins. In ADCC, once natural killer cells are bound to the Fc region of the anti- $\text{TNF}\alpha$ antibody, they can initiate a cell signaling cascade that eventually leads to apoptosis of activated immune cells (primarily monocytes and macrophages) expressing transmembrane $\text{TNF}\alpha$ (tm $\text{TNF}\alpha$). Similarly, for CDC, the Fc binding of anti- $\text{TNF}\alpha$ therapeutics to C1q proteins triggers the formation of a membrane attack complex (MAC) resulting in apoptosis of tm $\text{TNF}\alpha$ -expressing cells. Overall, the death of inflammatory cells is beneficial to IBD patients because it reduces the number of cells that are available to induce excessive immune responses and alleviates their symptoms.

One of the commonly prescribed anti- $\text{TNF}\alpha$ biopharmaceuticals is Humira[®] (adalimumab). Humira[®] is a fully humanized monoclonal antibody (mAb) therapeutic indicated for over 10 autoimmune diseases including rheumatoid arthritis, psoriatic arthritis, plaque psoriasis, ankylosing spondylitis, and irritable bowel disease, namely, ulcerative colitis (UC) and Crohn's disease (CD). Aside from Humira[®], there are two other full-length mAbs approved for similar indications, Remicade[®] (infliximab) and Simponi

Aria[®] (golimumab). While these three drug products are approved for overlapping disease states, they do differ in a number of other factors including route of administration (subcutaneous or intravenous), recommended dose (40 mg/ 2 weeks to 100 mg/ 8 weeks), TNF α binding stoichiometry, pharmacokinetics, and immunogenicity (Table 2.1). There are a range of factors that influence the clinical use of anti-TNF α mAbs. For example, Remicade[®] is considered to be a “rescue” drug for moderate-severe ulcerative colitis patients as it has been shown to invoke superior remission rates in this population. [82–86] However, unlike the fully humanized mAbs Humira[®] and Simponi Aria[®], Remicade[®] is chimeric, having both human and murine protein sequences. Because of this, patients taking Remicade[®] have a higher tendency to develop anti-drug antibodies (ADA), which can lead to immunogenic events and reduced efficacy. [87–89] In general, these ADA levels, indicative of immunogenicity and overall efficacy/safety, differ across all three products and among individual patients and patient populations (Table 2.2).

Another variable factor to highlight is route of administration. Humira[®] is administered subcutaneously, resulting in lower serum concentration levels, while Remicade[®] and Simponi Aria[®] are administered intravenously, yielding higher serum concentration levels compared to Humira[®] (Table 2.2). Despite these lower serum concentration levels, Humira[®] and Remicade[®] are approved for IBD while Simponi Aria[®] remains only in the arthritis space.

There are two other approved anti-TNF α biotherapeutics, Cimzia[®] (certolizumab pegol) and Enbrel[®] (etanercept), which are not full-length mAbs. Cimzia[®] is only the Fab region of an IgG1. It is not indicated as a treatment for IBD diseases, perhaps because it does not have an Fc region available to elicit effector functions- a secondary mechanism of action in IBD. Enbrel[®] is a fusion protein with an IgG1 Fc region and a TNF receptor. Despite the presence of an Fc region, Enbrel[®] does not induce Fc-mediated apoptosis to the same extent as full-lengths mAbs and, therefore, it is not indicated for IBD. [90, 91] Given the effector function limitations of Cimzia[®] and Enbrel[®], we analyzed only the full-length

Table 2.1: General product administration and dosing information for the three anti-TNF α mAbs.

Protein therapeutic	Structure	Route of administration	Frequency of dosing	Dosage form and strength	Clinician prescribing tendencies for UC & CD
Humira® (<i>adalimumab</i>)	Fully humanized	SC via an injection pen or pre-filled syringe	40 mg every 2 weeks	Single dose pre-filled pen or syringe: 40 mg/0.8 mL, 40 mg/0.4 mL, 10 mg/ 0.1 mL* *other dosage strengths available	Moderate-severe UC & CD ^{2,3,4}
Remicade® (<i>infliximab</i>)	Chimeric (30% murine, 70% human) ⁶	IV via a needle with an in-line filter	5 mg/kg at 0, 2, and 6 weeks followed by a maintenance regimen of 5 mg/kg every 8 weeks thereafter	100 mg of infliximab as a lyophilized powder in a single-dose vial	Moderate-severe UC & CD Rescue drug for UC ^{2,3,4}
Simponi Aria® (<i>golimumab</i>)	Fully humanized	IV via a needle with an in-line filter (Simponi is SC via an autoinjector or pre-filled syringe)	2 mg/kg over 30 minutes at weeks 0 and 4, and every 8 weeks thereafter	50 mg/4 mL (12.5 mg/mL) solution in a single-dose vial	Not approved for UC & CD

1("Humira Prices, Coupons & Patient Assistance Programs - Drugs.com,")

2(Järnerot et al., 2005)

3(Park et al., 2014)

4(Sjöberg et al., 2013)

5("AbbVie Reports Full-Year and Fourth-Quarter 2021 Financial Results | AbbVie News Center," 2022)

6(EMA, 2005)

7("Remicade Prices, Coupons & Patient Assistance Programs - Drugs.com,")

8(*Johnson & Johnson Reports Q4 and Full-Year 2021 Results*, 2022)

9("Simponi Aria Prices, Coupons & Patient Assistance Programs - Drugs.com,")

CD = Crohn's disease; UC = Ulcerative colitis

Table 2.2: Binding stoichiometry, pharmacokinetic properties and immunogenicity characteristics.

Protein therapeutic	Binding properties	Half-life ($t_{1/2}$)	Max serum concentration (C_{max})	Clearance rate	% ADA (package inserts)
Humira® (adalimumab)	- 3 mAb : 2 TNF - Interaction with 2 TNF protomers - Direct overlap with native TNF receptor binding site ^{1,2}	14 days (10-20 days) ³	Following a single 40 mg SC dose: 4.7 ± 1.6 µg/mL ³	12 mL/hr ³	RA: 5% CD: 3% PsA: 7% UC: 5% PS: 8% ³
Remicade® (infliximab)	- 3 mAb : 2 TNF - Interaction with 1 TNF protomer - Partial overlap with native TNF receptor binding site ^{1,2}	7.7 - 9.5 days ⁴	Following a single IV of 5 mg/kg dose: 129.2 ± 18.8 µg/mL ⁵	10.7 ± 2.9 mL/hr ⁵	RA: 10% PsA: 15% PS: 36% ⁴
Simponi Aria® (golimumab)	- 3 mAb : 2 TNF - Interaction with 1 TNF protomer - No overlap with native TNF receptor binding site ⁶ (Ono et al., 2018)	14 days (10-18 days) ⁷	Following a single IV dose of 2 mg/kg: 44.4 ± 11.3 µg/mL ⁷	7.6 ± 2.0 mL/day/kg ⁷	RA: 21% PsA: 19% AS: 19% ⁷

1(Lim et al., 2018)

2(Tran et al., 2017)

3(HIGHLIGHTS OF PRESCRIBING INFORMATION - HUMIRA, 2002)

4(HIGHLIGHTS OF PRESCRIBING INFORMATION - REMICADE, 1998)

5(Shin et al., 2015)

6(Ono et al., 2018)

7(HIGHLIGHTS OF PRESCRIBING INFORMATION - SIMPONI ARIA, 2009)

mAbs, Humira[®], Remicade[®] and Simponi Aria[®], in the study described here.

Effector functions are of special interest to our group and to others as they can be altered by the presence of certain post translational modifications and can lead to changes in therapeutic efficacy and safety. [92–94] For example, afucosylated and high-mannose glycans have been shown to increase FcγRIIIa binding and ADCC potency in therapeutic mAbs. [2, 11, 47, 48, 95] High-mannose glycans have also been linked to altered pharmacokinetics in the form of decreased half-life and increased clearance. [3, 96, 97] Therefore, to determine whether these trends held true for the three full-length anti-TNF α mAbs, we performed a number of binding affinity and *in vitro* efficacy experiments. Additionally, we characterized the glycosylation profile of each mAb and correlated it with Fc binding and ADCC.

While previous studies have measured TNF α binding affinity, Fc- binding affinity, glycosylation and effector function for these mAbs independently, to our knowledge, this is the first time all three therapies have been compared head-to-head. The benefit of performing these experiments for all three mAbs simultaneously is that we can control the types of experiments and the conditions they are run under. Mirroring elements of comparative studies used for small molecule products like statins allows us to simply compare physicochemical differences between the three products to see if there are significant differences in their structure, function and potential safety implications. [98–100] Then we can tie those properties with the drug products' published pharmacokinetic profiles to paint a full picture of each therapeutic. In doing so, we aim to identify potential product-related reasons why some of these therapeutics are prescribed and preferred more by physicians and patients. [101–104] It is worth noting that while we aim to identify possible reasons for drug preferences, we recognize the unique nature of each drug product and each patient, and understand that the trends we observe here are not a sure way to predict the *in vivo* efficacy and safety of these drug products.

2.2 Materials and Methods

2.2.1 Reagents and Kits

Digestion reagents, including iodoacetamide, TCEP and trypsin with Lys-c were acquired from Promega (Madison, WI). Sample plates for the digestion reaction were purchased through Agilent (Santa Clara, CA). LC-Fluorescence reagents were provided in the purchased RapiFluor kit by Waters (Milford, MA). The TNF α ELISA kits and required reagents were purchased from ThermoFisher Scientific (Waltham, MA). The AlphaLISA kits were purchased from PerkinElmer (Waltham, MA). The ADCC Reporter Bioassay kit and required reagents were purchased from Promega Corporation (Madison, WI).

2.2.2 mAb Sample Information

Drugs were purchased from the University of Michigan Hospital Pharmacy. Three lots of each drug were acquired. Humira[®] (AbbVie, Lake Bluff, IL) lots include 1080483, 1108313 and 1110162. Remicade[®] (Janssen, Raritan, NJ) lots include 17AD20231, 12BD20451 and 18LD39901. Simponi Aria[®] (Janssen, Raritan, NJ) lots include HESORO2, IJS4E00 and ILS0800. Each mAb lot was run in triplicate for the assays completed.

2.2.3 Glycosylation Analysis

2.2.3.1 Glycosylation Analysis by LC-MS/MS

Humira[®] and Simponi[®] were diluted down to 10 mg/mL from their native formulations using water. 6.08 mg of Remicade[®] was dissolved in 100 μ L of water to achieve a protein concentration of 10 mg/mL. A single reduction solution comprised of 2 M Tris-HCl, pH 8, 8 M guanidine hydrochloride, 100 mM TCEP and water was added into a 96-well Eppendorf PCR plate. Then 100 μ g of the mAbs were added into the wells of a separate 1.2 mL Deep Well AbGene plate and 300 mM iodoacetamide was added into wells on a third 96 well Eppendorf PCR plate. These plates were placed on the AssayMAP Bravo liquid handling

platform (Agilent) and an in-solution digestion protocol was completed. The reduction solution was added to the mAbs and incubated for 30 min at 37°C. Then the alkylant was added and incubated for 30 min at room temperature with a lid to prevent light exposure. Finally, a single digestion solution comprised of 2 M Tris-HCl, pH 8, calcium chloride, Lys-C and trypsin was added into a 1.2 mL Deep Well AbGene plate and placed on the liquid handling platform. After the alkylation incubation, the digestion solution was added into the sample plate. The sample plate was incubated overnight at 37°C as a final concentration of 1:1:10 Lys- C: trypsin: mAb. The following day, the reaction was terminated with TFA and samples were purified using stage tips for solid phase extraction. The elution buffer used during solid phase extraction was 70% acetonitrile, 0.1% TFA. The purified samples were lyophilized and reconstituted prior to LC- MS/MS injection.

LC was completed on a Waters Acquity UPLC and the MS was conducted on a ThermoFisher Orbitrap Fusion Lumos mass spectrometer (Waltham, MA). The sample peptides were loaded onto a C18 trapping column then eluted over a 75 um C18 analytical column at a flow rate of 350 nL/min. For the LC, a 30-minute reverse phase gradient was used. For the MS, a data dependent HCD mode was used with MS at a 60,000 FWHM resolution and MS/MS at a 15,000 FWHM resolution. Three second cycles were used throughout the duration of the MS and MS/MS run time. Data was processed using Protein Metrics' Byos PTM suite (Cupertino, CA), accounting for trypsin and Lys-c cleavage. Sequences were searched against existing library data derived from the FASTA file of each protein.

2.2.3.2 Glycosylation Analysis by LC-FLR

Samples were prepared for LC-FLR using the protocol and reagents provided in the RapiFluor N-glycan kit (Waters). In short, 15 µg of the mAb samples were treated with 5% RapiGest surfactant then heated for 3 min at 90°C to denature the protein. Then the samples were cooled and deglycosylated with PNGase F and incubated for 5 min at 50°C. mAbs were labeled with RapiFluor-MS reagent solution at room temperature and further

diluted with acetonitrile in preparation of HILIC solid phase extraction. For solid phase extraction, a HILIC μ Elution plate attached to a vacuum was used. After equilibration, samples were added to the plate and eluted with three 30 μ L volumes of the provided elution buffer (200 mM ammonium acetate in 5% acetonitrile). Finally, the samples were diluted with the GlycoWorks Sample diluent- DMF/ACN and injected on a BEH Glycan column (Waters) interfaced to an Acquity UPLC fitted with a fluorescence detector (Waters). The column temperature was set at 60°C, the flow rate was 0.4 mL/min, mobile phase A was 50 mM ammonium formate solution, pH 4.4 and mobile phase B was 100% acetonitrile. The gradient used increased % mobile phase A from 25% to 100% and back to 25% over the duration of the run.

2.2.4 TNF α Binding ELISA

Coating buffer was used to dilute TNF α down to 0.5 μ g/mL. Then 100 μ L of diluted TNF α was added into each well of a 96-well plate. Plates were covered and incubated at 4°C overnight. Plates were washed 3 times using the plate washer prior to the addition of 200 μ L of blocking buffer into each well. The plates then shook at 300 rpm at room temperature for 1 h. Next, 100 μ L of samples were added to each well except for the blanks, then plates were incubated shaking at 300 rpm at room temperature for 1 h. After the plates were washed 3 times, 100 μ L of diluted HRP conjugate was dispensed into each well prior to another incubation at room temperature for 1 h. Wells were washed 5 times with the plate washer and 100 μ L of TMB substrate was added into each well. The plates were developed at room temperature for 10–30 min. After adding 50 μ L of stop solution to each well, the absorbance of each well was read at 450 and 550 nm on a SpectraMax M3 plate reader (Molecular Devices). Subtracting the 550 nm values from the 450 nm values corrected for optical imperfections in the microplate. The sample starting concentration was at 0.01 μ g/mL and a dilution factor of 1:2 was used for a total of 12 points. Data was processed and interpreted via GraphPad Prism.

2.2.5 AlphaLISA for FcγRIIIa (V158 Variant) Binding Affinity

Samples were prepared and analyzed using the protocol provided by AlphaLISA FcγRIIIa (V158) kit (Perkin Elmer). mAbs were serially diluted in 1X HiBlock buffer to yield 4X protein for plating. Then 10 μL of 4X mAbs were added into a ½ area 96-well plate followed by the addition of 10 μL of 4X FcγRIIIa (final concentration of 2 nM). Next, 20 μL of the solution containing 2X human IgG Fc conjugated acceptor beads and 2X streptavidin donor beads (20 μg/mL) was added into the plate, yielding a final protein concentration of 20 μg/mL. The sample plate was incubated for 90 min at room temperature in the dark and read on a Synergy Neo2 plate reader (BioTek). Data was processed and interpreted via GraphPad Prism.

2.2.6 ADCC for Effector Function

The ADCC Reporter Bioassay was conducted according to the manufacturer's protocol (Promega) with optimizations in antibody concentrations. On day 1, 100uL (104 cells) per well of target cells (CHO-K1 cells expressing mTNFα) was transferred to the inner wells of a 96-well plate. On day 2, the cell culture media was removed, and 25uL of assay buffer containing the test antibodies was added. A final antibody concentration of 5 nM was selected and serially diluted 2.25-fold using the assay buffer. There were 8 dilutions per antibody and 6 replicates per concentration. The outer wells of a 96-well plate were left as blanks. After adding the antibody, 25 μL aliquots of the thawed effector cells (Jurkat cells stably expressing V158 variant FcγRIIIa receptors) were added into the reaction plate and the plate was incubated for 6 h at 37 °C in a humidified CO2 incubator. Once the plate was removed from the incubator and brought to room temperature, 75 μL of the Bio-Glo Luciferase Assay Reagent was added into each well. The plate was incubated for 15 min then luminescence was measured using a GloMax Explorer plate reader (Promega). The plate reader's built-in ADCC data analysis method, in conjunction with GraphPad Prism, was used to graph and interpret the data.

2.2.7 Statistical Analysis

For the binding assays, EC/IC50 values were obtained using GraphPad Prism's non-linear regression analysis for [Antibody] vs response- variable slope (four parameters). The EC/IC50 values were compared across the different antibodies using ANOVA with a Tukey's test for multiple comparisons. For glycan analysis, the average amount of each glycan present was compared using ANOVA with a Tukey's test for multiple comparisons. A p value <0.05 was considered significant.

2.3 Results

2.3.1 Glycan Profiling

Prior to further assessing the *in vitro* efficacy of each mAb with regards to effector function, we sought to compare the types and relative amounts of glycans present in each antibody. Numerous groups have noted the significance and desirability of afucosylated and high mannose glycans for enhancing ADCC potency. Assembling a glycan profile of each mAb enables more meaningful conclusions to be drawn from subsequent Fc effector function assays. In order to thoroughly analyze the glycans present in each mAb, we employed both LC-MS/MS and LC-FLR methods.

2.3.1.1 Glycan Analysis by LC-MS/MS

The MS data in panels A and B of Figure 2.1 demonstrate the similarities and differences in the glycans identified for each mAb. In the panel A, it is clear that the three mAbs studied have similar glycans with higher abundances. For example, as expected for human IgG1, G0F is the most abundant glycan for all of the mAbs. G1F, G0F-GlcNAc, Man5 and Man6 are also relatively prominent across at least two if not all three of the mAbs studied. However, despite their similar trends, there are differences in the total abundance and total number of glycans for each mAb. Remicade[®] had the highest percentage of afuco-

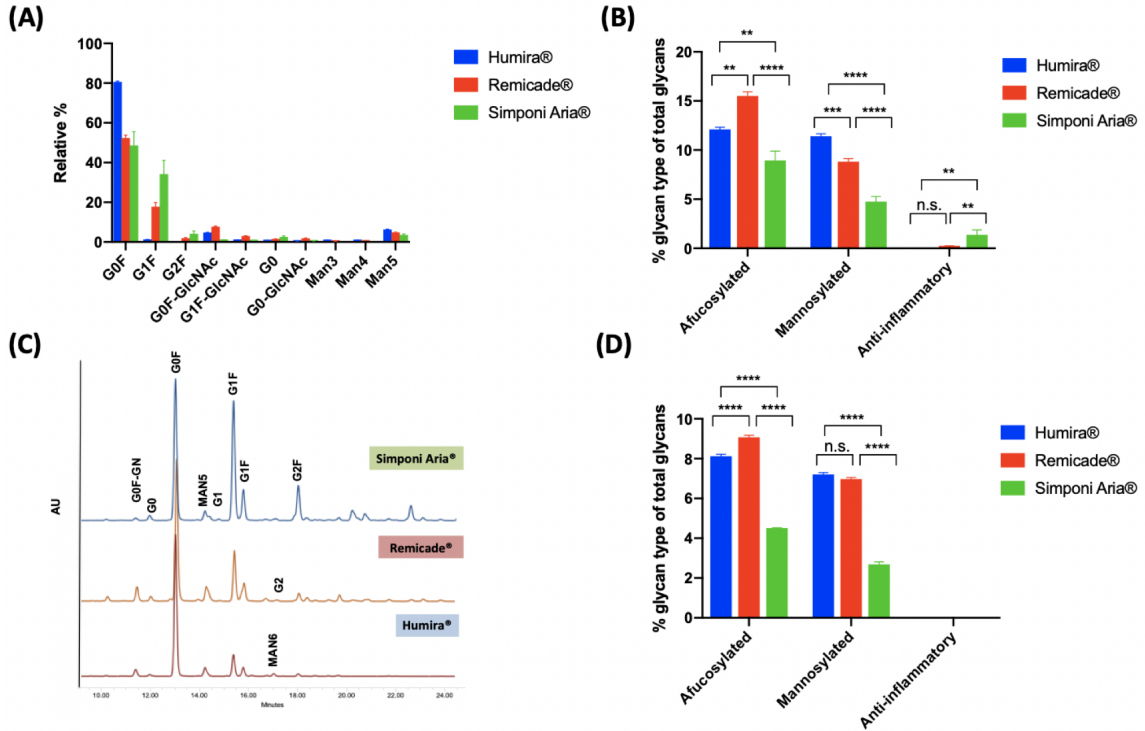


Figure 2.1: Glycan data collected for each mAb using two methods is presented for some of the most abundant glycans. (A) depicts the top 10 glycans identified for the mAbs by LC-MS/MS and (B) separates the LC-MS/MS detected glycans into their percent contribution based on glycan type. (C) Characteristic LC-FLR chromatograms for each mAb and (D) separates the LC-FLR detected glycans into their percent contribution based on glycan type. Error bars are SEM. ns: not significant, * $p < 0.05$, ** $p < 0.01$, *** $p < 0.001$, **** $p < 0.0001$.

sylated glycans, ($15.5 \pm 1.3\%$), but it also had the largest total number of unique glycans identified, 28. Humira® had the highest percentage of mannosylated glycans ($11.4 \pm 0.8\%$), which makes up most of the afucosylated glycans. Unlike Remicade®, Humira® only had 15 unique glycans. Simponi Aria® had 21 unique glycans identified, and very few of those were mannosylated and/or afucosylated (only $8.9 \pm 2.9\%$ were afucosylated). In looking at the broader picture of glycosylation profiles, Remicade® has the highest % afucosylated glycans, which is desirable since the presence of fucose on glycans causes steric hindrance and reduces Fc receptor binding and effector function. On the other hand, Humira®'s glycan profile has a lower number of unique glycans. It is important to note though that many of Humira's glycans are mannosylated and, as mentioned above, mannosylated glycans

have been linked to both enhanced ADCC and increased clearance rates of drugs *in vivo*.

2.3.1.2 Glycan Analysis by LC-FLR

The MS glycan trends were upheld in the LC-FLR experiments. As shown in panels C and D of Fig. 1, G0F and G1F were some of the most abundant glycans for the three mAbs studied. Man5, and Man6 in the case of Humira[®], were also large enough to be detected by the LC-FLR method. This correlates with their relatively high abundance detected by MS. We also noticed the same general patterns in % afucosylated and % mannosylated across the two methods. Remicade[®] had the highest relative % afucosylated glycans (9.1 ± 0.3), followed by Humira[®] (8.1 ± 0.3) then Simponi Aria[®] (4.5 ± 0.03). For % mannosylated, Remicade[®] and Humira[®] did not have a statistically significant difference, but the two were also close in the MS method. Despite differences in absolute values due to the varying numbers of total glycans identified by both methods, the FLR data matches the MS data well and corroborates the trends observed from the MS analysis.

2.3.2 TNF α Binding Affinity

The efficacy of anti-TNF α mAbs begins with binding to soluble or membrane-bound TNF α in order to eventually reduce pro-inflammatory signaling. In order to compare the binding affinities of Humira[®], Remicade[®], and Simponi Aria[®], we conducted an ELISA using 12 concentrations of each mAb to generate dose–response curves (Figure 2.2A). The TNF α ELISA data presented in Figure 2.2B shows that Humira[®] has the lowest average EC50 value, thus the highest soluble TNF α binding affinity, of the three drugs. Humira[®]'s EC50 value of 1.9 ± 0.1 pM is followed by Simponi Aria[®] (4.9 ± 0.2 pM) then Remicade[®] (6.4 ± 0.3 pM), with all of these differences being statistically significant (Figure 2.2B).

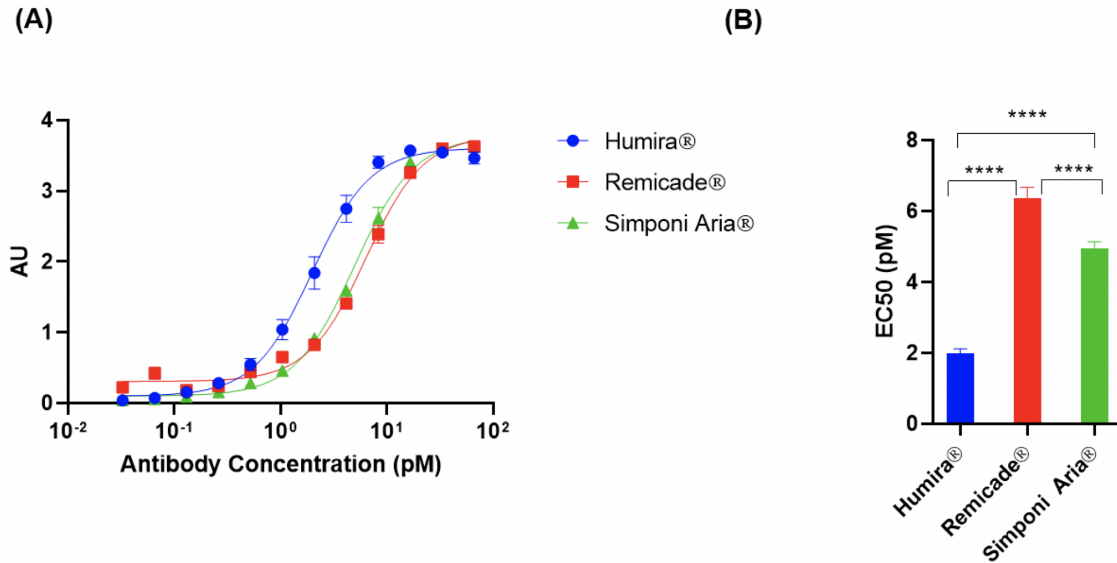


Figure 2.2: TNF α ELISA data for all three mAbs are shown as (A) an absorbance vs. mAb concentration curve and (B) EC $_{50}$ values derived from the ELISA curve in (A). Error bars are SEM. ****p < 0.0001.

2.3.3 Fc γ RIIIa binding

To further analyze the differences in glycosylation in the context of Fc effector function and efficacy, we compared the binding affinities of each mAb for Fc γ RIIIa (high affinity V variant) using AlphaLISA. Fc γ RIIIa is expressed on the surface of natural killer cells and its recognition of the Fc region of mAbs is highly dependent on the glycans present. Dose-response curves for each mAb are illustrated in Figure 2.3A, with a comparison of their respective IC $_{50}$ values provided in Figure 2.3B. Our results show that Humira $^{\text{®}}$ had the lowest average IC $_{50}$ value (10.6 ± 1.2 nM), thus the highest binding affinity to Fc γ RIIIa. Simponi Aria $^{\text{®}}$ had the next lowest average IC $_{50}$ value (35.4 ± 4.8 nM) followed by Remicade $^{\text{®}}$ (76.2 ± 6.6 nM) (Fig. 3). Based on these results, in conjunction with the TNF α ELISA results, Humira $^{\text{®}}$ is expected to trigger ADCC more readily than the other anti-TNF α mAbs.

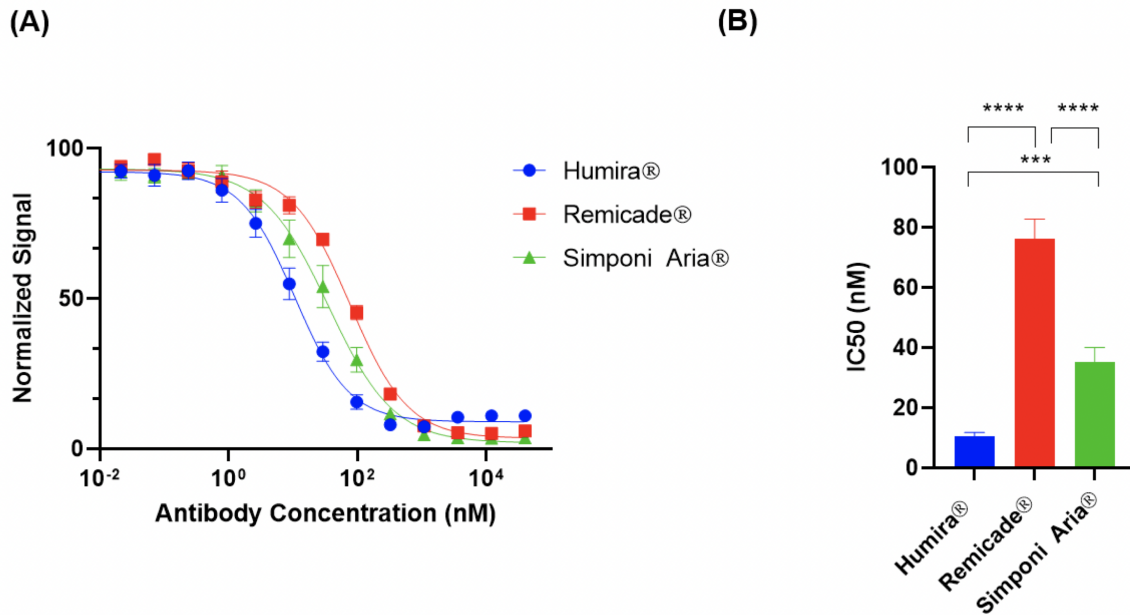


Figure 2.3: AlphaLISA V variant data for all three mAbs are shown as (A) a normalized luminescence signal vs. mAb concentration curve and; (B) IC₅₀ values derived from the AlphaLISA curve in (A). Error bars are SEM. ***p < 0.001, ****p < 0.0001.

2.3.4 Antibody-Dependent Cellular Cytotoxicity (ADCC)

In order to further understand how the differences observed thus far in terms TNF α and Fc γ RIIIa binding affect efficacy *in vitro*, we compared each mAb in an ADCC luciferase reporter assay (Figure 2.4). ADCC is dependent on both Fab binding and Fc binding. It requires Fab binding because the mAb must recognize and bind to TNF α on the membrane of target cells in the first stage of initiation. Then, once the antibody is bound to TNF α , the Fc portion of the mAb plays its role by binding to Fc γ R on effector cells. In the specific case of this reporter assay, the effector cells are engineered Jurkat cells, but *in vivo* they would be natural killer cells. Once the Fc γ R binding occurs, cell signaling leads to degranulation and, when *in vivo*, cell death of the target cell. Therefore, given our previous results that demonstrated Humira® had the highest affinity for TNF α and Fc γ RIIIa, it was expected that Humira® would perform the best in the ADCC assay. This prediction was supported by the results in the ADCC assay as Humira® had a statistically significant lower average EC₅₀ value compared to Remicade® and Simponi Aria®. Humira's average EC₅₀ was

measured as 0.55 ± 0.03 nM compared with Remicade[®] (0.64 ± 0.04 nM) and Simponi Aria[®] (0.67 ± 0.03 nM).

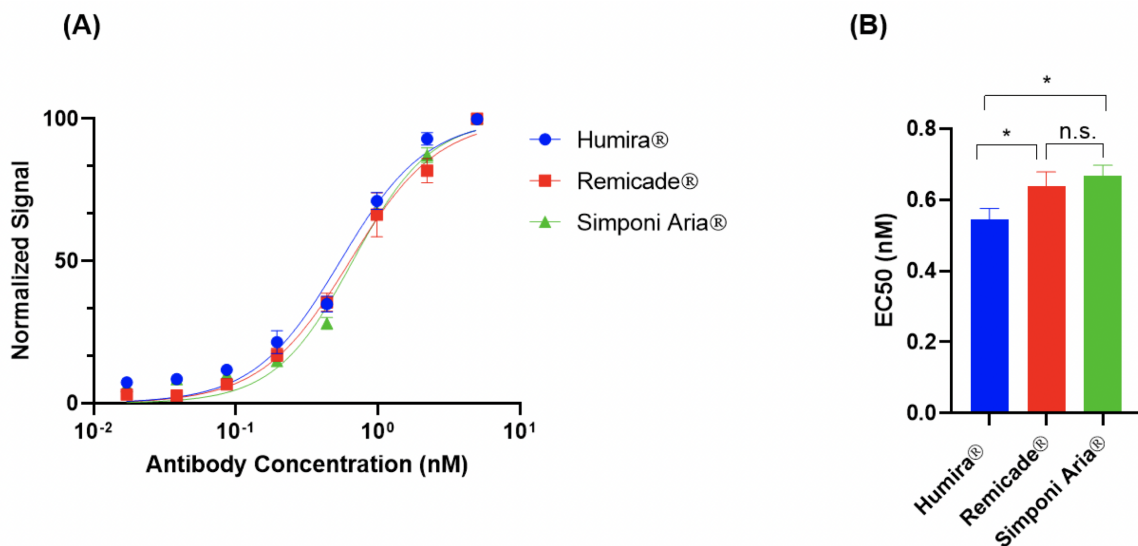


Figure 2.4: AlphaLISA V variant data for all three mAbs are shown as (A) a normalized luminescence signal vs. mAb concentration curve and; (B) IC₅₀ values derived from the AlphaLISA curve in (A). Error bars are SEM. ***p < 0.001, ****p < 0.0001.

2.4 Discussion

mAb products are notoriously challenging to produce and replicate due to their large size, structural complexity and reliance upon healthy cell cultures during manufacturing. Differences in sequences and folding patterns can influence how they bind to their targets of interest and elicit a therapeutic response. They also are subject to post-translational modifications, such as glycosylation, that can impact their safety and efficacy. Therefore, observing statistically significant binding and glycosylation differences between three anti-TNF α therapeutics is to be expected but intriguing, as it provides insight into why certain mAb treatments may elicit different patient responses.

Humira[®] yielded lower EC₅₀/IC₅₀ values than Remicade[®] and Simponi Aria[®] for the TNF α binding ELISA, Fc γ RIIIa binding AlphaLISA and ADCC bioassay. Simponi Aria[®] had lower EC₅₀/IC₅₀ values for the ELISA and AlphaLISA when compared with Remicade[®],

but the two had similar ADCC EC50 values. The exact reason for the similar ADCC EC50 values for Remicade[®] and Simponi Aria[®] despite statistically significant differences in binding to TNF α and Fc γ RIIIa, and % afucosylation levels, could be due to several reasons. The first is that the ELISA assay measured binding to immobilized soluble TNF α whereas the cellular ADCC depends on binding to membrane bound TNF α (mTNF α). In addition, differences in binding valency and dissociation time from mTNF α could result in differences in effector cell recruitment prior to adding the luciferase substrate.

A previous study conducted by Shealy et al. compared golimumab with infliximab and adalimumab in terms of their binding affinity to soluble and membrane-bound TNF α . [105] The surface plasmon resonance of (SPR) results from their experiments showed that immobilized golimumab had a higher binding affinity to soluble TNF α , as measured by dissociation equilibrium constants, (K_D =18 pM) compared to infliximab (44 pM) and adalimumab (127 pM). While the 2.4-fold difference between golimumab and infliximab was not statistically significant, the difference between golimumab and adalimumab was significant. It is also worth noting that they observed similar levels of cytotoxicity induced by all 3 mAbs upon binding to cells expressing mTNF α . While Shealy et al.'s data does not fully align with our data presented here, it is important to note that we used different methods for measuring antibody-antigen binding affinity. In the ELISA, TNF α was passively adsorbed on a plate and incubated with antibody for an hour, whereas the SPR protocol used by Shealy et al. immobilized the antibody and flowed TNF α over the coated chip over the course of minutes. Given this, it is possible for higher avidity antibody-antigen complexes to form during the ELISA and less likely with the antibody immobilized in SPR, which could impact the measured IC50 values.

Separate studies conducted by Kaymakcalan et al. and Arora et al. also compared TNF α binding and effector functions for adalimumab and infliximab. [90, 106] Kaymakcalan et al. observed similar binding affinities to soluble TNF α for adalimumab and infliximab by SPR (K_d of 3.04x10⁻¹¹M and 2.73x10⁻¹¹M, respectively). In addition, the authors observed

similar binding affinities to cells expressing mTNF α using radiolabeled mAbs (binding affinities of 0.48 nM and 0.47 nM for adalimumab and infliximab, respectively). The results from the experiments conducted by Arora et al. also highlighted comparable performances in ADCC, TNF α binding, and Fc γ R binding for adalimumab and infliximab. While we report here slight significant differences in TNF α binding, Fc γ R binding and ADCC between adalimumab and infliximab, we recognize that there are limitations in trying to make direct comparisons between results obtained via endpoint (ELISA, AlphaLISA) and kinetic (SPR) techniques.

In general, we conducted established and accessible functional assays on the three anti-TNF α mAbs, with our experiments having the additional focus on glycosylation differences between antibodies. We emphasized glycosylation in an effort to elucidate possible reasons behind differences observed for effector function. Any differences between our binding affinity results for these three drugs compared to other groups could stem from differences (i.e. sensitivity, reproducibility) in the exact assays used to quantify the interactions with TNF α and Fc γ RIIIa. This does not discount our data but rather showcases the variability between methods and highlights the importance of future method standardization. Since we have conducted only a handful of analytical methods, we recognize that our data might not be comprehensive/predictive of the data resulting from all other orthogonal methods. Another potential contributing factor is lot-to-lot variability for the individual mAbs studied, which is why we included three lots of each drug in our study compared to just one lot studied by previous groups.

Nevertheless, the binding affinities determined in our experiments, in conjunction with the total fewer number of glycans identified for Humira[®] compared to Simponi Aria[®] and Remicade[®], leads one to believe that Humira[®] may have higher efficacy *in vivo*. Theoretically, the better Fab binding of TNF α translates to more TNF neutralization and inflammation reduction, which is the drug's primary mechanism of action. Similarly, the better Fc γ RIIIa binding indicates that there is a greater potential for the drug to recruit

and activate effector cells to lyse mTNF α -expressing cells. While this could be construed as a compelling argument, it is important to note that there are other variables to consider when trying to predict *in vivo* drug performance.

For example, each patient is unique in their presentation of an autoimmune condition and needs to be treated on a case-by-case basis. There are genetic factors such as human leukocyte antigen (HLA) type, that can influence how therapeutics are taken up by antigen presenting cells and subsequently recognized by the immune system. This can increase the number of anti-drug antibodies present, leading to further immunogenicity, safety and efficacy concerns. [107–109] In addition, genetic polymorphisms in patient's FC γ RIIIa gene to contain valine or phenylalanine as residue 158 may contribute to the individual patient Fc γ RIIIa binding and response to treatment. [1] This is why there are patient specific differences in response to individual anti-TNF α product treatment, clearance of the drug and/or levels of anti-drug antibodies neutralizing its function.

2.5 Conclusion

Our results showed that Humira[®] had the highest soluble TNF α binding affinity, as measured by ELISA, the highest Fc γ RIIIa binding, as measured by AlphaLISA, and the greatest effector function, as measured by an ADCC bioassay. It also had the fewest number of total glycans identified by LC-MS/MS. Remicade[®], on the other hand, had the lowest soluble TNF α and Fc γ RIIIa binding affinity, highest number of identified glycans and lower effector functionality than Humira[®]. While we tested multiple lots of each drug to increase our statistical power for these methods, we are unable to state that one therapeutic is more efficacious and/or safe than the others based on *in vitro* data alone. We would need to confirm *in vitro* results with extensive clinical data before making such claims. The higher binding affinities and glycosylation profile of Humira[®] could feed into its market success, but likely other factors outside of our research scope (i.e. marketing, at-home administration, patient support, etc.) play an even larger role in its success. After all, all three drugs

are broadly prescribed, showcasing the fact that one is not the optimal “standard of care”. Rather, the unique nature of each drug product gives it both advantages and disadvantages when administered to certain individuals and/or patient populations. Nevertheless, by analyzing three different mAbs in one laboratory and under one set of conditions we observed significant differences in the drugs’ *in vitro* functionality and post translational modifications. Thus, we believe that these findings are worth sharing with the pharmaceutical and healthcare community at large. We hope that the work presented here sparks further comparisons of these mAbs and other biologics in a controlled manner, increasing our field’s knowledge of significant drug differences and potential safety/efficacy considerations to assess during biologic development and administration.

CHAPTER III

Disulfide Shuffling Analysis in mAb Innovators and Biosimilars

This chapter describes our study on disulfide bond shuffling within IgG1 innovator (originator) and biosimilar mAbs. We monitored disulfide shuffling over a incubation period via digestion and mass spectrometry techniques. We also measured changes in degradation patterns in addition changes in disulfide bond shuffling when protein were exposed to stressed conditions. In doing so, we aimed to compare two IgG1 mAbs with each other and with their biosimilar. This chapter is based on work published in *Frontiers in Bioengineering and Biotechnology*. [110]

3.1 Introduction

Mass spectrometry has gained traction among the biologics community for its ability to identify a myriad of protein modifications. Being able to identify, locate and quantify protein modifications is paramount when developing new biologics and biosimilars. After all, certain modifications can be indicators of protein degradation, immunogenicity, improper manufacturing conditions, etc. N and O-linked glycosylation is one example of a post translational modification (PTM) that has been well-studied in recent years. The presence of specific glycans can affect protein therapeutics' potency by conferring sta-

bility, controlling conformation, altering target binding, and increasing clearance rate. [3, 111–116] Aside from glycans, there are other noteworthy PTMs that influence protein activity and safety, including deamidation at asparagine and glutamine residues, oxidation at methionine and tryptophan residues, and disulfide bond shuffling. [117] Disulfide bond shuffling in IgG1 therapeutics, namely bevacizumab and rituximab, is the main focus of this research as, upon our literature search, we discovered a limited number of publications studying this topic.

In IgG1s there are normally 16 disulfide bonds: 4 interchain and 12 intrachain (Figure 3.1). These bonds are critical in maintaining proper protein folding and stability. Interchain bonds are more susceptible to reduction and, therefore, are more susceptible to an incomplete formation of bonds and shuffling than intrachain bonds. [71, 114, 118–123] For example, the larger number and hinge region arrangement of disulfide bonds in IgG2 increases its potential for covalent dimerization, which leads to an increased binding avidity. [72, 121] Similarly, antibody-drug conjugates (ADCs) that are conjugated via thiol-maleimide chemistry are dependent upon the partial reduction of disulfide bonds. These bonds are then able to participate in forming the connection between the antibody and the drug. [124] The success of ADCs in treating diseases such as cancer is evidenced by the fact that 10 ADCs are FDA approved and over 80 others are in clinical trials. [125]

Then again, sometimes unconventional disulfide bond formation can be detrimental. Normally, cysteines pair with their correct partner residue, but occasionally a cysteine or “free thiol” will bond with a second cysteine in an unexpected way. This unexpected, incorrect bonding of cysteines is referred to as disulfide bond shuffling or scrambling. Usually disulfide bond shuffling occurs as a protein is exposed to stressors such as heat, oxygen radicals, high pH and agitation. [72, 126–128] Disulfide bond shuffling can negatively impact a therapeutic protein’s safety and functionality by increasing its aggregation and degradation, modifying its folding, and/or reducing its target binding. [6, 121, 126] In addition to disulfide bond shuffling, a rare modification called a trisulfide bond can oc-

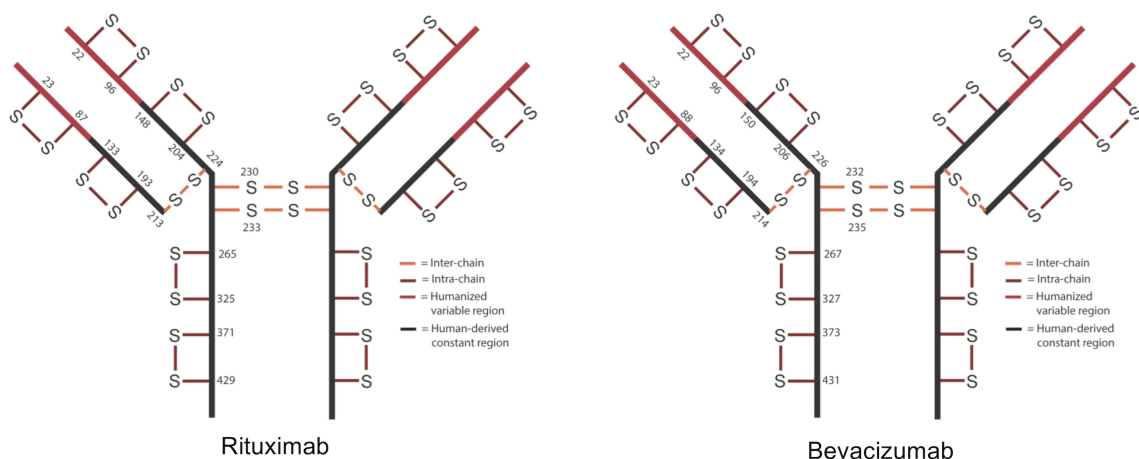


Figure 3.1: Schematic of expected disulfide bond locations for rituximab and bevacizumab. Fc region is shown in black and Fv region is shown in red. 12 intrachain (red) and 4 inter-chain (orange) bonds are typical for IgG1.

cur in IgGs. A trisulfide bond is described as the insertion of a third sulfur between the cysteines of a disulfide bond. While trisulfide bonds have not yet been shown to affect a protein’s safety and functionality, they are indicators of unhealthy cell cultures being used during protein production. [74, 75]

Disulfide bonds are clearly important contributors to the proper functioning of a therapeutic IgG1. When they are shuffled, they can have detrimental effects on the protein’s stability and, therefore, potentially its safety and potency as well. Due to this, disulfide bonds are considered to be a subset of a “cysteine form” critical quality attribute (CQA) for biologics. Free thiols, unexpected linkages and modifications such as trisulfides are embedded within this CQA. [129] The designation of disulfide bonds as CQAs is recognized by regulatory bodies including the FDA, EMA and ICH. [29, 130–132] Additionally, an ICH guidance states that scrambled/exchanged disulfide bonds are a common protein degradation mechanism. [131]

It is especially important to quantify disulfide bonds during biosimilar characterization as regulators note that disulfide bonds affect the protein’s physicochemical properties and can influence the efficacy of the product. In a comparison between Humira® and a

biosimilar, disulfide linkages were listed as CQAs and the authors remarked that mismatched disulfide linkages could impact the conformation and function of the drug. [133] Others have conducted similar studies on disulfide bond comparisons across biosimilar and originator biologics to monitor and control changes in disulfide bond number and position. Again, these studies were completed because incorrect disulfide bond linkages can negatively affect the activity, potency, immunogenicity and overall “similarity” of biosimilars. [134–136]

However, despite all of the possible negative side effects of shuffled disulfide bonds, there are more publications on the issue for IgG2 and IgG4 as compared to IgG1. It is likely that there are more publications for IgG2 and IgG4 because disulfide bond shuffling occurs more frequently in them and can sometimes be beneficial to the proper functioning of these proteins. Likewise, disulfide bond shuffling is also frequently discussed with regards to proteins derived from *E.coli* cells because *E.coli* lack an endoplasmic reticulum. For proteins produced in mammalian cell lines, such as the CHO cell lines used to produce rituximab and bevacizumab, the endoplasmic reticulum acts a center for disulfide bond modulation, checking for the proper formation of bonds. [6, 137] Nevertheless, IgG1 therapeutics are not fully immune to disulfide bond shuffling.

Sung et al. (2016) have studied disulfide bond shuffling in bevacizumab under different pH and enzymatic conditions. [126] While this research is useful in determining preferential protein digestion conditions to minimize disulfide shuffling, it does not discuss in great detail how the process of identifying disulfide bonds can be optimized. Similarly, Nie et al. (2022) analyzed two IgG1 proteins to suggest sample preparation improvements to minimize the number of the disulfide bond artifacts. [122] Again, this group focused on sample preparation conditions rather than disulfide bond identification and quantification methods. Dong et al. (2021) studied disulfide bond shuffling in the NIST monoclonal antibody, focusing on generating a mass spectral library of disulfide linkages for the monoclonal antibody rather than discussing method optimization. [128] Mass spectrometry

instrumentation companies such as Waters and Shimadzu have also characterized disulfide bonds on biosimilar and originator IgG1 therapeutics to showcase how they can detect any product/batch variability on their latest platforms. [134, 136] None of these reports emphasized optimizing a disulfide bond identification and quantitation method, especially for shuffled bonds, for multiple IgG1s. Nor did any group measure the effects that normal vs. prolonged stressed conditions had on disulfide bond shuffling and subsequent IgG1 biosimilar and originator degradation.

To address this lack of knowledge, we have designed a semiautomated, streamlined method for characterizing disulfide bonds on two IgG1s, rituximab and bevacizumab, using an Agilent AssayMAP Bravo liquid handling platform and LC-MS/MS. Performing this method, in conjunction with typical degradation analytical techniques (SEC and SDS-PAGE), allowed us to increase our knowledge of how these two proteins are modified and degraded overtime. This gave us insights into antibody variability as antibodies can act differently, especially when exposed to undesirable conditions. [138–140] Additionally, we compared originator and biosimilars versions of the drugs to determine their batch comparability and biosimilarity levels when exposed to various periods of stress. Previous research in our lab and in other labs have shown structural and functional differences between originators and biosimilars after forced degradation, so we were curious as to how our treatment conditions may impact the overall degradation and disulfide shuffling profiles of the rituximab and bevacizumab originators and biosimilars studied here. [2, 141–143]

In sum, our analytical methodology provided us with a way to preliminarily test our hypothesis that as proteins unfold during degradation, exposing buried cysteine residues, they increase their likelihood to form shuffled disulfide bonds. Although we recognize that degradation and disulfide shuffling are not directly proportional, completing these studies helps justify future research and innovation in this space.

3.2 Materials and Methods

3.2.1 mAb Sample Information

The following originator drugs were purchased and stored at 4°C until analysis: Avastin[®] (Genentech) and Rituxan[®] (Genentech). The following biosimilar drugs were purchased and stored at 4°C until analysis: Acellbia[®] (Biocad) and Avegra[®] (Biocad). The two rituximabs (Rituxan[®] and Acellbia[®]) are referred to as Rit throughout the manuscript. The two bevacizumabs (Avastin[®] and Avegra[®]) are referred to as Bev throughout the manuscript. Originators are referred to as OR and biosimilars are referred to as BS.

3.2.2 Digestion Reagents

Digestion reagents, including AccuMAP denaturing solution, 10x low pH AccuMAP reaction buffer, N-ethylmaleimide (NEM), Trypsin Platinum and AccuMAP low pH resistant rLys-C were acquired from Promega Corporation. Sample plates for the digestion reaction were purchased through Agilent.

3.2.3 Incubation of Proteins

Rituximab lots were aliquoted in 50 µl increments into 0.5 ml Eppendorf tubes. Bevacizumab lots were diluted from 25 mg/ml down to 10 mg/ml with water to match the aliquot concentration of rituximab. Bevacizumab samples at 10 mg/ml were aliquoted in 50 µl increments into 0.5 ml Eppendorf tubes. For each timepoint (0, 2 and 4 weeks), there were three aliquots per lot of each mAb. Tubes were placed on an orbital shaker at 240 RPM, incubating at 37°C for up to 4 weeks. 0-week samples were instead left at 4°C and 2-week samples, upon removal from the incubator, were moved to 4°C until the 4-week samples were finished incubating.

3.2.4 Protein Digestion and Data Analysis

3.2.4.1 Sample Preparation on AssayMAP Bravo

3 μ l of 10 mg/ml antibody samples (0, 2, 4-week; N = 3 per sample type) were added into a 96 well Eppendorf PCR plate and placed on the Agilent AssayMAP Bravo liquid handling platform (referred to herein as the “robot”). A single solution containing Promega’s AccuMAP Denaturing Solution, 10x low pH AccuMAP reaction buffer and 200 mM NEM were added in 32 μ l aliquots into a 96 well Eppendorf PCR plate and placed on the robot. The addition of 17 μ l of this solution into the protein plate, followed by a 30-minute incubation at 37° C, yielded denatured mAbs with blocked free cysteines. Also on the robot were two other plates, one containing an AccuMAP low pH resistant rLys-C pre-digest and a second containing a digestion solution comprised of 10x low pH reaction buffer, AccuMAP low pH resistant rLys-C, Trypsin Platinum and water. The robot added 35 μ l of the pre-digest to the sample plate, incubated for 2.5 h at 37°C, then added 81 μ l of digestion solution. Then samples were left at 37°C overnight. The pH for the digestion reaction was 5.4. The next day samples were acidified with 20% TFA and prepared for lyophilization prior to reconstitution and MS injection.

3.2.4.2 LC-MS/MS

The samples were analyzed using an Acquity LC (Waters) interfaced to an Orbitrap Fusion Lumos mass spectrometer (ThermoFisher). The sample peptides were loaded onto a 75 μ m analytical trapping column packed with Luna C18 resin (Phenomenex) then eluted at a flow rate of 350 nl/min. For the LC, a 30-minute reverse phase gradient was used. For the MS, a data dependent HCD mode was used with MS at a 60,000 FWHM resolution and MS/MS at a 15,000 FWHM resolution. 3 s cycles were used throughout the duration of the MS and MS/MS run time.

3.2.4.3 LC-MS/MS Data Processing

Data was processed using the Byos disulfide bond workflow (Protein Metrics, Inc.), accounting for trypsin and Lys-C cleavage. Sequences were searched against existing library data derived from the FASTA file of each protein. The designation of disulfide bond type (i.e. expected vs. shuffled) was based on FASTA protein sequences. By using the FASTA protein sequence and existing databases, the software was able to match the bonds detected from our samples with known, expected disulfide bonds. Label free quantitation was used to create an extracted ion chromatogram (XIC) from the summation of the MS1 isotope area(s) over an elution time range for the peptides resulting after digestion. The XIC is then integrated to determine area under the curve, and this integrated value is compared with other peptides to report the relative abundances of the peptide. The label free quantitation method we used in reporting our data was a single isotope mechanism. This means that the integrated XICs are representative of the monoisotopic, or most intense isotope, peak detected for a peptide. These monoisotope peaks can be compared with the unmodified peptides of the same protein to identify modifications (i.e., disulfide bonds) on the peptide.

For shuffled disulfide bonds, we reported the disulfide bond data as the XIC sum contribution of all shuffled disulfide bonds relative to the total XIC sum of all (shuffled and expected) detected disulfide bonds. For the trisulfide bonds, we repeated the same process looking at the total XIC sum of all trisulfides bonds compared to the XIC sum of all detected disulfide bonds. When analyzing the frequency of specific disulfide bond locations, we normalized the number of times that each bond type was measured relative to the total number of disulfide bonds. All data was analyzed for statistical significance using a 2-way ANOVA, * $p < 0.05$, ** $p < 0.01$, *** $p < 0.001$, **** $p < 0.0001$. Each sample was run in triplicate and results were reported as averages \pm standard deviation.

3.2.5 Protein Degradation Analysis

3.2.5.1 SEC

All samples were diluted down to 1.5 mg/ml with water. 10 μ l of 1.5 mg/ml mAb samples were injected onto the column (Acquity UPLC BEH 450 SEC 2.5 μ m, 4.6 \times 150 mm, Waters) attached to an Acquity UPLC (Waters) and run for 10 min at a flow rate of 0.4 ml/min. The column was maintained at room temperature. The mobile phase used for the isocratic method was 1x phosphate buffered saline, pH 7.4 (Gibco, Fisher Scientific). Antibodies were detected at dual wavelengths of 214 and 280 nm. Data was reported as average % contribution of each peak type (monomer, aggregate and fragment) \pm standard deviation. For the aggregate and fragment peaks, our average % contribution data accounted for the summation of areas of all fragment and aggregate peaks, when applicable. % contribution values were based off of the entire area under the curve reported for each sample type. Samples were run in triplicate. A 2-way ANOVA (* $p < 0.05$, ** $p < 0.01$, *** $p < 0.001$, **** $p < 0.0001$) was conducted to compare the statistical significance of BS and OR results for the same protein at the same timepoint.

3.2.5.2 SDS-PAGE

Representative samples from each antibody at each timepoint (0, 2, and 4 weeks) were run on an Invitrogen NuPAGE 3%–8% Tris-Acetate Gel. Protein samples were diluted from 10 mg/ml down to 0.33 mg/ml with water. To each of the 0.33 mg/ml samples, 5 μ l of loading buffer (NuPAGE LDS Sample Buffer 4X, Invitrogen) were added, yielding 1:3 sample:loading buffer, with a final antibody concentration of 0.25 mg/ml. 10 μ l of the 0.25 mg/ml antibodies were added into individual wells. 15 μ l of the ladder (HiMark™ pre-stained protein standard, Invitrogen) were added into well 1. The gel was run under the following conditions: 150 V, 50 mA, 5 W for 1 h on a PowerEase500 electrophoresis system (Invitrogen). Upon completion of the run, the gel was washed 3 times with water, shak-

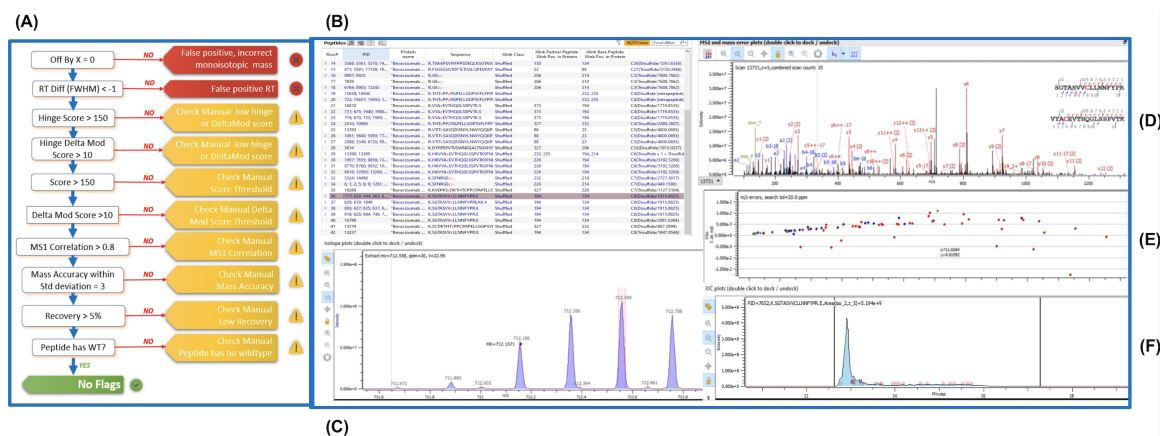


Figure 3.2: (A) Schematic of the Byos disulfide bond workflow. (B) Highlighted bevacizumab shuffled disulfide bond used for representation of LC-MS/MS data plots. Generated data depicted as a (C) MS1 plot; (D) MSMS plot; (E) Mass error plot; and (F) XIC intensity plot.

ing each time for 5 min. Then the gel was washed with SimplyBlue SafeStain (Invitrogen) for 1 h with shaking and with water for 1 h with shaking. The gel was imaged using a FluorChem M Imaging System (Protein Simple).

3.3 Results

3.3.1 Disulfide Bond Quantification and Qualification by LC-MS/MS

To assess the extent and location of disulfide bond shuffling in our monoclonal antibodies, we completed a non-reduced protein digestion using a modified version of the robot's in-solution digestion protocol. After identifying the measured bond locations via LC-MS/MS, we used Protein Metrics' Byos software to designate whether each bond was an expected or shuffled disulfide bond (Figure ??).

Aside from designating bond type, the Byos disulfide bond workflow flags samples that need to be checked manually due to concerns over threshold, recovery and/or scores (Figure 3.2A). We confirmed that the samples marked as true positives and false positives were indeed properly labeled or changed them to true or false positives based on our manual analysis. We did so by monitoring the MS1 isotope plots, looking for the characteristic

isotopic distribution for peptides, and matching it to the charge state (Figure ??C). We also confirmed that the MS1 plots were created by using both the most abundant isotopic peak (apex identified within the pink bar across the isotope on the isotope plot panel, Figure 3.2C) and the MSMS scan location in relation to the retention time (shown in the blue XIC intensity plot, Figure 3.2F). Users can select whether an isotope or an averagine calculation is applied for the label-free quantitation of samples. As described in the methods section, we used a single isotope mechanism. If we had chosen the averagine calculation, we would have extrapolated the monoisotopic peak via the averagine distribution, yielding a theoretical monoisotope. [144] Finally, we assessed the MSMS and mass error plots (Figures 3.2D,E) and ensured that we were seeing good fragmentation and ion coverage. If samples did not meet these criteria, they were marked as false positive and were not included in our disulfide bond analysis.

From our LC-MS/MS data we determined that the unstressed, 0-week bevacizumab samples trended towards higher shuffled disulfide bond levels initially when compared with rituximab samples. This held true for both the originator and biosimilar samples. As depicted in Figure 3.3A,C, we observed that over the course of 4 weeks under stressed conditions, both rituximab sample types had minor, possibly artificial increases in their average relative percent contribution of shuffled disulfide bonds: $0.24 \pm 0.21\%$ to $0.51 \pm 0.11\%$ for the originator and $0.27 \pm 0.07\%$ to $0.35 \pm 0.08\%$ for the biosimilar. The bevacizumab originator sample had a more pronounced increase in the average relative percent contribution of shuffled bonds, from $0.58 \pm 0.08\%$ to $1.46 \pm 1.10\%$ after the 4-week incubation. The bevacizumab biosimilar samples saw a marginal increase, potentially due to analytical variability, between the 2-week ($1.10 \pm 0.50\%$) and 4-week samples ($1.25 \pm 0.20\%$). According to our results, the bevacizumab biosimilar 0-week samples had the highest level of shuffled bonds ($1.62 \pm 0.78\%$) which is unexpected given other trends, but this can be explained by analytical variability at such low levels as well as the relatively small sample size ($n = 3$). None of the four sample types had any statistical significance

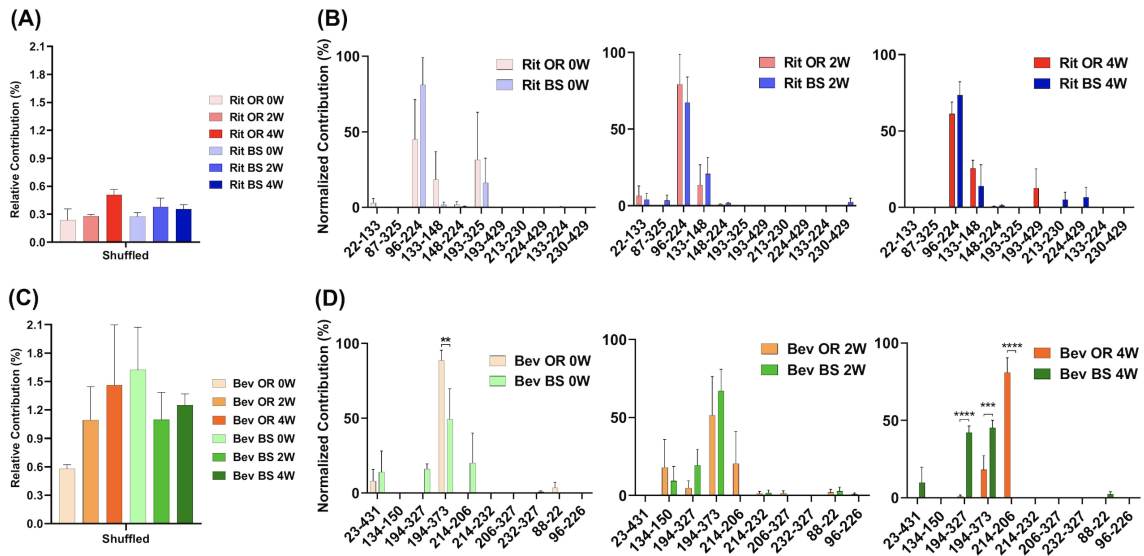


Figure 3.3: (A) Schematic of the Byos disulfide bond workflow. (B) Highlighted bevacizumab shuffled disulfide bond used for representation of LC-MS/MS data plots. Generated data depicted as a (C) MS1 plot; (D) MSMS plot; (E) Mass error plot; and (F) XIC intensity plot.

in the relative percent contribution of shuffled disulfide bonds measured across all of the timepoints. This suggests that there are not any significant increases in the number of shuffled disulfide bonds over time. However, since minimal disulfide bond shuffling is expected when samples are treated at pH 7 or below [126, 128], as ours were, seeing these general upwards trends in shuffling supports our hypothesis that disulfide shuffling occurs more frequently as a protein is exposed to stress and begins degrading.

In addition to monitoring the relative contribution of the shuffled disulfide bonds, we also monitored the location of the shuffled bonds to see whether they would change over time (Figure 3.3B). We studied this to see how protein residue exposure and unfolding may differ after varying incubation times. We also were curious as to whether the most prominent shuffled disulfide bond locations would be intrachain or interchain. As mentioned in the introduction, interchain bonds are more susceptible to reduction, incomplete formation and, therefore, shuffling than intrachain bonds. For rituximab originator and biosimilar, the shuffled bond at position Cys96-Cys224 was the most prominent across all

of the timepoints. Position 224 is normally involved in an interchain bond, which may be why it was participating in the most prominent shuffled bond. Cys133-Cys148 was also relatively prominent in across all timepoints, but more so in the incubated samples. Cys193-Cys325 had a higher abundance for the unstressed sample. These bonds are all normally involved intrachain binding. There was no statistically significant difference in the bond locations for the originator vs. biosimilar.

A similar story played out for bevacizumab. Its most prominent shuffled bond location was at Cys194-Cys373 for all samples except bevacizumab originator at 4-weeks, whose most prominent location was Cys214-Cys206. Cys194, Cys373 and Cys206 are typically involved in intrachain bonds but Cys214 is typically involved in an interchain bond. Other common shuffled bond locations included Cys194-Cys327 (intrachain) and Cys214-Cys206. Unlike rituximab, there were some significant differences in the bond locations between the originator and biosimilar. For the 4-week samples, Cys214-Cys206 (80.97 ± 16.49) became the most prominent disulfide bond location for the originator while Cys194-Cys327 (42.20 ± 7.26) and Cys194-Cys373 (45.39 ± 8.10) were nearly equal in their contribution for the biosimilar (Figure 3.3D). It should be noted that given constraints in our current technology, we were unable to determine whether these disulfide bonds were inter- or intra- antibody.

3.3.2 Detection of Trisulfide Formation by LC-MS/MS

We were also curious about the number of trisulfide bonds present in the samples. By using the disulfide workflow in the Byos software and manually checking the outputs, we were able to identify 5 unique trisulfides in the bevacizumab originator samples and 8 unique trisulfides in the bevacizumab biosimilar samples. The initial average levels of trisulfides, based on XIC values for trisulfides bonds compared to all detected disulfide bonds, were $0.07 \pm 0.70\%$ for the originator and $0.19 \pm 0.14\%$ for the biosimilar. This level is low but is still worth mentioning because it was significantly greater than rituximab,

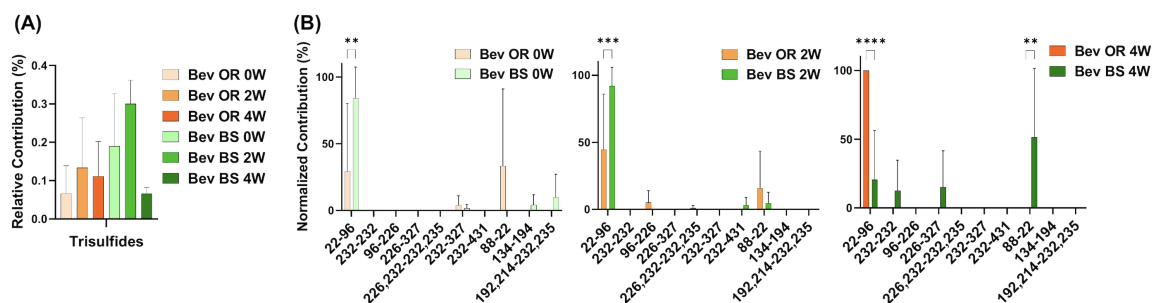


Figure 3.4: Trisulfide bonds detected for bevacizumab samples by LC-MS/MS. (A) Total trisulfide bond contribution relative to the XIC sum of all identified disulfide bonds for bevacizumab OR (0 week—peach, 2 weeks—orange, 4 weeks—red orange) and BS (0 week—teal, 2 weeks—green, 4 weeks—dark green). (B) Prevalence of the shuffled bond locations normalized to the total number of shuffled bonds for bevacizumab OR (0 week—peach, 2 weeks—orange, 4 weeks—red orange) and BS (0 week—teal, 2 weeks—green, 4 weeks—dark green) ($N = 3$, mean \pm SD, 2-way ANOVA, * $p < 0.05$, ** $p < 0.01$, *** $p < 0.001$, **** $p < 0.0001$).

which had no detectable trisulfides. These were most commonly found at position Cys22-Cys96 in the variable region of the antibody, which is an expected disulfide bond location (Figure 3.4B).

3.3.3 Protein Degradation Measurement by SEC

Since our research hypothesis hinges on the fact that stressed proteins degrade and, in doing so, increase their propensity for disulfide bond shuffling, we wanted to verify that we were indeed seeing protein degradation via more traditional chromatography methods. To track protein degradation over time, we measured the changes in percent aggregates, fragments and monomer for each sample type by size exclusion chromatography (Figure 3.5; Table 3.1). In this study we observed a small increase in aggregates from 0 to 4 weeks for the rituximabs: $0.76 \pm 0.02\%$ to $1.37 \pm 0.08\%$ for the originator and $2.11 \pm 0.05\%$ to $2.41 \pm 0.11\%$ for the biosimilar. We also measured more fragments than aggregates initially in rituximab, with fragment formation in the rituximab samples slightly increasing over time. The originator fragment contribution increased from $6.76 \pm 0.24\%$ (0 weeks) to $7.61 \pm 0.24\%$ (4 weeks) and the biosimilar fragment contribution increased from $7.09 \pm$

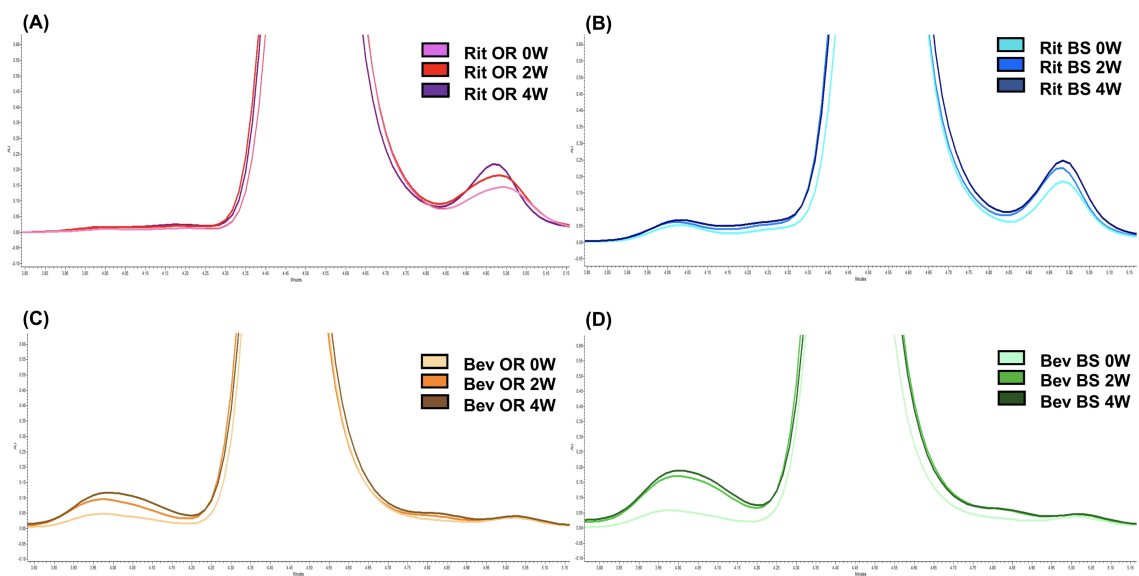


Figure 3.5: Representative SEC chromatograms at 214 nm for 15 µg of antibody. (A) Rituximab OR at 0 (pink), 2 (red) and 4 (purple) weeks; (B) Rituximab BS at 0 (light blue), 2 (blue) and 4 (navy) weeks; (C) Bevacizumab OR at 0 (peach), 2 (orange), and 4 (brown) weeks; (D) Bevacizumab BS at 0 (teal), 2 (green) and 4 (dark green) weeks. Stressed samples were shaking at 240 RPM, incubating at 37°C for 2 or 4 weeks. Chromatograms are zoomed in to depict the increase in aggregates and/or fragments detected in each sample across each timepoint.

0.05% (0 weeks) to $8.02 \pm 0.38\%$ (4 weeks). Conversely, we observed that the bevacizumab samples had more degradation in the form of aggregates. From 0 to 4 weeks the relative contribution of aggregates for the bevacizumab originator increased from $2.91 \pm 0.39\%$ (0 weeks) to $7.09 \pm 0.37\%$ (4 weeks) and for the biosimilar, $3.30 \pm 0.06\%$ (0 weeks) to $10.60 \pm 0.52\%$ (4 weeks). There were fragments present in the bevacizumab samples, but those stayed relatively steady over time. The originator fragment contribution was $1.76 \pm 0.06\%$ at 0 weeks and $1.78 \pm 0.01\%$ at 4 weeks. The biosimilar fragment contribution was $1.91 \pm 0.07\%$ at 0 weeks and $1.75 \pm 0.01\%$ at 4 weeks.

We noticed that there was a greater decrease in the percent monomer for bevacizumab compared to rituximab (Table 3.1). The percent monomer for the rituximab originator changed from $92.48 \pm 0.26\%$ to $91.03 \pm 0.26\%$ and the biosimilar changed from $90.79\% \pm 0.01$ to $89.57 \pm 0.50\%$ over the course of 4 weeks. The percent monomer for the bevacizumab originator changed from $95.34 \pm 0.33\%$ to $91.14 \pm 0.38\%$ and the biosimilar changed from

Table 3.1: SEC data depicted as average % concentration contributions of monomer, aggregate, fragment peaks (N = 3, mean \pm SD). Aggregates and fragments include summations of multiple peaks, where applicable. Stressed samples were shaking at 240 RPM, incubating at 37°C for 2 or 4 weeks. All samples were diluted to 1.5 mg/ml to load 15 μ g of antibody on the column. N = 3, mean \pm SD, 2-way ANOVA, *p < 0.05, **p < 0.01, ***p < 0.001, ****p < 0.0001. *Denotes statistical significance of BS, compared to OR, at same timepoint for the same protein type.

	% Monomer	% Aggregates	% Fragments
Rit OR 0w	92.48 \pm 0.26	0.76 \pm 0.02	6.76 \pm 0.24
Rit OR 2w	91.15 \pm 1.33	1.37 \pm 0.61	7.49 \pm 0.72
Rit OR 4w	91.03 \pm 0.26	1.37 \pm 0.08	7.61 \pm 0.24
Rit BS 0w	90.79 \pm 0.01	2.11 \pm 0.05**	7.09 \pm 0.05
Rit BS 2w	90.51 \pm 0.63	1.89 \pm 0.58	7.60 \pm 0.40
Rit BS 4w	89.57 \pm 0.50	2.41 \pm 0.11*	8.02 \pm 0.38
Bev OR 0w	95.34 \pm 0.33	2.91 \pm 0.39	1.76 \pm 0.06
Bev OR 2w	92.43 \pm 0.64	5.85 \pm 0.78	1.71 \pm 0.13
Bev OR 4w	91.14 \pm 0.38	7.09 \pm 0.37	1.78 \pm 0.01
Bev BS 0w	94.78 \pm 0.02	3.30 \pm 0.06	1.91 \pm 0.07
Bev BS 2w	89.88 \pm 0.21****	8.38 \pm 0.21***	1.74 \pm 0.03
Bev BS 4w	87.65 \pm 0.53****	10.60 \pm 0.52****	1.75 \pm 0.01

94.78 \pm 0.02% to 87.65 \pm 0.53% over the course of 4 weeks. The larger reduction in percent monomer confirmed that the bevacizumab degraded more over time relative to rituximab. Given our hypothesis, this would be expected because bevacizumab had higher levels of shuffled disulfide bonds. With regards to biosimilar vs. originator comparisons, we noticed more significant differences between the two for bevacizumab than for rituximab. The biosimilar bevacizumab had a larger formation of aggregates, thus a smaller average % monomer, when compared to the originator bevacizumab.

While aggregation and fragmentation are both degradation products, it is interest-

ing that the two IgG1s had differing degradation profiles. Then again, the two proteins varied in their LC-MS/MS disulfide bond profiles. Bevacizumab had more shuffled bonds appear over time under stressed conditions compared to rituximab. This correlates with the greater percent decrease in monomer for bevacizumab as detected by SEC across the 4-week incubation. We also saw similarities in the LC-MS/MS disulfide bond trends over time between biosimilar and originator drugs for both rituximab and bevacizumab. These trends were further confirmed by the SEC data.

3.3.4 Protein Degradation Characterization by SDS-PAGE

As an orthogonal method to SEC, we completed SDS-PAGE at varying protein concentrations. Shown in Figure 3.6 is a gel that contains data from all of the samples across the different stressed and unstressed timepoints. The monomer bands are at ~150 kDa, which matches the molecular weights of intact rituximab (145 kDa) and bevacizumab (149 kDa).

We observed more aggregates in the bevacizumab samples at a molecular weight of ~240 kDa compared to the rituximab samples. The aggregate contributions also increased, yielding darker gel bands, in the stressed samples for both the bevacizumab originator and biosimilar. This matches our SEC data and continues to exemplify how exposure to stressed conditions degrades antibodies. We also saw fragments present at ~115 and ~85 kDa in both proteins. Since we used SDS-PAGE as a qualitative orthogonal method, we did not determine exactly which fragments these bands corresponded to. The fragment bands at 115 kDa were consistent and prominent for rituximab. The fragment bands at 85 kDa increased, becoming darker, across the 0, 2 and 4-week samples for rituximab. The fragment bands at 115 and 85 kDa were similar across the bevacizumab originator. The fragments at 115 and 85 kDa were larger in the 0-week bevacizumab biosimilar sample compared to the 2 and 4-week sample, but this could be accounted for by differences in the protein concentration loaded on the gel. In general, this SDS-PAGE data matches the SEC data. Both protein types also have a variety of other less abundant fragments below

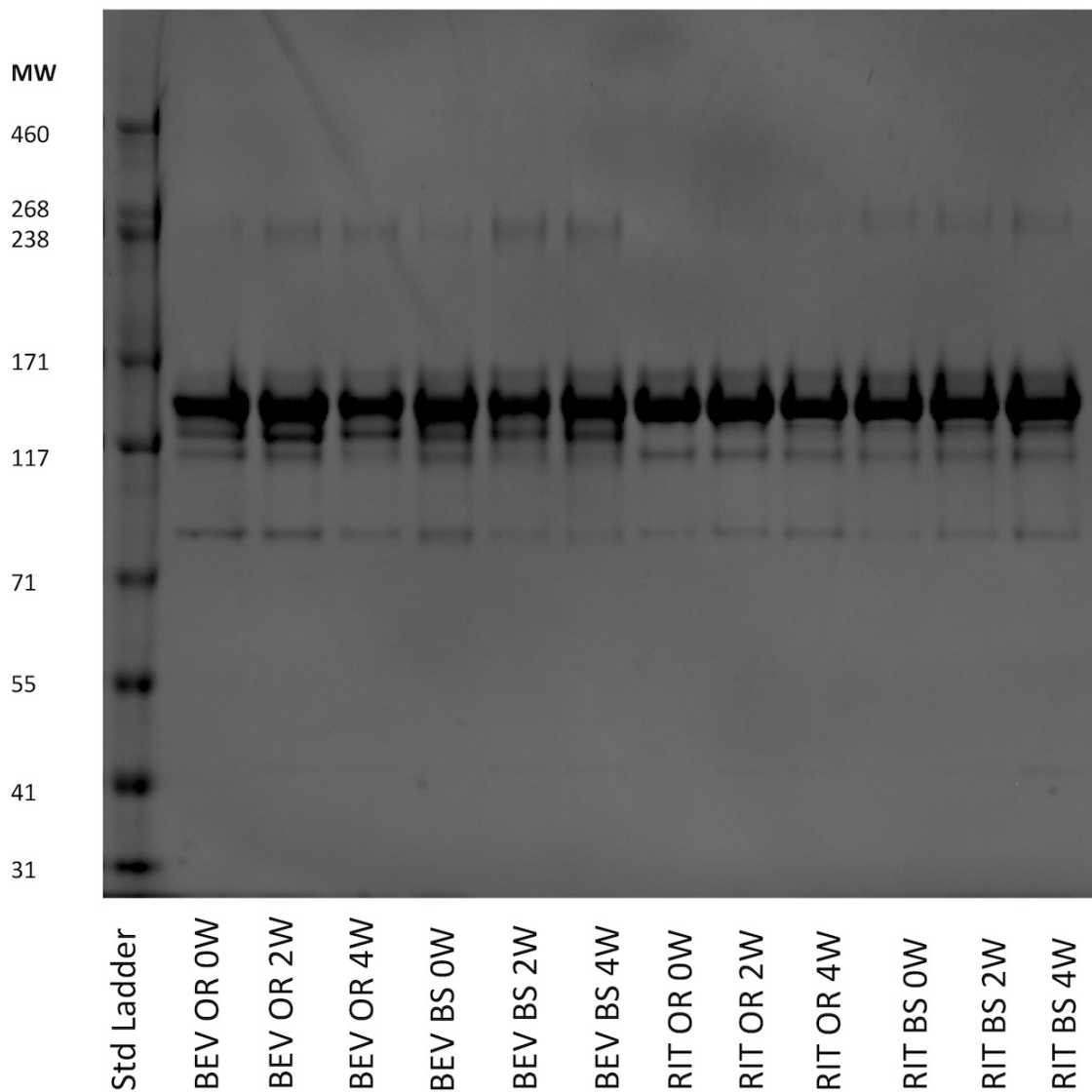


Figure 3.6: SDS-PAGE of representative 0.25 mg/ml samples for bevacizumab OR and BS and rituximab OR and BS depicting the fragmentation and aggregation of the samples at each timepoint. Samples were incubated 0, 2 or 4 weeks at 37°C, shaking at 240 RPM.

the main monomer band at ~150 kDa.

3.4 Discussion

By performing the semi-automated mass spectrometry method for characterizing disulfide bonds, as well as the SEC and SDS-PAGE methods, we were able to more seamlessly identify how bevacizumab and rituximab differ in their disulfide bond profile and degradation propensity. Low levels of shuffled disulfide bonds were detected in both antibodies. The total amount of shuffled bonds and changes in shuffled bond levels over time differed between rituximab and bevacizumab. Similarly, both antibodies showed degradation over the course of the 4-week incubation, but the two varied in how they changed over time.

Rituximab maintained relatively consistent, low levels of disulfide bonds throughout the duration of the stress experiment. At 4 weeks, we detected only $0.51 \pm 0.11\%$ shuffled disulfide bonds for the originator and $0.35 \pm 0.08\%$ for the biosimilar. Bevacizumab had higher levels of disulfide bond shuffling initially, averaging $0.58 \pm 0.08\%$ relative contribution for the originator and $1.62 \pm 0.78\%$ relative contribution for the biosimilar. By 4 weeks, the average relative percent contribution of shuffled disulfide bonds reached $1.46 \pm 1.10\%$ for the originator and $1.25 \pm 0.20\%$ for the biosimilar. We attribute the higher relative percent contribution of shuffled bonds in the 0-week bevacizumab biosimilar sample to analytical variability, especially given the low levels at which we are measuring, and sample size ($N = 3$). We did see an increase in shuffled bond contribution between the 2 and 4-week samples. This suggests that the biosimilar should follow similar disulfide shuffling trends compared to the ones we observed in the originator. We also identified trisulfide bonds in all of the bevacizumab samples but none of the rituximab samples. This perhaps points to poor bevacizumab manufacturing conditions, as trisulfide bonds are indicative of unhealthy cell cultures. [74, 75]

In the end, there was no statistically significant difference across the timepoints and between the originator and biosimilar for each protein. To further confirm this finding, we

would need to perform these studies on additional lots of each drug product. However, that does not discount the fact that we were seeing increases in the average relative percent contribution of shuffled bonds, especially in the bevacizumab samples. After all, under neutral or slightly acidic conditions, disulfide bond shuffling should be minimal. [126, 128] Therefore, increases in shuffled bond contributions at low levels can still support our hypothesis—as a protein unfolds during degradation, buried cysteine residues are exposed and can participate in disulfide bond shuffling. Additionally, the higher levels of shuffled disulfide bonds present in the bevacizumab samples compared with the rituximab samples suggest that bevacizumab is overall less stable, thus more prone to degradation.

While the disulfide bond data indicated that bevacizumab has lower stability and, subsequently, a greater chance for degradation to occur, the SEC and SDS-PAGE data told their own version of the story. As depicted in Figures 3.5, 3.6 and Table 3.1, bevacizumab was more likely to aggregate than fragment when exposed to stress while the opposite was true for rituximab. In comparing biosimilars with their originators, we generally saw similar trends. We detected more significant differences between the bevacizumab biosimilar and originator with regards degradation overtime when compared with rituximab. According to our SEC data, the biosimilar bevacizumab had a greater increase in the % contribution of aggregates after the 2- and 4-week incubations. This also translated to an average lower % monomer for the biosimilar bevacizumab compared with the originator bevacizumab. It is not yet understood exactly why we are seeing these differences in degradation patterns, both between biosimilars and originators and across different IgG1s, but the variability in degradation is interesting given that all of the studied proteins are IgG1s. It should be noted, though, that to further bolster our findings and ensure that intra- and inter-batch variability are not dictating our results and theorized trends, we need to perform these same studies on more than one lot per originator and biosimilar. Nevertheless, these initial studies are important for proof of concept and give us an idea of what trends we may expect. They also exemplify the uniqueness and complexity of protein therapeutics, as

well as documents how not all IgG1s can be expected to act similarly.

Although bevacizumab and rituximab differed in how they responded to stress conditions, the broad applicability of our methods made it possible to run samples from both proteins in tandem. The disulfide bond LC-MS/MS method was instrumental in showcasing how we can more efficiently characterize unexpected disulfide bonds in monoclonal antibodies. The established SEC and SDS-PAGE methods were critical in demonstrating the variability in degradation pathways across IgG1 therapeutics. By combining these methods, we were able paint a full picture on the stability of IgG1 therapeutics exposed to normal and stressed conditions.

In conclusion, our use of a semi-automated, streamlined approach for identifying, characterizing and quantifying disulfide bonds on rituximab and bevacizumab has allowed us to more fully understand differences in the aggregation/ degradation propensity between drugs of the same IgG subclass. Many published studies have characterized aggregation/degradation profiles of these and other IgG1 therapeutics, but few have focused on providing, improving and/or optimizing methods by which to measure disulfide bond shuffling. Based on our data, disulfide bond shuffling does occur in IgG1s, even when they are unstressed. As the proteins are exposed to prolonged heat and shaking, a greater level of shuffling occurs. Similarly, we noticed that disulfide bond shuffling trends matched those of protein degradation, as measured by SEC and SDS-PAGE. This bolsters our hypothesis that as proteins unfold during degradation, exposing buried cysteine residues, they increase their likelihood to form shuffled disulfide bonds. While we recognize that correlation is not causation and other factors could be influencing IgG1 degradation propensity, this initial study justifies our further exploration into how disulfide bond shuffling and protein degradation may be linked.

The implementation of our semi-automated LC-MS/MS method, SEC and SDS-PAGE during antibody development can be useful to a number of stakeholders including the pharmaceutical industry and regulatory agencies. By identifying shuffled disulfide bonds

upfront, companies can save themselves the inevitable headache that will occur if a product fails to meet its designated specifications. This would be especially beneficial to the pharmaceutical industry as disulfide bond characterization is a CQA that is monitored during the development of new therapeutics and biosimilars. Companies can also reduce project related time, money and operator variability by implementing robotics and established MS data processing workflows in their protein characterization. With regards to regulatory agencies, our experimental workflow can become a standardized way to characterize expected and shuffled disulfide bonds within a protein therapeutic. Providing a standardized disulfide bond identification method in product specific guidances would help streamline the approval of BLAs. In sum, our methodology for identifying, quantifying and characterizing disulfide bonds and protein degradation profiles provides the groundwork necessary to further standardize such methods across the pharmaceutical industry and regulatory bodies.

CHAPTER IV

Comparison of Glycan Profiling Methods for mAbs

This chapter describes our study comparing five glycan analysis methods using NIST mAb as our standard with further application in Herceptin[®] and its biosimilars Kanjinti[®] and Ogivri[®]. We initially profiled the glycans on NIST mAb using three released glycan FLR kits, peptide digestion followed by LC-MS/MS and intact MS. As the digestion followed by LC-MS/MS method was the most sensitive of the methods, we used that to compare glycan profiles across the trastuzumabs. From this project we found that while approved biosimilars are may be similar to their reference product, they can be statistically different from their competitors. This chapter is based on a manuscript in preparation for *mAbs*.

4.1 Introduction

Critical quality attributes (CQAs) are physical, chemical, biological or microbiological properties or characteristics that must be within an appropriate limit, range or distribution to ensure desired product quality, safety and efficacy. [145] For monoclonal antibody (mAb) therapeutics, there are many CQAs ranging from excipient content to pH to sub-visible particles to charge-related variants and beyond. [129] One CQA of interest for our group as well as for industry and regulatory bodies is N-glycosylation. [94]

N-glycosylation is omnipresent on the Fc portion of therapeutic IgG1 mAbs. Given

its widespread presence and location, N-glycosylation dictates structural and functional characteristics of mAbs. Since N-glycans have varying sugar compositions or motifs, they are heterogenous in their therapeutic impact. [37] There are certain compositions within glycans, herein referred to as glycan types, that are known to influence a mAb's functionality and safety. The glycan types that are of particular interest to our group include (a)fucosylated, mannosylated, sialylated (sialic acid), galactosylated, and bisecting N-acetylglucosamine (GlcNAc). While these are generally less abundant glycans, their impact on a mAb can be great.

Table 4.1 gives a brief overview of these five glycan types and their impact on the functionality and safety, or immunogenicity, of mAbs. Fucosylated glycans can reduce an antibody's Fc binding affinity. This is attributed to the steric hindrance that the presence of fucose provides. Reduced binding affinity results in diminished therapeutic efficacy, primarily through reduced antibody-dependent cellular cytotoxicity (ADCC) and complement-dependent cytotoxicity (CDC). Thus, afucosylated glycans are generally preferred as they enhance ADCC and CDC, mechanisms of action for many therapeutics IgG1 mAbs. [34, 49, 50]

Mannosylated, or high mannose, glycans are an example of an afucosylated glycan that can enhance ADCC. However, mannosylated glycans can increase the clearance rate of the drug due to their recognition by endogenous mannose (ManR) and asialoglycoprotein (ASGPR) receptors. [50] Upon recognition of the high mannose glycan, the endogenous receptors bind, uptake, and degrade the high-mannose containing mAb. This results in a decrease in the number of therapeutic mAbs in circulation and, in turn, an overall increase in the therapeutic clearance rate. [34, 49, 50] Increased clearance rates are problematic because they require more frequent dosing in order to achieve the therapeutic levels. Additionally, the formation of anti-drug antibodies, hallmarks of immunogenicity and patient safety concerns, can occur more rapidly if the therapeutic is readily recognized. [50–53]

Sialylated glycans, which contain sialic acid, can be both beneficial and detrimental to

patients. They can be beneficial in that they initiate anti-inflammatory effects by upregulating FcγRIIb, an immune checkpoint that suppresses immune responses. For patients with autoimmune diseases, this can reduce the inflammation and swelling associated with their disease. For patients with cancer though, this can inhibit the immune response in tumor micro environments, allowing the malignancy to survive. In fact, there is even a new clinical-stage FcγRIIb antibody being developed by BioInvent targeting FcγRIIb. [57] It aims to improve the outcome of current antibody treatments like trastuzumab or rituximab by enhancing efficacy and overcoming current resistance challenges. Additionally, sialic acids have been associated with reduced FcγRIIIa binding and ADCC. Non-human sialic acids, like the murine-derived sialic acid, NGNA, may also potentially increase immunogenicity. [34, 49, 50, 58, 59]

Galactosylated glycans, which have a terminal galactose, are known to increase ADCC and CDC through enhanced FcγRIIIa binding. Their role in enhancing CDC is more prominent as there is high affinity for C1q, a critical component of the complement cascade, to galactosylated glycans. Galactose has also been affiliated with anti-inflammatory responses by binding to FcγRIIb. Terminal galactose may increase the clearance rate of mAbs as well because the asialoglycoprotein receptors can recognize and bind galactose. [34, 49, 50, 59]

Bisecting GlcNAc glycans increase binding affinity to FcγRIIIa and therefore enhance ADCC. It is still unknown whether this phenomenon is due to the presence of the bisecting GlcNAc or due to the lack of fucose. [34, 49, 50] Bisecting GlcNAc has also been classified as a proinflammatory trait in autoimmune diseases such as Crohn's Disease. This can perhaps be linked to methylation, which is related to disease progression and pathogenesis of Crohn's disease. [60]

To detect, identify and quantify these and other, more abundant glycans on mAbs, researchers conduct a number of methods. Some methods include intact mass spectrometry (MS), intact and denatured MS, IdES enzyme treatment for subunit analysis via liquid

Table 4.1: List of glycan sugar types and their influence on therapeutic mAb efficacy and safety.

Glycan type	FcγRIIIa binding	FcγRIIb binding	ADCC	CDC	Clearance (PK)	Immunogenicity	Inflammatory response	Notes
Fucose	Decreases	No effect	Decreases	Minimal effect	No effect	Minimal	Minimal	Steric bulk hinders Fc binding, reducing effector function
Mannose	Increases	No effect	Increases	Decreases	Increases	Increases	Minimal	Faster clearance due from endogenous receptor recognition; increased ADCC without fucose present
Sialic acid	Decreases	Increase	Decreases	Decreases	No effect	Increases for NGNA (non-human)	Anti-inflammatory	Upregulates FcγRIIb and inhibits CDC; active component of IVIG; interferes with FcγRIIIa binding and ADCC
Galactose	Increases	Increase	Increases	Increases	Increases	Minimal	Anti-inflammatory	Increases binding to C1q for CDC and ADCC; binding to FcγRIIb, inhibiting proinflammatory response
Bisecting GlcNAc	Increases	No effect	Increases	Minimal effect	No effect	Minimal	Pro-inflammatory	Enhances binding to FcγRIIIa and ADCC – potentially attributed to afucosylation

chromatography – tandem mass spectrometry (LC-MS/MS), peptide digestion and subsequent analysis via LC-MS/MS, and released glycan kits analysis via liquid chromatography – fluorescence (LC-FLR) and/or LC-MS. [5, 65] Other MS techniques such as electron spray ionization mass spectrometry (ESI-MS), ion-mobility mass spectrometry (IM-MS), capillary electrophoresis mass spectrometry (CE-MS) and matrix-assisted laser desorption ionization mass spectrometry (MALDI-MS) have also been conducted to determine glycoforms. [67, 146, 147] As if the current options were not enough, one group is modifying current HILIC-MS libraries to overcome current limitations by using accurate mass values instead of glucose units and retention times. [148]

Despite measuring the same target species, these methods yield differing results with regards to relative glycan contribution. The result output variability can be attributed to differences in the sensitivity, resolution, reliability and reproducibility of each method. User-specific and site-specific variability, which our group experienced first-hand as members of a second multi-institution NIIMBL study characterizing glycans on the NIST mAb,

are also known to affect data outcomes. [149]

Understanding why there is variability across orthogonal methods is important, but it is only half of the battle. In order to confidently and consistently characterize glycans on antibody therapeutics, there needs to be a consensus on how to best identify and quantify glycans. Although there are multiple publications comparing the glycosylation analysis techniques used for mAbs, there are no glycan characterization “best practices” that are followed by all biologics developers. [66–70] However, with the reauthorization of Biosimilars User Fee Amendments (BsUFA III) in 2022, there is now a push from regulators to improve upon biologics development guidances. In early 2023, the FDA published a research roadmap that establishes goals for the BsUFA III regulatory science research pilot program. [150] Broadly, these goals are to advance the development of interchangeable products and improve the efficiency of biosimilar product development. To achieve these goals, the FDA is seeking to increase the accuracy and capability of analytical (structural and functional), and chemistry, manufacturing, and controls (CMC) characterizations. In doing so, the FDA is studying approaches for standardizing the assessment and reporting of product quality attributes, characterizing relationships between product quality attributes and clinical outcomes, and improving and/or developing new analytical technologies for protein characterization. [150] As recipients of a BsUFA grant, we have been working closely with members of the FDA to establish ways in which to further the BsUFA research program’s goals.

Glycans provide a great starting point for standardizing assessment and reporting methods given the aforementioned influence of glycans on drug safety/efficacy, as well as associated challenges in current glycan analysis practices. Challenges in glycan analysis arise not only from inconsistencies across reported method outcomes, but also from knowledge gaps on the acceptable limits of low abundance glycans. Understanding acceptable limits for glycans, especially those associated with potentially negative clinical impacts, is paramount for the biologics industry. Glycan acceptance criteria may dictate

whether a project can advance into later development or submission stages. Further clarity on these limitations could also benefit biosimilar developers. If biosimilars yield desirable glycan profiles with acceptable deviations from the innovator, and do not have impact *in vitro* efficacy, the perhaps this evidence could justify reducing and/or eliminating phase 3 bioequivalency clinical studies of biosimilars.

Given the criticality of correctly characterizing glycans, we have begun studying and comparing the current methods by which to identify and quantify on mAb therapeutics. Our studies have comprised of released glycans analysis via commercial kits – 2AB Express (2AB), RapiFluor-MS (RF) and InstantPC (PC)– and LC-FLR, intact MS, and protein digestion followed by LC-MS/MS. For our initial study, we performed all methods on the NIST mAb. This provided the foundational knowledge necessary to understand the expected resolution, sensitivity, reproducibility and reliability of each method. Studying NIST mAb also allowed us to compare our results with published glycan profiles.

As the closest thing to a mAb standard, the NIST mAb has been well-characterized by a number of different groups across numerous methods. What is worth noting, and what corroborates our point earlier, is that no glycan characterization “best practices” exist. The initial interlaboratory study conducted by NIST exemplifies this well. Of the 103 reports from the 76 groups that participated in the study, 74% performed released glycans methods (2-AA, InstantAB, InstantPC, or RapiFluor with fluorescence detectors), 20% monitored glycopeptides via LC-MS, CE-MS or MADLI-MS, and 6% measured glycans on the intact protein or protein fragments, again using LC-MS. The majority of industrial contributors analyzed released glycans whereas the majority of academic institutions analyzed glycopeptides. Due to the disparities in method choice, the number of unique glycans identified ranged from 4-48. [149]

Aside from the interlaboratory study, there are other labs that have published NIST mAb glycan data using a variety of methods. In a 2015 American Chemical Society book chapter, Prien et al. described how they used a National Institute for Bioprocessing Re-

search and Training (NIBRT) glycomics platform to assess the repeatability of NIST mAb glycan identification across 6 separate days. [151] In this platform they implemented a Hamilton liquid handling robot for sample preparation and HILIC separation with FLR detection. Using this method, they were able to detect 24 unique glycans with standard deviations of $\leq 0.4\%$ for peak areas $\geq 0.5\%$ of the total peak area. They also described additional techniques including fluorescent labeled released glycans, HILIC peak fractionation followed by reversed phase LC-FLR-MS, and LC-MS based peptide mapping. In a workflow using 2-AA to label the released glycans, followed by HILIC separation, FLR detection and ion-trap MS analysis, the group identified 29 glycans. They explained that differences in the numbers of glycans identified could be due to co-eluted glycans in the NIBRT method that were able to be resolved in the HILIC fractionation method. [151] Again, this showcases how the choice of method used can influence the number of glycans identified.

Those examples do not stand alone. A paper by Zhao et al. discussed glycopeptide profiling after tryptic digestion. They identified 42 glycopeptides, however, of those only 24 were $\geq 0.05\%$ relative abundance. [152] The lower abundance ones are more questionable, especially since their % coefficient of variance values were extremely high – sometimes more than 100%. Another paper by Hilliard et al. reported the identification of 35 glycans with relative abundances $\geq 0.1\%$ using the RapiFluor released glycan method. [153] Clearly, the range of methods and, subsequently, the range of results is large enough to warrant further research into method standardization.

Although performing NIST mAb glycan analyses using the same site and same scientist for future method standardization is important, we wanted to expand our research beyond the NIST mAb. Therefore, we subsequently applied these techniques to Herceptin[®] and its biosimilars Kanjinti[®] and Ogivri[®] to showcase how there is variability in lower level glycans (i.e. afucosylated, high mannose, sialic acid) across biosimilars. While the biosimilars have been approved because they are similar enough to Herceptin[®], differences between the glycan profiles of multiple biosimilars could indicate problems in the

future with therapeutic switching in patients.

The results from our glycan analysis comparison study reaffirmed the presence of variability between methods in regards to relative glycan contributions. They also highlighted the differences in lower-level glycan abundances for Herceptin[®] and two of its biosimilars. In sum, the glycan data presented here emphasizes experimental expectations, limitations and nuances for several glycan analysis methods tested against multiple mAbs. This data can be used in improving current biologics development and approval practices by setting the foundation for future method standardization and validation, spurring the creation of related biologic development guidances, and justifying the reduction of burdensome phase 3 clinical studies for biosimilars.

4.2 Materials and Methods

4.2.1 mAb Sample Information

NIST mAb was provided by NIIMBL in 800 uL aliquots of 10 mg/mL mAb in its native formulation buffer. Herceptin[®] (trastuzumab), Kanjinti[®] (trastuzumab) and Ogivri[®] (trastuzumab) were all procured from the University of Michigan hospital pharmacy. They are provided as 100 mg lyophilized powders for reconstitution. All samples were run in triplicate for each method.

4.2.2 Released Glycan Commercial Kits

4.2.2.1 Sample Preparation

GlyX N-glycan prep with 2-AB Express (Agilent, Santa Clara, CA), Glycoworks RapiFluor-MS N-glycan kit (Waters, Milford, MA) and GlyX N-glycan prep with InstantPC (Agilent, Santa Clara, CA) were purchased through their respective vendors. The RapiFluor-MS and Instant-PC kits were for 96 samples while the 2-AB Express kit was for 24 samples. For the RapiFluor-MS samples, we used a RapiFluor labeled dextran ladder (Waters) as our

standard. For the 2-AB samples, we used a 2-AB labeled dextran ladder (Waters) as our standard. For the InstantPC samples, we used the InstantPC (Agilent) as our standard.

Due to buffer incompatibility with the kits, NIST mAb was buffer exchanged into water using 0.5mL, 10 kDa MWCO Amicon spin filters and further concentrated to 2 mg/mL. Protein concentrations after centrifugation were then recorded using the protein A280 IgG setting on a NanoDrop. The trastuzumab samples were reconstituted in water at a protein concentration of 2 mg/mL. Protein concentrations after centrifugation were then recorded using the protein A280 IgG setting on a NanoDrop.

After buffer exchanging or reconstituting the samples, vendor protocols were followed to perform the released glycan assays. The three kits used for sample preparation and analysis were GlyX N-glycan prep with 2-AB Express (Agilent, Santa Clara, CA), Glycoworks RapiFluor-MS N-glycan kit and GlyX N-glycan prep with InstantPC (Agilent, Santa Clara, CA). The eluted released glycans were collected upon completion of the assay and were either run on the LC-FLR-MS on the day of the sample preparation or were frozen at -20°C until analysis, as recommended in the vendor protocols. If samples were frozen, they were thawed within a week of preparation and analyzed via LC-FLR-MS on the same day as their freeze-thaw.

4.2.2.2 LC-FLR-MS

For the LC-FLR-MS, we created methods based on the vendor recommended methods provided for each kit. The methods were similar for all 3 kits with some minor variations. The instrument system was a Waters Acquity H Class HPLC interfaced with a Waters fluorescence detector and a Waters Xevo G2-XS QTOF. The column used for all kits and samples was a Waters ACQUITY UPLC Glycan BEH Amide, 130 Å, 1.7 μm, 2.1 x 150 mm column kept at 60° C. The flow rate was 0.4 mL/min over the 60-minute run time. We injected 1 uL on column for the labeled samples. A gradient method was used with increasing amounts of aqueous phase over time from 25% up to 100% then back to 25% for

equilibration. Mobile phase A was 50 mM ammonium formate pH 4.4 and mobile phase B was 100% acetonitrile. For 2AB Express, the fluorescence excitation wavelength was 360nm and emission wavelength was 428nm. For RapiFluor-MS, the fluorescence excitation wavelength was 265nm and emission wavelength was 425nm. For InstantPC, the fluorescence excitation wavelength was 285nm and emission wavelength was 345nm.

For all samples, the following qTOF parameters were used: positive mode, capillary voltage 2.8 kV, cone voltage 30 V, source temperature 120 °C, desolvation temperature 350 °C, scan time 0.8 second, and m/z range 300-2,000 Da.

4.2.2.3 Data Processing

We processed our samples using Waters' UNIFI software for released glycan analysis. We first identified glucose units by setting the labeled Dextran ladder as our standard. Then the UNIFI software was able to determine glycan identity based on the glucose units and retention time detected by the LC-FLR system (Figure 1). We also mass confirmed the glycans using the QTOF m/z values. As there was no Dextran ladder for InstantPC, we manually integrated the fluorescence peaks in UNIFI to quantify glycans and compared fluorescence peak retention times and m/z with the InstantPC standard to identify the glycans. Therefore, we could only identify confidently 8 glycans. There were more peaks integrated on the FLR spectra, but even with the m/z values it was challenging to assign glycan identities with high certainty. Thus, we elected to omit any inferred glycan identities based on m/z.

4.2.3 Intact MS

The samples were diluted to 1 pmol/ uL with water. Five pmol of protein were loaded onto the column in a 5 uL injection. A 9-minute gradient with an increasing percentage of organic solvent from 2% to 20% was used. Mobile phase A was 0.1% formic acid in water and mobile phase B was 0.1% formic acid in acetonitrile. The flow rate was 50 ul/min and

the column was kept at 60°C. The mass spectrometer was operated in full scan, positive ion mode with an in-source CID at 45 eV. The scan range was 1000 – 4000 m/z with 10 microscans per second. The resolution was 17,500, ACG target was 3×10^6 and the max IT was 250 ms.

An Acquity M Class HPLC (Waters, Milford, MA) was interfaced with a Q-Exactive mass spectrometer (ThermoFisher, Waltham, MA) for intact MS data acquisition. The column used was a XBridge Protein BEH C4 column, 300A, 3.5 μ m, 2.1 mm x 50 mm (Waters, Milford, MA). Byos Intact workflows (Protein Metrics Inc., Cupertino, CA) were used to process data and identify and quantify glycans.

4.2.4 Peptide Mapping

4.2.4.1 Protein Digestion

An AccuMAP Low pH Protein Digestion kit (Promega Inc., Madison, WI) was purchased to perform the protein digestion for peptide mapping. The digestion process was conducted using an AssayMAP Bravo liquid handling platform (Agilent, Santa Clara, CA).

Samples were prepared following the vendor's AccuMAP Low pH Protein Digestion protocol for 5 mg/mL protein samples. The only deviation from the protocol was changing the concentration of iodoacetamide from 300 mM to 100 mM and increasing the volume of the iodoacetamide added from 2 μ L to 6 μ L per sample. This adjustment was made to accommodate the AssayMAP Bravo pipetting volume limitations. Samples were left incubating at 37° C overnight upon addition of the trypsin and Lys-C. The following morning, samples were acidified with 20% TFA and were purified using C18 solid phase extraction cartridges on the AssayMAP Bravo. For purification, the equilibration/utility buffer was 0.1% formic acid and the priming/syringe wash and elution buffers were 80% ACN in 0.1% FA. We eluted 50 μ L of sample at a flow rate of 5 μ L/ min.

The peptide concentration of each sample was measured using a Pierce Fluorometric Quantitative Peptide Assay (ThermoScientific, Waltham, MA). The sample were then

normalized to 0.1 ug/uL using the AssayMAP Bravo with 0.05% TFA as the diluent. After normalization, 500 ng sample were loaded onto the column for LC-MS/MS analysis.

4.2.4.2 LC-MS/MS and Data Processing

An Acquity M Class HPLC (Waters, Milford, MA) was interfaced with an Orbitrap Exploris mass spectrometer (ThermoFisher, Waltham, MA) for peptide mapping data acquisition. The column used was Luna C18 column (Phenomenex, Torrance, CA). Samples were run using a 30-minute gradient with 0.1% formic acid in water as mobile phase A and 0.1% formic acid in acetonitrile as mobile phase B. The gradient gradually increased the amount of organic from 2% to 90% throughout the run before equilibrating at 2% mobile phase B. Ten uL, equivalent to 500 ng of protein, were injected on the column at room temperature and flowed at a rate of 0.350 uL/min. The Orbitrap was operated in positive ion mode at a resolution of 6000 and scan range of 300-1600 m/z. The RF lens was set to 40%, normalized ACG target set to 300%, mass tolerance set to 10 ppm, intensity threshold set to 5.0E3 and charge state set to 2-6. The HCD collision energy was set at 30% using a fixed, normalized collision energy mode. Byos PTM workflows (Protein Metrics Inc., Cupertino, CA) were used to process data and identify and quantify glycans.

4.3 Results

4.3.1 Released Glycan Kits with NIST mAb

Figure 4.1 depicts a 2AB fluorescence chromatogram. From this chromatogram we can see that most peaks we detected by the UNIFI software automatically. Peaks that were not automatically detected, like the second isomer peak for G1F at 21 minutes, were manually integrated later. We also noticed that in general, the PC FLR traces and MS spectra had better resolution between peaks, higher signal intensity and better overall sensitivity, especially when we zoomed in on the smaller peaks. However, without access

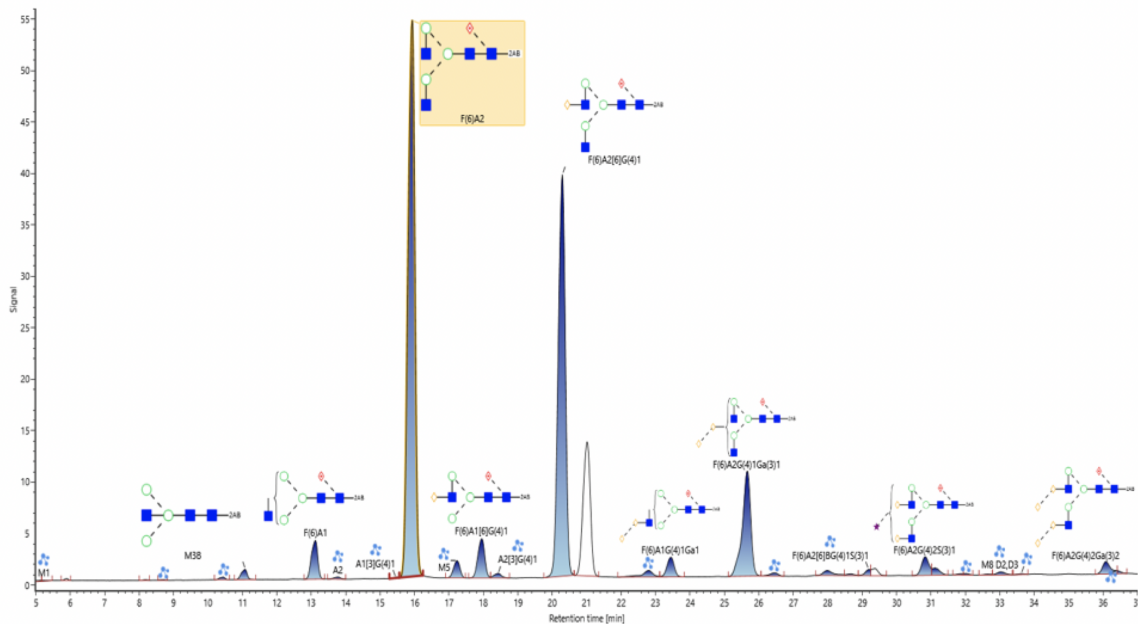


Figure 4.1: Example NIST mAb fluorescence chromatogram with glycans labeled with the 2AB express kit. Glycans were identified using a UNIFI algorithm based on a Dextran calibration ladder. Highlighted at a retention time of 16 minutes is the F(6)A2 glycan, or G0F, which is expected to have the highest signal for NIST mAb.

to an analysis software that can perform a direct head-to-head comparison between PC, 2AB and RF, it is challenging to make quantitative claims about differences in sensitivity and resolution across all three methods.

Nevertheless, our observations that all three kits had varying signal intensities and peak shapes, leading to differences in sensitivity and resolution, were supported by quantitative differences in the number and type of glycans identified (table 4.2). InstantPC had the highest average number of total glycan peaks identified (19) while 2AB and RF were comparable in their number of glycans identified at 16.33 and 16.67 glycans, respectively. The more common glycans such as G0F, G1F and G2F were similar in average normalized % area across all 3 methods. For example, G0F had average normalized % areas of 39.92 (2AB), 40.10 (RF) and 38.17 (PC). Likewise, for G1F we saw values of 40.99 (2AB), 39.58 (RF), 36.70 (PC) and for G2F we saw values of 8.33 (2AB), 7.42 (RF) and 7.21 (PC). However, when it came to lower abundance glycans, there was greater variability not only in

Table 4.2: Comparison of the total number of glycans, broken down by glycan type, detected on NIST mAb via the five methods. N = 3; shown is mean \pm standard deviation.

NIST mAb (LC-FLR)	Average total # glycan type				
	2AB	RF	PC	Intact	Digestion
Total # unique glycans	16.33 \pm 0.58	16.67 \pm 0.58	19.00 \pm 0.00	4.00 \pm 0.00	22.33 \pm 1.15
Total # afucosylated	6.33 \pm 1.53	2.00 \pm 0.00	3.00 \pm 0.00	0.00 \pm 0.00	8.33 \pm 0.58
Total # mannosylated	4.33 \pm 0.58	1.00 \pm 0.00	0.00 \pm 0.00	0.00 \pm 0.00	5.00 \pm 1.00
Total # sialylated	2.67 \pm 0.58	1.33 \pm 0.58	2.00 \pm 0.00	0.00 \pm 0.00	3.33 \pm 0.58
Total # galactosylated	1.67 \pm 0.58	4.00 \pm 0.00	0.00 \pm 0.00	0.00 \pm 0.00	4.00 \pm 0.00
Total # bisecting GlcNAc	1.00 \pm 0.00	0.00 \pm 0.00	1.00 \pm 0.00	0.00 \pm 0.00	2.00 \pm 0.00

the number of glycans detected but also in the identities UNIFI assigned to these glycan peaks.

Lower abundance glycans are important because often times they are the ones that can influence therapeutic efficacy and safety in patients. As described in the introduction, glycans we were particularly interested in monitoring were afucosylated, mannosylated, sialylated, galactosylated and bisecting GlcNAc. As shown in figure 4.2, there was variability across the methods in their ability to detect relative % contribution of different glycan types. Relative % contribution was calculated across all integrated peaks, including ones that were not automatically identified by the UNIFI software but were manually integrated.

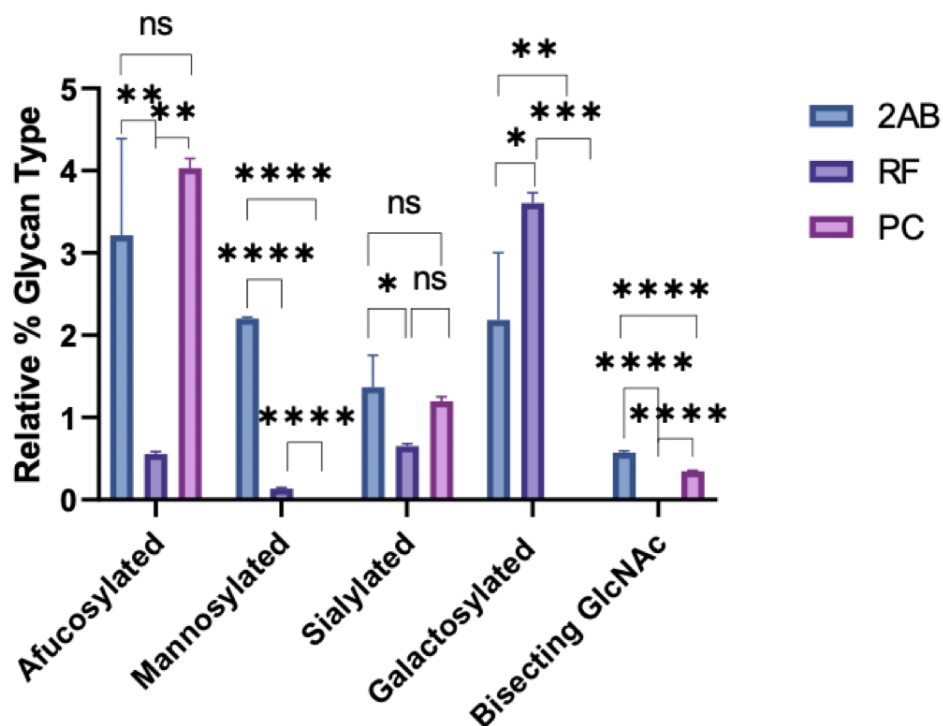
Based on UNIFI outputs, 2AB yielded the highest relative % contribution of mannosylated (2.20 ± 0.02), sialylated (1.37 ± 0.38), and bisecting GlcNAc (0.57 ± 0.02) glycans. PC yielded the highest relative % contribution of afucosylated (4.03 ± 0.12) glycans and RF yielded the highest relative % contribution of galactosylated (3.61 ± 0.13) glycans. While challenging to compare PC directly with RF and 2AB due to the inability to identify over

half of the integrated peaks, it is readily apparent that RF and 2AB are different in their ability to identify these lower abundance peaks. Theoretically, we should be seeing similar % contribution across the methods because we are analyzing only the NIST mAb in this case. In practice, we see minimal contributions (<1% relative contributions) for most of our glycan types of interest in the RF samples whereas we see over 1% relative contribution in four of the five glycan types for 2AB (figure 4.2). Even for the glycans that we do know in the PC samples, we are seeing higher contributions for afucosylated, sialylated and bisecting-GlcNAc when compared with RF.

We recognize that we do not have a large enough sample set to state whether one glycan kit is more robust or preferred than the others at the moment. What we can say is that there are significant differences across the lower abundance glycan identifications for the three kits (figure 4.2). Given the potential importance that these less abundant glycans could have on the therapeutic's efficacy and safety, we wanted to quantify them in an orthogonal manner. From our prior experience and knowledge of mass spectrometry lower-level sensitivity capabilities, we hypothesized that LC-MS/MS would be a more sensitive method to perform and would yield more unique glycans compared to the FLR kits.

4.3.2 Peptide Mapping LC-MS/MS of NIST mAb

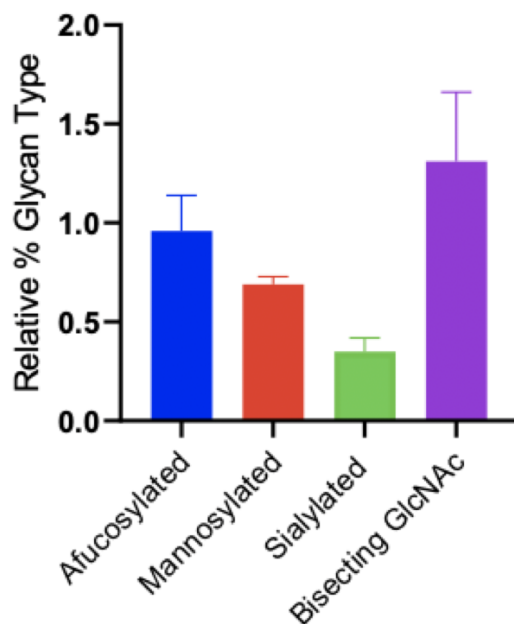
Our hypothesis held true as we were able to identify an average of 22.33 glycans via LC-MS/MS compared with an average of 16.33 for RF, 16.67 for 2AB and 19 for PC. Additionally, we detected glycans in all of the types we were monitoring – afucosylated, mannosylated, sialylated, galactosylated and bisecting GlcNAc. The relative % contribution of these glycan types were under 1.5%, but the standard deviations were generally small, giving us higher confidence that the glycans were correctly identified (figure 4.3).



	Relative % Afucosylated	Relative % Mannosylated	Relative % Sialylated	Relative % Galactosylated	Relative % Bisecting GlcNAc
2AB	3.21 ± 1.17	2.20 ± 0.02	1.37 ± 0.38	2.19 ± 0.82	0.57 ± 0.02
RF	0.56 ± 0.03	0.13 ± 0.02	0.65 ± 0.03	3.61 ± 0.13	0.00 ± 0.00
PC	4.03 ± 0.12	0.00 ± 0.00	1.20 ± 0.06	0.00 ± 0.00	0.35 ± 0.01

Figure 4.2: Example NIST mAb fluorescence chromatogram with glycans labeled with the 2AB express kit. Glycans were identified using a UNIFI algorithm based on a Dextran calibration ladder. Highlighted at a retention time of 16 minutes is the F(6)A2 glycan, or G0F, which is expected to have the highest signal for NIST mAb.

LC-MS/MS Glycans Grouped by Type



	Relative % Afucosylated	Relative % Mannosylated	Relative % Sialylated	Relative % Bisecting GlcNAc
NIST mAb	0.96 ± 0.18	0.69 ± 0.04	0.35 ± 0.07	1.31 ± 0.35

Figure 4.3: Relative % contribution of each glycan type for NIST mAb as identified by LC-MS/MS after protein digestion. Glycans were identified using the Protein Metrics PTM workflow. N=3; Error bars are standard deviation.

4.3.3 Intact MS of NIST mAb

To further prove the better sensitivity of the protein digestion followed by LC-MS/MS, we measured the intact MS of NIST. After processing the intact data with the Protein Metrics workflow, we only identified 4 unique glycans – G0F, G1F, G2F, G0F-GN (figure 4.4). These glycans comprised 7 readily identified glycoforms bearing 2 glycans each, with 4 other potential glycoforms not confidently identified by the Protein Metrics software (figure 4.4A). The identified glycans are all common glycans on human IgGs, which also yielded higher abundances in the FLR and LC-MS/MS methods. Therefore, it was unsurprising that they were the ones readily identified by Protein Metrics after intact MS.

4.3.4 NIST mAb Glycan Profile Summary

Table 4.2 shows a summary comparison of the average total number of glycans data collected for the five methods described. From this table, it is clear to see that the protein digestion followed by LC-MS/MS was the most sensitive of the methods. Not only did it yield the highest number of total glycans (22.33), but it also detected the most unique glycans for each glycan type we monitored. From this table, it is also worth noting that 2AB, while having similar total number of glycans to RF did detect more unique afucosylated, mannosylated, sialylated and bisecting GlcNAc glycans. Unlike 2AB or RF, PC had no mannosylated or galactosylated glycans identified. However, we can explain that due to the inability to confidently identify all integrated peaks based off of the provided standard. As expected, the intact MS yielded the fewest number of unique glycans (4) and therefore did not identify low level glycans.

4.3.5 Glycan Characterization of Trastuzumabs

As we are ideally trying to recommend the use of certain glycan methods, understanding the sensitivity, signal intensity, resolution and reliability of each method was important in making recommendations. Given our experience with NIST mAb, we decided to

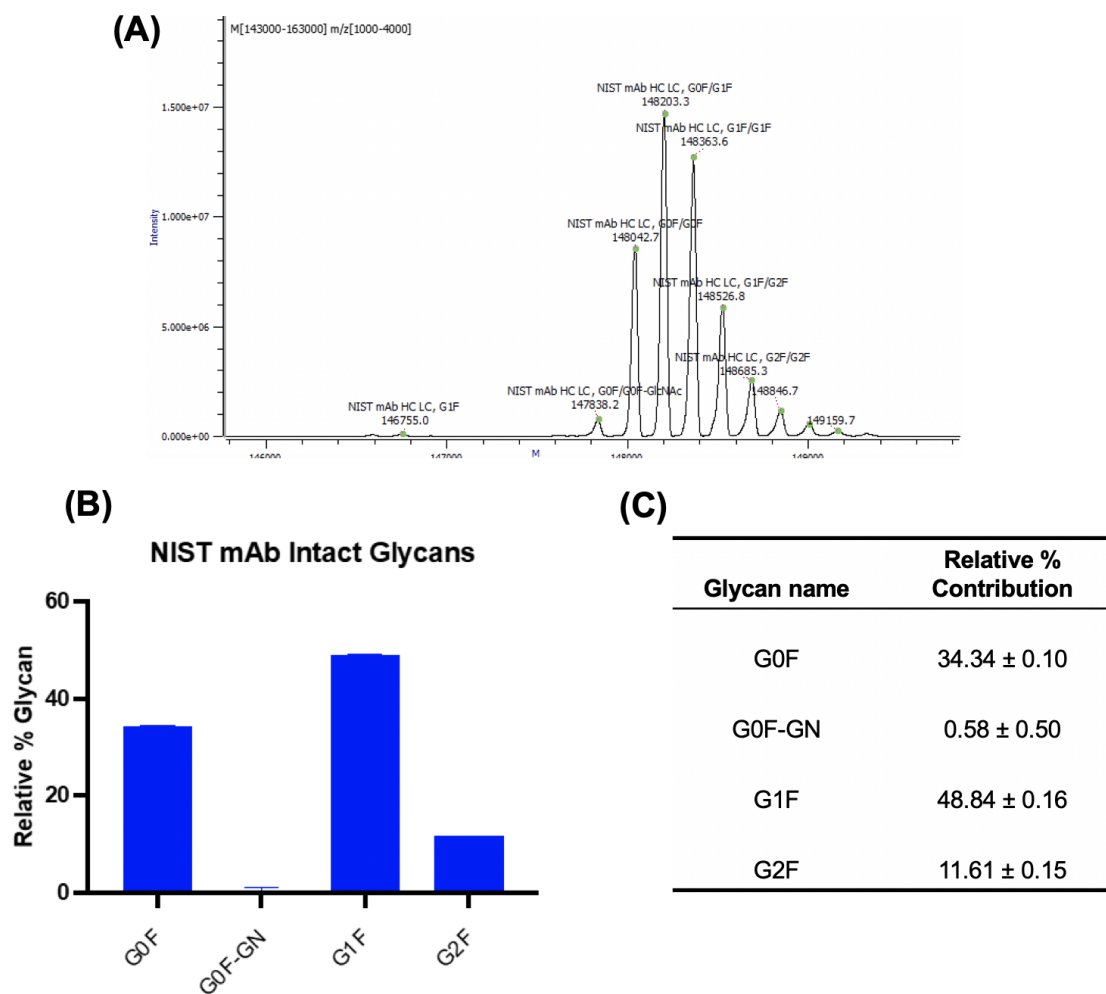


Figure 4.4: Relative percent contribution of glycans as detected by intact MS. (A) Deconvoluted spectra from Protein Metrics Intact workflow; (B) Visual representation of the Relative % contribution of the detected glycans detailed in table (C). N = 3; shown is mean ± standard deviation. Note: glycans shown as pairs in the spectra were subsequently normalized to depict individual glycan contribution.

Table 4.3: Comparison of the total number of glycans, broken down by glycan type, detected on trastuzumabs via the five methods. N = 3; shown is the average value.

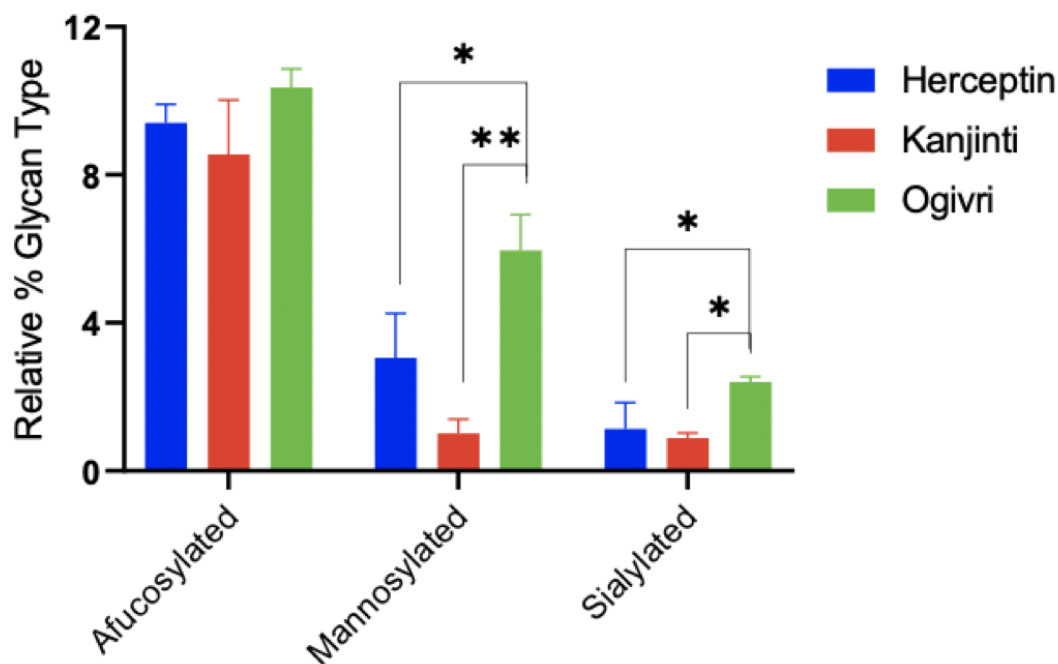
Average total # glycan type															
Total #	Herceptin®					Kanjinti®					Ogivri®				
	2AB	RF	PC	Intact	LC-MS/MS	2AB	RF	PC	Intact	LC-MS/MS	2AB	RF	PC	Intact	LC-MS/MS
Unique glycans	15.67	12.33	13	6	25	13.67	12.33	11	4	21	14.33	13	14.33	6	24.67
Afucosylated	9.33	4	3	0	15	6.67	4	3	0	10.67	6.67	5.33	3	0	11
Mannosylated	4.67	2.33	0	0	6.67	2	0.67	0	0	4	3	2.33	0	0	7
Inflammatory	1.33	3.33	0	1	5.67	2.67	3.67	0	1	4.67	1.67	3.67	0	2	5
Sialylated	1.33	3	1	1	5.67	1	3.67	1	0.67	4.67	1.67	3	1	1.33	5
Galactosylated	0	0.33	0	0	0	0	0	0	0	0	0	0.67	0	0	0
Bisecting GlcNAc	2	0	1	0	0	1.67	0	1	0	0	1	0	1	0	0

perform protein digestion followed by LC-MS/MS as our “gold standard” moving forward with other mAbs. We also performed the three FLR kits and intact MS on Herceptin® (trastuzumab) and its biosimilars Kanjinti® and Ogivri® to confirm that our NIST mAb data trends were not protein specific.

Our results and trends across all methods for the trastuzumab samples mirrored those of NIST mAb. For one, the LC-MS/MS method yielded the highest number of unique glycans followed by FLR kits and intact MS (table 4.3). There were differences in the average total number of unique glycans identified for the innovator Herceptin® (25) and its biosimilars Kanjinti® (21) and Ogivri® (24.6). All had similar number of glycans identified across the three FLR methods – anywhere from 11 to 15.67 glycans. There was no distinct FLR kit method that was consistently identifying more glycan peaks for all of the trastuzumab samples.

Since we determined that LC-MS/MS was the most sensitive method, we further explored differences between the types of glycans across the innovator and biosimilar trastuzumabs as measured by LC-MS/MS. What we discovered was that there were significant differences in the relative % contribution of mannosylated and sialylated glycans across the three trastuzumabs. Interestingly, the two biosimilars were more different from each other

LC-MS/MS Glycans Grouped by Type



	Relative % Afucosylated	Relative % Mannosylated	Relative % Sialylated
Herceptin®	9.40 ± 0.50	3.05 ± 1.21	1.14 ± 0.71
Kanjinti®	8.55 ± 1.47	1.01 ± 0.38	0.88 ± 0.14
Ogivri®	10.35 ± 0.51	5.95 ± 0.97	2.40 ± 0.14

Figure 4.5: Relative % contribution of each glycan type for NIST mAb as identified by LC-MS/MS after protein digestion. Glycans were identified using the Protein Metrics PTM workflow. N=3; Error bars are standard deviation.

than from Herceptin[®]. For example, the relative % mannosylated for Kanjinti[®] was 1.01 ± 0.38 while Ogivri[®] was 5.95 ± 0.97 . Herceptin[®] fell in the middle of both with a relative % mannosylated of 3.05 ± 1.21 . Similar trends held true for relative % sialylated and relative % afucosylated (figure 4.5). Kanjinti[®] in general had the fewest unique glycans identified and statistically less % contribution of mannosylated and sialylated glycans whereas Ogivri[®] had statistically higher % contribution of mannosylated and sialylated glycans when compared with Kanjinti[®] and Herceptin[®].

4.4 Discussion

Based on our results, we determined that the peptide mapping (protein digestion followed by LC-MS/MS) gave us the most in-depth glycan profile. The sensitivity of the high-resolution mass spectrometer meant that the LC-MS/MS method was able to identify more of the unique, less abundant glycans compared to the orthogonal FLR and intact MS methods. For the NIST mAb, we identified an average of 22.33 unique glycans by LC-MS/MS compared to 16 – 19 glycans by LC-FLR released glycan kits and 4 by intact MS. Similarly, for the trastuzumabs we detected over 20 glycans by the LC-MS/MS method but no more than 16 by FLR. Most importantly, the LC-MS/MS method detected glycans that fell into the types we were interested in monitoring – afucosylated, mannosylated, sialylated, galactosylated and bisecting GlcNAC. While the LC-MS/MS relative % contribution for these glycan types was lower than that of the FLR kits for NIST mAb, the fact that it could identify more low abundance glycans made it useful for our research.

We do want to recognize the fact that the number of glycans identified by our methods differed from those described in the introduction. For example, for RF labeled released glycans Hilliard et al. identified 35 glycans whereas we only identified an average of 16.67 glycans. [153] Prien et al. identified 29 glycans using a 2-AA fluorescence label, again suggesting that we should have identified more glycans after treating samples with a released glycan kit. [151] With regards to digestion, Zhao et al. confidently identified 24

glycans, although they reported up to 42 potential candidates, whereas as we confidently identified an average of 22.33 glycans. [152] The exact reasons for our generally lower glycan identifications remains unknown. Many factors could have contributed including sample preparation, MS method conditions, software capabilities and/or individuals' level of conservatism when manually identifying lower abundance glycans. Nevertheless, it continues to bolster the idea that depending on the method, instrumentation and the user, differing results for the same antibody can be reported.

For intact MS, our 4 unique glycans and 7 glycoforms may seem lower than expected. However, it is still similar to the 7 glycoforms identified by Chen et al. who performed intact MS on NIST mAb using CE-MS. [154] In the interlaboratory study, 5 specific glycoforms containing abundant glycans such as G0F, G1F, G2F were also reported. [149] This further confirms that 7 glycoforms is not out of the realm of expectations for intact MS results. Any variability again may be explained by factors ranging from instrumentation sensitivity to acquisition parameters to software capabilities. It also reiterates the conclusion that higher sensitivity can be achieved with alternative methods.

With all of this information in mind, we want to continue to emphasize the ability of protein digestion followed by LC-MS/MS to detect less abundant glycans because those are frequently influential to a mAb's safety and efficacy, as described in table 4.1 and the introduction. As shown in figures 4.2, 4.3, and 4.5, the composite relative contribution of these glycans is frequently in the single percentage range (0-9%). Therefore, they could be easily missed if a less sensitive, lower resolution method was performed – a phenomenon exhibited in the intact MS data and, to some extent, the FLR data. Therefore, to capture all glycans we would recommend peptide mapping via protein digestion followed by LC-MS/MS. This recommendation seems to be one that many biologics companies would agree with given the rising implementation of MS based glycosylation analysis techniques in BLA submissions. [146]

However, given the costs associated with owning and maintaining a high-resolution

mass spectrometer, we recognize that not every lab can attain these results. Thus, we also highlight our experiences with the LC-FLR released glycan kits and note that the InstantPC kit exhibited the highest signal intensity, along with better sensitivity and resolution compared to RapiFluor and 2AB. One drawback with the InstantPC kit, as is apparent in tables 2 and 3, is that it is not compatible with the UNIFI software for released glycan analysis. While we had an average of 19 integrated peaks in the PC samples for NIST mAb, and anywhere from 11 (Kanjinti[®]) to 14.33 (Ogivri[®]) peaks for the trastuzumabs, we were unable to confidently identify them based on the LC-FLR spectra of the standard alone. Therefore, we need to employ a third-party software, such as Protein Metrics, which has libraries built in for all common fluorescence tags, in order to directly compare the three kits. The released glycan workflow from Protein Metrics can take the back-end QTOF data and process it to output glycan identifications and quantifications. We plan to complete this head-to-head comparison in the future once the Protein Metrics software is integrated with the QTOF. It is also worth noting that other publications, including the aforementioned ones, have reported data for different fluorescence labels that can act as references.

With regards to Herceptin[®] and its biosimilars Kanjinti[®] and Ogivri[®], we did notice significant differences in the relative contribution of lower abundance glycans. We found that the two biosimilars, Kanjinti[®] and Ogivri[®], tended to be significantly different from each other but not always significantly different from Herceptin[®]. This is apparent in the mannosylated data shown in figure 5 where we observed a significantly higher % mannosylated for Ogivri[®] compared to Kanjinti[®] and Herceptin[®]. While there was no statistical significance between Kanjinti[®] and Herceptin[®] with regards to % mannosylated, Kanjinti[®] was lower (1.01 ± 0.38) compared to Herceptin[®] (3.05 ± 1.21). The % sialylated had a similar trend with Ogivri[®] being significantly greater than Kanjinti[®] and Herceptin[®]. No statistical significance was detected between Kanjinti[®] and Herceptin[®], but Kanjinti[®] was the lowest of the three trastuzumabs.

Similarity to Herceptin[®] is expected as these products have been approved and should be matching Herceptin[®] closely in glycan profile. That is why it is unsurprising that there are no differences between Herceptin[®] and Kanjinti[®], but is it unexpected that there are significant differences between Herceptin[®] and Ogivri[®] with regards to % mannosylated and % sialylated glycans. However, our sample set was rather small and we only looked at one lot per trastuzumab for the case study, which may explain these differences.

What is more interesting from this data though is that the Ogivri[®] and Kanjinti[®] appear to be more different from each other than from Herceptin[®]. Generally, most developers are concerned with their products' comparability to the innovator rather than to their biosimilar competitors because similarity to the reference is what matters for approval. Therefore, there are few publications discussing the glycan heterogeneity between the multiple biosimilars for the same reference product. [155, 156] Ones that do compare biosimilars may still focus on biosimilar comparability to innovator rather than to other biosimilars for the same reference product. [157] Yet, the differences we noted here and the differences Grampp et al. and Kaur et al. observed in their studies beg the question of whether these products could be used interchangeably in the future. If they do have significantly different glycan profiles from each other, would they satisfy the safety and efficacy requirements needed to be met for patient switching studies? Does this call into question the acceptable range for glycan heterogeneity of biosimilars? As interchangeability is another area of interest for BSUFA III, more research from our group and others needs to be conducted in order to determine the extent to which biosimilars for the same reference product may be significantly different from each other, yet still safe and effective. We need to increase the number of lots studied for each protein and expand our studies into other mAbs in order to identify trends and highlight consistent discrepancies in glycan profiles across multiple biosimilars.

Tangential to this future work is the idea that there needs to be more dissemination of information on "failed" mAbs products. While our data can provide the foundation for

building out a guidance for glycan analysis, we recognize that we have only tested a small subset of mAbs with well-characterized glycan profiles and, in the case of trastuzumab, ones that are known to be tolerable in patients. This means we are working with the cream of the crop to design a standardized set of methods. Working with approved proteins perhaps does not appropriately account for acceptable deviations from the norm. We need to also understand the extremes, by studying “failed” mAb products, in order to establish goalposts and adequate ranges for acceptable glycan criteria. Currently, there is limited public data of detailing the glycan profiles of “failed” mAb products or batches that did not move forward due to possible concerns related to glycosylation. Without such knowledge, it can be challenging to make statements that specific glycans are known to reduce *in vitro* efficacy, pose safety concerns, alter protein folding, etc. If this “failed” mAb data was published, it could benefit industry and the FDA alike as it may shape the acceptance criteria ranges for glycans. It also plays a hand in the standardization and validation of glycan analysis methods – perhaps even leading to new guidances in this field.

In a similar vein, publications on “negative clinical studies”, which would show how despite differences in the relative contribution of mannosylated glycans, for example, there is no clinically meaningful impact on safety or efficacy in patients, are also lacking. Contrary to the concern about switching patients between Kanjinti[®] and Ogivri[®] given their significantly different glycan profiles, these studies would dispel concerns about interchangeability. As it stands, we can attempt to retroactively compare published clinical data and determine whether there are significant differences that could point to poor structural features. For example, we found that Ogivri[®] had significantly higher % contributions of mannosylated and sialylated glycans compared with Kanjinti[®]. As described above, these two glycans have been linked to immunogenicity and/or increased clearance rates. Given this information, we hypothesize that there could be differences in ADA formation and/or pharmacokinetics between the two biosimilars. We would expect Ogivri[®] to have more ADA formation and faster clearance rates compared with Kanjinti[®] because

it has larger contributions of mannosylated and sialylated glycans.

When reading the Ogivri[®] European assessment report, we discovered that 9 patients (3.9%) in the clinical study reported ADAs by week 48. Of those, only 1 patient (0.4%) had neutralizing antibodies. Meanwhile, the Herceptin[®] studied in tandem reported overall ADA formation in 10 patients (4.4%), of which 3 patients (1.3%) had neutralizing antibodies. [158] From this study, it appears that the two drugs are highly similar and, if anything, Ogivri[®] had slightly favorable immunogenicity. Yet, due to patient specific factors, it is hard to draw a definitive conclusion as to how each individual would respond. With regards to pharmacokinetics, Ogivri[®] did have slightly a faster half-life (6.95 days) and clearance rate (0.296 L/day) compared to Herceptin[®] (7.02 days and 0.278 L/day, respectively). [158] However, these differences were not deemed significant. Nevertheless, it is interesting because perhaps the mannosylated glycans are having a slight impact on the pharmacokinetics.

When looking through the Kanjinti[®] European assessment report, we had a much harder time finding similar data. This is more evidence yet about the inability to directly compare two biosimilars. Rather than half-lives or clearance rates, our preferred values for direct pharmacokinetic comparison, C_{trough} levels were reported in the Kanjinti[®] assessment report. Kanjinti had a C_{trough} of 53.5 vs. 52.8 µg/mL for Herceptin[®] during the adjuvant phase after the sixth dose. [159] These two values suggest highly similarity and while we observed that Kanjinti[®] had a lower % contribution of mannosylated glycans than Herceptin[®], it was not statistically significant. Therefore, this data corroborates our results. During the adjuvant phase, 0.6% of patients receiving Kanjinti[®] formed ADA and 1.2% receiving Herceptin[®] formed ADA. None of those were reportedly neutralizing ADA. [159] It was noted in the assessment report that these immunogenicity levels were very low compared with other biosimilar/innovator studies. Therefore, this could call into question the types of methods that were used to detect the ADA.

Given the inability to directly compare multiple biosimilars for the same reference

based on retrospective analyses, clinical studies with arms for each biosimilar and the reference product would be necessary to make more confident claims. These clinical studies might be “negative” in that, in theory, they should not show significant differences across all groups. While these would be expensive up-front, they could benefit the field as a whole. These multiple biosimilar, “negative” clinical studies, in conjunction with new glycan analysis guidances, could act as evidence to reduce or even eliminate burdensome phase 3 studies, provided *in vitro* analyses and early phase clinical studies showed no apparent concerns in safety or efficacy. Although this clinical work is out of the scope of our group’s expertise, we could continue performing glycan characterization in tandem with animal studies. In these animal studies we could measure pharmacokinetics, ADAs, provided we use humanized mice, and/or therapeutic activity. The results from our glycan analyses and subsequent animal studies could prove useful in justifying the reduction or elimination of phase 3 clinical trials.

Our data presented here is far from making waves in the biologics industry. Nevertheless, it provides groundwork for glycan method standardization, guidance development, and potential modifications to biosimilar clinical trial requirements. It also highlights that there is not only variability in the data outputs from various glycan analysis methods, but also variability in how this data can be interpreted and implemented. Our data might be useful in clarifying interchangeability designations and requirements. On the other hand, it might be useful in supporting claims that some significant differences in relative contribution of low abundance glycans are not clinically meaningful. Regardless of the final impact it makes in the field, our data comparing mAb glycan profiles identified via LC-FLR released glycan kits, intact MS and LC-MS/MS after protein digestion can spark conversation between stakeholders to improve current practices for glycan analysis. Further work applying these methods, especially protein digestion with LC-MS/MS detection, on multiple innovator mAbs and available biosimilars treated under normal and stressed conditions is needed to truly make substantial claims. As we continue expanding our data

set with more innovators and biosimilars, we hope to provide industry, regulatory and academic affiliates with more knowledge to draw from as they streamline their respective areas of expertise.

CHAPTER V

Research Summary and Future Directions

The previous chapters have highlighted our research on PTM characterization methods and *in vitro* functional assays for mAb products. Our overarching goals for this thesis was to aid in enhancing the knowledge of therapeutic mAb characteristics prior to patient administration. Ideally, in doing so, we help streamline the biologics development and approval timelines. In this final chapter we have summarized how we have met the over arching goal, along with how we have attained other project-specific goals. We also describe potential areas for future work to broaden the research impact.

5.1 Introduction of Concluding Thoughts

Throughout this thesis, I described characterizing PTMs on mAbs with the intention of applying our findings to identify structure-function relationships, streamline and automate methods, highlight innovator/biosimilar differences, and establish standardized best practices. The outcomes of each project varied, yet all emphasized the importance of analyzing PTMs on mAbs in order to better understand possible safety, efficacy, activity, immunogenicity, and/or pharmacokinetic concerns that could arise in patients. After all, while we envision that the pharmaceutical industry and regulatory agencies will be the main beneficiaries and primary users of this research, it is the health of the patients that we are ultimately striving to improve with our work.

5.2 Chapter Summaries

5.2.1 Chapter II: Anti-TNF α mAb Structure and Function Characterization

Three anti-TNF α mAbs, Humira[®], Remicade[®] and Simponi Aria[®], are all approved for similar autoimmune indications, so it is important to understand how they differ prior to administration in patients. Method, user, and site variability can impact data outcomes, thus preventing unbiased comparisons. To address this, we became the first group, to our knowledge, to perform a direct comparison of these products by studying their glycosylation patterns via LC-MS/MS and binding activities via Fab ELISA, Fc γ RIIIa AlphaLISA, and ADCC. Upon conclusion of our experiments, we found that Humira[®] had the fewest unique glycans (15) along with the highest Fc binding affinity (IC₅₀: $2.14 \times 10^{-6} \pm 1.13$ g/mol) and ADCC potency (EC₅₀: 0.55 ± 0.03 nM). This perhaps suggests that Humira[®] is more efficacious than Remicade[®] or Simponi Aria[®] since it has stronger effector functionality. It is worth noting, though, that there are other confounding variables such as genetics and disease state that can influence efficacy, safety and pharmacokinetics in patients. Therefore, the main takeaway from this study is that significant differences in the structure and function of three approved anti-TNF α mAbs do exist and should be considered not only during novel and biosimilar drug development, but also when physicians are determining appropriate treatments for their patients.

5.2.2 Chapter III: Disulfide Shuffling Analysis in mAb Innovators and Biosimilars

Shuffled disulfide bonds are PTMs known to alter protein conformation, potentially leading to reduced target binding and/or increased aggregation. Despite the impacts on efficacy and safety that shuffled disulfide bonds may induce, not many groups have published methods for shuffled disulfide bond characterization on IgG1 mAbs. Even fewer have studied shuffled bonds across innovator/biosimilar pairs. By monitoring the forma-

tion of shuffled disulfide bonds and degradation of rituximabs and bevacizumabs over time, we established streamlined protocols for such analyses. We also highlighted that while the innovator/biosimilar pairs behaved similarly, as one may expect given that they are approved as the same protein, different IgG1 mAbs can vary in their structural features and their degradation propensity. Innovator bevacizumab had an upward trend in shuffled disulfide bonds ($0.58\pm 0.08\%$ to $1.46\pm 1.10\%$) and formed more aggregates over time, whereas innovator rituximab maintained its shuffled disulfide bond level ($0.24\pm 0.21\%$ to $0.51\pm 0.11\%$) and formed more fragments over time. While it is important to understand under what conditions and with what modifications mAbs begin to degrade, one of the bigger takeaways from this research was learning how to apply newer technologies to PTM characterization. By digesting our samples using an AssayMAP Bravo Liquid Handling Platform and processing LC-MS/MS data using the Protein Metrics disulfide bond workflow, we were able to streamline the time and effort put in to analyzing lower abundance, yet still important, PTMs.

5.2.3 Chapter IV: Comparison of Glycan Profiling Methods for mAbs

Numerous glycan analysis methods currently exist, yet there is no established guidance detailing best practices and expected data outcomes for the available methods. Without such a guidance, it can be challenging for industry to know what is acceptable data in the eyes of the FDA. Therefore, by performing five different glycan analysis techniques: three FLR released glycans kits, protein digestion followed by LC-MS/MS and intact MS using NIST mAb as a standard mAb, we aimed to determine the most sensitive, reproducible, and robust method. From this initial study, as expected, we found that the protein digestion followed by LC-MS/MS identified the most glycans, including some low abundance glycans. We then applied these methods to Herceptin[®] and its biosimilars, Kanjinti[®] and Ogivri[®] to see whether the digestion method was still the most sensitive. The trastuzumabs did have similar trends compared to NIST mAb and the di-

gestion was able to tease out significant differences between the trastuzumab biosimilars. Interestingly, Kanjinti[®] and Ogivri[®] were more different from each other than they from Herceptin[®] (Kanjinti[®] had a relative % mannosylated contribution of $1.01 \pm 0.38\%$ while Ogivri[®] was $5.95 \pm 0.97\%$ and Herceptin[®] was $3.05 \pm 1.21\%$). These findings call into question the feasibility of approving and prescribing interchangeable biosimilars of the same reference product. Key conclusions from this research include the need for glycan method standardization, validation and implementation, as well as the fact the biosimilars of the same product might be similar enough to their reference, but different enough from competitors to warrant caution while switching patients.

5.3 Broader Future Directions

As an extension of this thesis work, our group plans to continue expanding our knowledge by analyzing other mAbs and their biosimilars under various storage conditions, as well as by exploring other PTMs including oxidation, methylation and deamidation. Ideally, we would like to create a toolkit down the line that has optimized, validated methods for common PTMs on mAbs (figure 5.1). To do so, we have to begin working at a higher throughput by analyzing large sample sets containing multiple types of mAbs, along with multiple batches of the each mAb, on the same plate. This requires us to further explore automation both for benchwork and for data processing. Fortunately, the timing for increasing automation is aligned with many advances in the field.

The use of artificial intelligence (AI) has been exponentially growing as accessibility and feasibility for using it has increased over the past few years. People are becoming more confident in utilizing AI to help design and test methods for sample preparation and processing. Take ChatGPT for example - scientists are now asking it questions ranging from “what are ideal formulation conditions for a therapeutic mAb?” to “how does one develop a protocol for in-solution protein digestion on a liquid handling platform?” and beyond. By learning scientific protocols through crowdsourced knowledge, ChatGPT and other AI

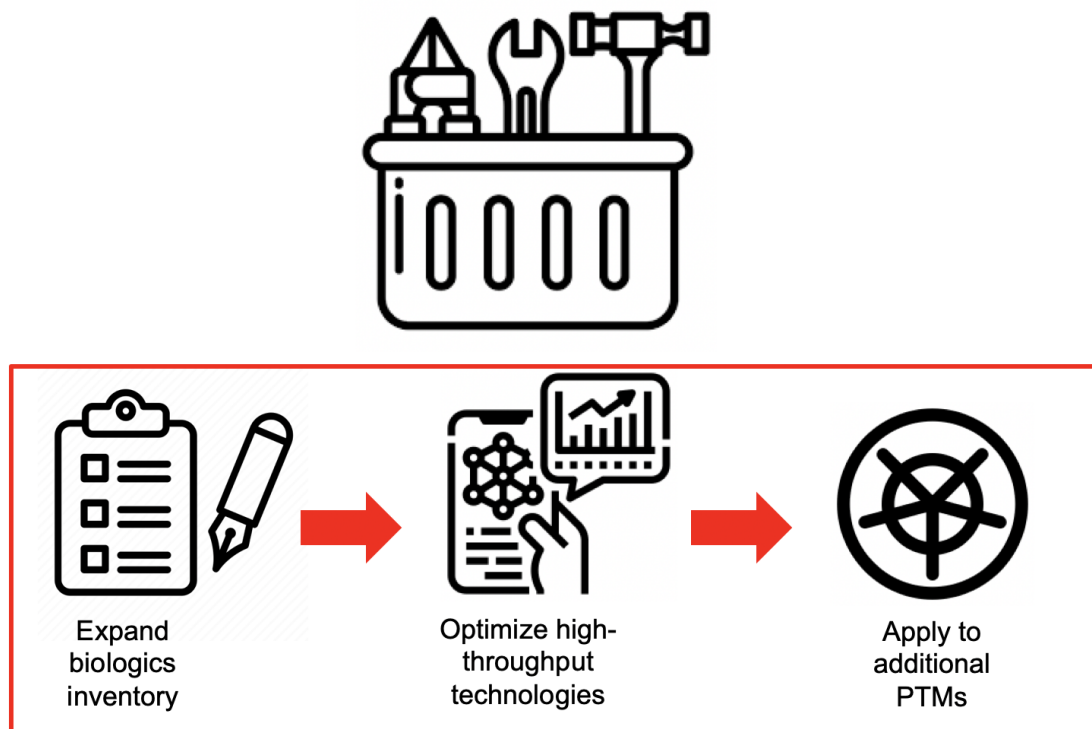


Figure 5.1: Proposed workflow for designing a broadly applicable PTM toolkit.

platforms can not only share appropriate method suggestions, but can aid in streamlining drug development and identifying potential drug development challenges. Therefore, we believe that with more training AI can be used to design and implement automation platforms. Perhaps it may be able to sequentially test sample preparation methods on a robotic system, independent of human interference, in order to determine an optimized protocol. The options for utilizing AI are endless provided creative minds are asking it the right questions.

Automation for the data processing is already in place, as described in all of the prior thesis chapters. We used a mass spectrometry software called Protein Metrics to deconvolute and analyze our raw files. The default workflows are relatively straightforward, easy to learn and can be adjusted to suit one’s needs. For the purposes of this thesis research, we also went back through the automatically processed data to flag any false positives or missing peptides. By doing so, we aimed to ensure the presented data was correct to

the best of our abilities. In the future we may train AI to complete the “second check”, looking for signs of potential false positives in the processed data and flagging them for a follow-up. The more fine-tuned the AI gets at reading the processed data, the better it should be at identifying potential false positives or missing peptides.

Of course, there are always caveats with automation that we have to be aware of. With regards to sample processing, we have to be wary of potential mechanical issues within the robot that the AI might not detect (i.e. a broken syringe head that is not picking up the full volume of reagent). Additionally, when it comes to mAbs and other proteins, not every therapeutic thrives under the same conditions. Therefore, just because AI recognized that one method works for previous samples does not mean it can be applied to all samples. Scientists still need to comb through data and determine whether the method worked well and can be reproduced on a larger scale.

Within some mass spectrometry software packages there are concerns about the imputation and matching between runs that can occur. Automatic imputation could impact the total number and types of proteins, peptides or other species identified by the software. This, in turn, may lead to artificially increased protein discovery within samples, perhaps leading to false identification of proteins. False identification of proteins could influence whether a project or drug candidate progresses, so it is critical to understand how to appropriately use AI without solely relying on default settings and automatic processing. To address such issues, there are various q-value and p-value filtering options within these platforms that can be applied.

Additionally, recent advancements in mass spectrometry instrumentation will make high throughput more feasible. ThermoFisher recently unveiled their latest mass spectrometer – an Orbitrap Astral – that allegedly enables the analysis of 180 samples per day with a cycle time of 8 minutes. High sensitivity is another hallmark of the Orbitrap Astral. It can identify over 8,000 proteins in the 8-minute cycles or 12,000+ proteins in 60-minute cycles for human cell lysates. [160] This is far faster than existing runs times and, if it

performs as claimed, could drastically alter the expected norms for sensitivity, resolution, protein identification and overall efficiency.

Circling back to the idea of the toolkit, we believe that we can start developing a list of PTM best practices using our existing methods in parallel with AI generated methods. We would like to incorporate more automation and AI in our protocols to mirror advancements available for the pharmaceutical industry. Once we have that in hand, we need to expand our inventory by procuring more mAb lots and multiple lots of other protein types (i.e. Fc fusion proteins, Fabs, nanobodies). With the expanded inventory, we aim to perform our “toolkit” methods at a higher throughput, monitoring for multiple attributes including glycosylation, deamidation, oxidation, methylation, etc. We envision that once we have data from additional samples, this toolkit can be approved by the FDA as a guidance, setting the precedent for the FDA’s expectations on reported data prior to BLA submissions. In doing so, we would be reducing the uncertainty from the drug sponsor’s end regarding what data needs to be collected, all while creating unified guidelines and acceptance criteria for FDA reviewers.

Along with the *in vitro* toolkit and utilization of automation/AI, another area for further exploration would be *in vivo* animal studies. As described in chapters II and IV, immunogenicity is a concern for mAbs as they relate not only to the efficacy of the drug, but also to patient safety. To test for immunogenicity, we have to monitor the ADA formation *in vivo* after administration of a therapeutic. While there are a number of factors that influence the immunogenicity of a therapeutic and the likelihood of adverse events – including patient-specific and manufacturing factors beyond the scope of this thesis research – we are interested in determining the extent to which PTMs could be inducing immunogenicity.

As described earlier, certain glycans are known to be precursors of immunogenicity. For example, since mannosylated glycans are recognized by endogenous mannose receptors on antigen presenting cells, they can be flagged as foreign by the immune system

faster than other glycan species. Therefore, it is likely that the body will more readily generate ADAs for mannosylated mAb therapeutics. As ADAs are precursors for immunogenicity and adverse events, measuring their formation over the course of a dosing regimen is critical to maintaining patient safety. Similarly, the quicker recognition and uptake of mannosylated species translates to faster clearance rates. Thus, the mAb pharmacokinetics are altered and overall efficacy is reduced. To measure ADAs and pharmacokinetics, we have to conduct *in vivo* animal studies.

There are many iterations by which we could perform such studies – looking at different disease states, looking at different therapeutic classes, looking at different animal models, etc. However, to extend the research described in this thesis, namely the research detailed in chapter IV, we want to study biosimilar-innovator and biosimilar-biosimilar mAb pairs with significantly different glycan profiles *in vivo*. In chapter IV we found that there were significant differences in % mannosylated glycans between biosimilars (Kanjinti[®] and Ogivri[®]) of the same reference product (Herceptin[®]). While the two were relatively similar to Herceptin[®] in their % mannosylated glycan contributions, they were significantly different from each other. This begs the question of whether the two biosimilars could be safely and effectively interchanged with each other. To understand the effects that glycans can have on the interchangeability of products, we again have to test *in vivo*. *In vivo* studies will give us a clearer picture as to how body systems respond to different treatments. If the *in vivo* pharmacokinetics, therapeutic activity and ADA formation are similar across treatment groups, then we will have more confidence in the interchangeability of biosimilars for the same reference product. If there are significant differences in how well a biosimilar performs and/or is tolerated, then further research needs to be conducted to identify all potential causes.

Additionally, performing these *in vivo* studies may help in elucidating acceptance ranges for glycan profiles. During interviews with biosimilar companies, we learned that there is a gap in knowledge regarding guidances explicitly detailing the acceptance cri-

teria for differences in glycan profiles across biosimilars and innovators. Therefore, it is challenging for companies to know whether their slightly varied glycan profile will appreciably impact the overall safety and efficacy of the drug product. To address these possible concerns, companies perform numerous *in vitro* and *in vivo* experiments to exemplify the comparable safety and efficacy of their biosimilar product. If we could perform preemptive *in vivo* studies within our lab, we may be able to establish general criteria and expectations for varied glycan profiles and their impact on *in vivo* efficacy, immunogenicity, safety and pharmacokinetics. These studies could act as a reference for pharmaceutical companies as they design appropriate experiments with their own biosimilar products. Similarly, if implemented as an FDA approved guidance document, it could become a “gold standard” for reviewers and sponsors alike to reference as a protein product moves throughout its development, submission and approval processes.

In tandem with the *in vitro* toolkit, we would also conduct *in vivo* animal studies to give a deeper context for potential safety, efficacy and/or pharmacokinetic adverse events. For example, if we find that there are significant differences in % mannosylated glycans between biosimilars of the same reference product, which are hypothesized to influence pharmacokinetics, we might conduct animal studies to determine if the significant differences we detected *in vitro* correlate to significant differences in clearance rates *in vivo*. This *in vivo* data would help bolster our claims that certain *in vitro* methods are more most sensitive, reproducible, reliable and robust.

To achieve our lofty goals, we need buy-in from various stakeholders. The capabilities of our lab are limited in that we currently can perform routine PTM analyses on approved products, allowing us to set “gold standards” and “goalposts” in conjunction with regulatory agencies. We also can conduct *in vivo* animal studies on different approved biosimilars and innovators, monitoring for clearance rate, ADA formation, and disease improvement. However, our capabilities to implement certain AI technologies and access state-of-the-art instruments are dependent on collaborations. We need to maintain relationships with



Figure 5.2: Schematic of relevant stakeholders involved in biologics research, development, approval and administration.

people from the pharmaceutical/biotech industry, healthcare systems, academic institutions and regulatory agencies in order to progress in the field of antibody and protein therapeutic research (Figure 5.2).

Another key point to emphasize is that our lab can only test approved products that can be acquired through our hospital pharmacy. Without access to failed products with non-ideal PTM profiles, we cannot stress test these methods to determine the appropriate method and parameters extremes. For example, just because a product may not fall within the % shuffled disulfide bonds range established based on approved products tested in our lab, does not necessarily mean that the product will be ineffective in patients. In fact, the product may prove to be just as, if not more, effective and safe than its competitors when tested in animals and clinical studies. Unless we have access to failed products to determine “breaking points” where we start to see adverse events or therapeutic non-

response in animals, acceptance criteria may remain tight. Hence another reason we are discussing *in vivo* studies to monitor multiple biosimilars and innovators over time. Again, to further broaden the scope of our research we would not only study approved and failed mAb products, but also expand into other biologics like Fc fusion proteins or Fabs.

In sum, this thesis work provides groundwork for future PTM method optimization, validation and standardization. To continue building off of the foundation, more mAbs and other biologics have to be analyzed, with their PTMs characterized, through multiple orthogonal methods. *In vivo* studies should also be conducted to bolster available data in areas such as innovator/biosimilar or biosimilar/biosimilar pharmacokinetic, immunogenicity and/or activity comparisons. This data can be correlated with various significant *in vitro* structural and functional characterization features on the therapeutic. We believe that this advancement can occur, but it will require collaborative work to generate novel techniques, access state-of-the-art technologies, implement AI, and develop applicable method systems. An overarching goal of this research is to foster relationships between individuals in academia, the pharmaceutical industry, regulatory agencies, and clinical practices to create robust enough methods that can be applied to many future products. Hopefully years down the line substantive PTM guidances exist and are used regularly in practice. Perhaps the availability of guidances and *in vivo* reference materials can spark conversations around ways to minimize the long, expensive, arduous studies currently required for FDA submissions. This research, if expanded upon and applied to related products and processes, has the potential to initiate positive growth in the biologics field.

BIBLIOGRAPHY

BIBLIOGRAPHY

- [1] J. Kang, *et al.*, “Infliximab biosimilars in the age of personalized medicine”, *Trends in Biotechnology* **36**, 987 (2018). DOI: 10.1016/j.tibtech.2018.05.002.
- [2] K. Pisupati, *et al.*, “A multidimensional analytical comparison of remicade and the biosimilar remsima”, *Analytical Chemistry* **89**, 4838 (2017). DOI: 10.1021/ACS.ANALCHEM.6B04436.
- [3] A. M. Goetze, *et al.*, “High-mannose glycans on the fc region of therapeutic igg antibodies increase serum clearance in humans”, *Glycobiology* **21**, 949 (2011). DOI: 10.1093/GLYCOB/CWR027.
- [4] B. J. Scallon, S. H. Tam, S. G. Mccarthy, A. N. Cai, T. S. Raju, “Higher levels of sialylated fc glycans in immunoglobulin g molecules can adversely impact functionality”, *Molecular Immunology* **44**, 1524 (2007). DOI: 10.1016/j.molimm.2006.09.005.
- [5] S. Carillo, *et al.*, “Comparing different domains of analysis for the characterisation of n-glycans on monoclonal antibodies”, *Journal of Pharmaceutical Analysis* **10**, 23 (2020). DOI: 10.1016/J.JPHA.2019.11.008.
- [6] L. Zhang, C. P. Chou, M. Moo-Young, “Disulfide bond formation and its impact on the biological activity and stability of recombinant therapeutic proteins produced by escherichia coli expression system”, *Biotechnology Advances* **29**, 923 (2011). DOI: 10.1016/j.biotechadv.2011.07.013.
- [7] H. Shion, *et al.*, “Smartms-enabled lc-ms system for biotherapeutic development in regulated/non-regulated environments”, *CASSS Conference* (2019).
- [8] B. Buntz, “The 50 best-selling pharmaceuticals of 2022: Covid-19 vaccines poised to take a step back” (2023).
- [9] X. Lyu, *et al.*, “The global landscape of approved antibody therapies”, *Antibody Therapeutics* **5**, 233 (2022). DOI: 10.1093/abt/tbac021.
- [10] FDA, “Fda biologics definitions”.
- [11] J. Kang, *et al.*, “Multifaceted assessment of rituximab biosimilarity: The impact of glycan microheterogeneity on fc function”, *European Journal of Pharmaceutics and Biopharmaceutics* **146**, 111 (2020). DOI: 10.1016/J.EJPB.2019.12.003.

- [12] N. Nupur, N. Chhabra, R. Dash, A. S. Rathore, "Assessment of structural and functional similarity of biosimilar products: Rituximab as a case study", *mAbs* **10**, 143 (2018). DOI: 10.1080/19420862.2017.1402996.
- [13] K. Pisupati, *et al.*, "Biosimilarity under stress: A forced degradation study of remicade® and remsima™", *mAbs* **9**, 1197 (2017). DOI: 10.1080/19420862.2017.1347741.
- [14] J. Lee, *et al.*, "Evaluation of analytical similarity between trastuzumab biosimilar ct-p6 and reference product using statistical analyses", *mAbs* (2018). DOI: 10.1080/19420862.2018.1440170.
- [15] B. Gürel, *et al.*, "Optimized methods for analytical and functional comparison of biosimilar mab drugs: A case study for avastin, mvasi, and zirabev", *Scientia Pharmaceutica* **90** (2022). DOI: 10.3390/scipharm90020036.
- [16] D. D. Vallejo, *et al.*, "Collision-induced unfolding reveals stability differences in infliximab therapeutics under native and heat stress conditions" (2021). DOI: 10.1021/acs.analchem.1c03946.
- [17] M. Sorensen, *et al.*, "Comparison of originator and biosimilar therapeutic monoclonal antibodies using comprehensive two-dimensional liquid chromatography coupled with time-of-flight mass spectrometry", *mAbs* **8**, 1224 (2016). DOI: 10.1080/19420862.2016.1203497.
- [18] N. Lee, *et al.*, "Evaluation of similar quality attribute characteristics in sb5 and reference product of adalimumab", *mAbs* (2019). DOI: 10.1080/19420862.2018.1530920.
- [19] X. Wang, Z. An, W. Luo, N. Xia, Q. Zhao, "Molecular and functional analysis of monoclonal antibodies in support of biologics development" (2018).
- [20] K. D. Ratanji, J. P. Derrick, R. J. Dearman, I. Kimber, "Immunogenicity of therapeutic proteins: Influence of aggregation" (2014).
- [21] T. Mouchahoir, J. E. Schiel, "Development of an lc-ms/ms peptide mapping protocol for the nistmab", *Analytical and Bioanalytical Chemistry* **410**, 2111 (2018). DOI: 10.1007/s00216-018-0848-6.
- [22] Y. Cheng, Y. Chen, C. Yu, "Fast and efficient non-reduced lys-c digest using pressure cycling technology for antibody disulfide mapping by lc-ms", *Journal of Pharmaceutical and Biomedical Analysis* **129**, 203 (2016). DOI: 10.1016/j.jpba.2016.07.002.
- [23] B. Shah, X. G. Jiang, L. Chen, Z. Zhang, "Lc-ms/ms peptide mapping with automated data processing for routine profiling of n-glycans in immunoglobulins", *Journal of the American Society for Mass Spectrometry* **25**, 999 (2014). DOI: 10.1007/s13361-014-0858-3.
- [24] P. Jiang, F. Li, J. Ding, "Development of an efficient lc-ms peptide mapping method using accelerated sample preparation for monoclonal antibodies", *Journal of Chromatography B: Analytical Technologies in the Biomedical and Life Sciences* **1137** (2020). DOI: 10.1016/j.jchromb.2019.121895.

- [25] C. Proteomics, “Orbitrap fusion lumos tribrid mass spectrometer”.
- [26] B. Sissolak, N. Lingg, W. Sommeregger, G. Striedner, K. Vorauer-Uhl, “Impact of mammalian cell culture conditions on monoclonal antibody charge heterogeneity: an accessory monitoring tool for process development”, *Journal of Industrial Microbiology and Biotechnology* **46**, 1167 (2019). DOI: 10.1007/s10295-019-02202-5.
- [27] WHO, “Guidelines for the production and quality control of monoclonal antibodies and related products intended for medicinal use” (2022).
- [28] L. Zhang, *et al.*, “Analysis of monoclonal antibody sequence and post-translational modifications by time-controlled proteolysis and tandem mass spectrometry”, *Molecular and Cellular Proteomics* **15**, 1479 (2016). DOI: 10.1074/mcp.O115.056721.
- [29] L. Christl, “Overview of the regulatory pathway and fda’s guidance for the development and approval of biosimilar products in the us”.
- [30] FDA, “Guidance for industry q8(r2) pharmaceutical development” (2009).
- [31] FDA, “Biosimilars info sheet level 2: Regulatory and scientific concepts variation in biological products”.
- [32] R. Upton, *et al.*, “Hybrid mass spectrometry methods reveal lot-to-lot differences and delineate the effects of glycosylation on the tertiary structure of herceptin®”, *Chemical Science* **10**, 2811 (2019). DOI: 10.1039/c8sc05029e.
- [33] S. Colombo, *et al.*, “Improvement of monoclonal antibody stability by modulating trace metal iron concentration in cell culture media: A case study”, *Process Biochemistry* **125**, 130 (2023). DOI: 10.1016/j.procbio.2022.12.013.
- [34] L. Liu, “Antibody glycosylation and its impact on the pharmacokinetics and pharmacodynamics of monoclonal antibodies and fc-fusion proteins”, *Journal of Pharmaceutical Sciences* **104**, 1866 (2015). DOI: 10.1002/jps.24444.
- [35] J. Coghlan, H. He, A. S. Schwendeman, “Overview of humira® biosimilars: Current european landscape and future implications”, *Journal of Pharmaceutical Sciences* **110**, 1572 (2021). DOI: 10.1016/J.XPHS.2021.02.003.
- [36] C. J. Janeway, P. Travers, M. Walport, *The structure of a typical antibody molecule - Immunobiology - NCBI Bookshelf* (Garland Science, 2001).
- [37] F. Higel, A. Seidl, F. Sörgel, W. Friess, “N-glycosylation heterogeneity and the influence on structure, function and pharmacokinetics of monoclonal antibodies and fc fusion proteins”, *European Journal of Pharmaceutics and Biopharmaceutics* **100**, 94 (2016). DOI: 10.1016/j.ejpb.2016.01.005.
- [38] G. Vidarsson, G. Dekkers, T. Rispens, “Igg subclasses and allotypes: From structure to effector functions”, *Frontiers in Immunology* **5**, 520 (2014). DOI: 10.3389/fimmu.2014.00520.

- [39] FDA, CDER, “Guidance for industry immunogenicity assessment for therapeutic protein products” (2014).
- [40] G. R. Gunn, *et al.*, “From the bench to clinical practice: understanding the challenges and uncertainties in immunogenicity testing for biopharmaceuticals” (2016).
- [41] M. Abrouk, *et al.*, “The impact of pasi 75 and pasi 90 on quality of life in moderate to severe psoriasis patients”, *Journal of Dermatological Treatment* **28**, 488 (2017). DOI: 10.1080/09546634.2016.1278198.
- [42] J. A. Goldman, H. A. Xia, B. White, H. Paulus, “Evaluation of a modified acr20 scoring system in patients with rheumatoid arthritis receiving treatment with etanercept”, *Annals of the Rheumatic Diseases* **65**, 1649 (2006). DOI: 10.1136/ard.2005.047266.
- [43] D. T. Felson, M. P. LaValley, “The acr20 and defining a threshold for response in rheumatic diseases: Too much of a good thing”, *Arthritis Research and Therapy* **16** (2014). DOI: 10.1186/ar4428.
- [44] “Validity of outcome measures” (2017).
- [45] D. Houde, Y. Peng, S. A. Berkowitz, J. R. Engen, “Post-translational modifications differentially affect igg1 conformation and receptor binding”, *Molecular Cellular Proteomics* **9**, 1716 (2010). DOI: 10.1074/mcp.M900540-MCP200.
- [46] C. L. Pierri, *et al.*, “Molecular modeling of antibodies for the treatment of tnfa-related immunological diseases”, *Pharmacology Research and Perspectives* **4**, e00197 (2016). DOI: 10.1002/prp2.197.
- [47] T. Shinkawa, *et al.*, “The absence of fucose but not the presence of galactose or bisecting n-acetylglucosamine of human igg1 complex-type oligosaccharides shows the critical role of enhancing antibody-dependent cellular cytotoxicity”, *Journal of Biological Chemistry* **278**, 3466 (2003). DOI: 10.1074/jbc.M210665200.
- [48] R. L. Shields, *et al.*, “Lack of fucose on human igg1 n-linked oligosaccharide improves binding to human fcγriii and antibody-dependent cellular toxicity”, *Journal of Biological Chemistry* **277**, 26733 (2002). DOI: 10.1074/jbc.M202069200.
- [49] B. Radovani, I. Gudelj, “N-glycosylation and inflammation; the not-so-sweet relation”, *Frontiers in Immunology* **13** (2022). DOI: 10.3389/fimmu.2022.893365.
- [50] S. Boune, P. Hu, A. L. Epstein, L. A. Khawli, “Principles of n-linked glycosylation variations of igg-based therapeutics: Pharmacokinetic and functional considerations”, *Antibodies* **9**, 1 (2020). DOI: 10.3390/antib9020022.
- [51] M. J. Buettner, S. R. Shah, C. T. Saeui, R. Ariss, K. J. Yarema, “Improving immunotherapy through glycodeign”, *Frontiers in Immunology* **9** (2018). DOI: 10.3389/fimmu.2018.02485.

- [52] K. P. Pratt, “Anti-drug antibodies: Emerging approaches to predict, reduce or reverse biotherapeutic immunogenicity”, *Antibodies* **7** (2018). DOI: 10.3390/antib7020019.
- [53] A. Vaisman-Mentesh, M. Gutierrez-Gonzalez, B. J. DeKosky, Y. Wine, “The molecular mechanisms that underlie the immune biology of anti-drug antibody formation following treatment with monoclonal antibodies”, *Frontiers in Immunology* **11** (2020). DOI: 10.3389/fimmu.2020.01951.
- [54] F. Kuhne, *et al.*, “The impact of immunoglobulin g1 fc sialylation on backbone amide h/d exchange”, *Antibodies* **8**, 49 (2019). DOI: 10.3390/antib8040049.
- [55] X. Zhou, *et al.*, “Antibody glycosylation in autoimmune diseases”, *Autoimmunity Reviews* **20** (2021). DOI: 10.1016/j.autrev.2021.102804.
- [56] M. H. C. Biermann, *et al.*, “Sweet but dangerous – the role of immunoglobulin g glycosylation in autoimmunity and inflammation”, *Lupus* **25**, 934 (2016). DOI: 10.1177/0961203316640368.
- [57] C. Hofvander, “Bioinvent’s bi-1607 to extend reach of anti-fcyriib approach to breast cancer”, *BioInvent Press Release* (2022).
- [58] Y. Mimura, *et al.*, “Glycosylation engineering of therapeutic igg antibodies: challenges for the safety, functionality and efficacy”, *Protein and Cell* **9**, 47 (2018). DOI: 10.1007/s13238-017-0433-3.
- [59] K. T. C. Shade, R. M. Anthony, “Antibody glycosylation and inflammation”, *Antibodies* **2**, 392 (2013). DOI: 10.3390/antib2030392.
- [60] M. Klasić, *et al.*, “Promoter methylation of the mgat3 and bach2 genes correlates with the composition of the immunoglobulin g glycome in inflammatory bowel disease”, *Clinical Epigenetics* **10** (2018). DOI: 10.1186/s13148-018-0507-y.
- [61] W. Afif, *et al.*, “Clinical utility of measuring infliximab and human anti-chimeric antibody concentrations in patients with inflammatory bowel disease”, *American Journal of Gastroenterology* **105**, 1133 (2010). DOI: 10.1038/ajg.2010.9.
- [62] B. Chastek, *et al.*, “Treatment persistence and healthcare costs among patients with rheumatoid arthritis changing biologics in the usa”, *Advances in Therapy* **34**, 2422 (2017). DOI: 10.1007/s12325-017-0617-5.
- [63] J. E. Gottenberg, *et al.*, “Nontnf-targeted biologic vs a second anti-tnf drug to treat rheumatoid arthritis in patients with insufficient response to a first anti-tnf drug: A randomized clinical trial”, *JAMA - Journal of the American Medical Association* **316**, 1172 (2016). DOI: 10.1001/jama.2016.13512.
- [64] K. J. Johnson, H. N. Sanchez, N. Schoenbrunner, “Defining response to tnf-inhibitors in rheumatoid arthritis: the negative impact of anti-tnf cycling and the need for a personalized medicine approach to identify primary non-responders”, *Clinical Rheumatology* **38**, 2967 (2019). DOI: 10.1007/s10067-019-04684-1.

- [65] X. Zhang, C. E. Reed, R. E. Birdsall, Y. Q. Yu, W. Chen, “High-throughput analysis of fluorescently labeled n-glycans derived from biotherapeutics using an automated lc-ms-based solution”, *SLAS Technology* **25**, 380 (2020). DOI: 10.1177/2472630320922803.
- [66] B. L. Duivelshof, *et al.*, “Quantitative n-glycan profiling of therapeutic monoclonal antibodies performed by middle-up level hilic-hrms analysis”, *Pharmaceutics* **13** (2021). DOI: 10.3390/pharmaceutics13111744.
- [67] D. Reusch, *et al.*, “Comparison of methods for the analysis of therapeutic immunoglobulin g fc-glycosylation profiles-part 2: Mass spectrometric methods”, *mAbs* **7**, 732 (2015). DOI: 10.1080/19420862.2015.1045173.
- [68] M. Kotsias, *et al.*, “Method comparison for n-glycan profiling: Towards the standardization of glycoanalytical technologies for cell line analysis”, *PLoS ONE* **14** (2019). DOI: 10.1371/journal.pone.0223270.
- [69] T. Keser, T. Pavic, G. Lauc, O. Gornik, “Comparison of 2-aminobenzamide, procainamide and rapifluor-ms as derivatizing agents for high-throughput hilic-uplc-flr-ms n-glycan analysis”, *Frontiers in Chemistry* **6** (2018). DOI: 10.3389/fchem.2018.00324.
- [70] S. Hamla, *et al.*, “A new alternative tool to analyse glycosylation in pharmaceutical proteins based on infrared spectroscopy combined with nonlinear support vector regression†”, *Analyst* **147**, 1086 (2022). DOI: 10.1039/d1an00697e.
- [71] H. Liu, K. May, “Disulfide bond structures of igg molecules: Structural variations, chemical modifications and possible impacts to stability and biological function”, *mAbs* **4**, 17 (2012). DOI: 10.4161/MABS.4.1.18347.
- [72] B. Moritz, J. O. Stracke, “Assessment of disulfide and hinge modifications in monoclonal antibodies”, *Electrophoresis* **38**, 769 (2017). DOI: 10.1002/ELPS.201600425.
- [73] P. Pristatsky, *et al.*, “Evidence for trisulfide bonds in a recombinant variant of a human igg2 monoclonal antibody”, *Analytical Chemistry* **81**, 6148 (2009). DOI: 10.1021/ac9006254.
- [74] S. Gu, *et al.*, “Characterization of trisulfide modification in antibodies”, *Analytical Biochemistry* **400**, 89 (2010). DOI: 10.1016/J.AB.2010.01.019.
- [75] R. Kshirsagar, K. McElearney, A. Gilbert, M. Sinacore, T. Ryll, “Controlling trisulfide modification in recombinant monoclonal antibody produced in fed-batch cell culture”, *Biotechnology and Bioengineering* **109**, 2523 (2012). DOI: 10.1002/BIT.24511.
- [76] J. L. Kinzer, *et al.*, “Physicochemical characterization and functionality comparison of humira®(adalimumab), remicade®(infliximab) and simponi aria®(golimumab)”, *International Journal of Pharmaceutics* **635**, 122646 (2023). DOI: <https://doi.org/10.1016/j.ijpharm.2023.122646>.

- [77] N. I. of Environmental Health Sciences, “Autoimmune diseases” (2022).
- [78] C. Monaco, J. Nanchahal, P. Taylor, M. Feldmann, “Anti-tnf therapy: past, present and future”, *International Immunology* **27**, 55 (2015). DOI: 10.1093/INTIM-M/DXU102.
- [79] U. Billmeier, W. Dieterich, M. F. Neurath, R. Atreya, “Molecular mechanism of action of anti-tumor necrosis factor antibodies in inflammatory bowel diseases”, *World Journal of Gastroenterology* **22**, 9300 (2016). DOI: 10.3748/wjg.v22.i42.9300.
- [80] A. D. Levin, M. E. Wildenberg, G. R. van den Brink, “Mechanism of action of anti-tnf therapy in inflammatory bowel disease”, *Journal of Crohn’s and Colitis* **10**, 989 (2016). DOI: 10.1093/ECCO-JCC/JJW053.
- [81] B. L. McRae, *et al.*, “Fc receptor-mediated effector function contributes to the therapeutic response of anti-tnf monoclonal antibodies in a mouse model of inflammatory bowel disease”, *Journal of Crohn’s and Colitis* **10**, 69 (2016). DOI: 10.1093/ECCO-JCC/JJV179.
- [82] A. N. Ananthakrishnan, *et al.*, “Comparative effectiveness of infliximab and adalimumab in crohn’s disease and ulcerative colitis”, *Inflammatory Bowel Diseases* **22**, 880 (2016). DOI: 10.1097/MIB.0000000000000754.
- [83] G. Järnerot, *et al.*, “Clinical-alimentary tract infliximab as rescue therapy in severe to moderately severe ulcerative colitis: A randomized, placebo-controlled study” (2005). DOI: 10.1053/j.gastro.2005.03.003.
- [84] M. Sjöberg, *et al.*, “Infliximab as rescue therapy in hospitalised patients with steroid-refractory acute ulcerative colitis: a long-term follow-up of 211 swedish patients”, *Alimentary Pharmacology Therapeutics* **38**, 377 (2013). DOI: 10.1111/APT.12387.
- [85] K. Thorlund, E. Druyts, E. J. Mills, R. N. Fedorak, J. K. Marshall, “Adalimumab versus infliximab for the treatment of moderate to severe ulcerative colitis in adult patients naïve to anti-tnf therapy: An indirect treatment comparison meta-analysis”, *Journal of Crohn’s and Colitis* **8**, 571 (2014). DOI: 10.1016/J.CROHNS.2014.01.010/2/8-7-FIG011.JPEG.
- [86] K. Thorlund, E. Druyts, K. Toor, E. J. Mills, “Comparative efficacy of golimumab, infliximab, and adalimumab for moderately to severely active ulcerative colitis: A network meta-analysis accounting for differences in trial designs”, *Expert Review of Gastroenterology and Hepatology* **9**, 693 (2015). DOI: 10.1586/17474124.2015.1024657/SUPPL_FILE/IERH_A_1024657_SM1080.DOC.
- [87] M. L. Barclay, *et al.*, “Infliximab and adalimumab concentrations and anti-drug antibodies in inflammatory bowel disease control using new zealand assays”, *Internal Medicine Journal* **49**, 513 (2019). DOI: 10.1111/IMJ.14064.

- [88] S. J. Bots, *et al.*, “Anti-drug antibody formation against biologic agents in inflammatory bowel disease: A systematic review and meta-analysis”, *BioDrugs : clinical immunotherapeutics, biopharmaceuticals and gene therapy* **35**, 715 (2021). DOI: 10.1007/S40259-021-00507-5.
- [89] K. Herszényi, *et al.*, “Antidrug antibody formation during tumor necrosis factor α inhibitor treatment of severe psoriatic patients in the real-life practice”, *Advances in Dermatology and Allergology/Postpy Dermatologii i Alergologii* **36**, 589 (2019). DOI: 10.5114/ADA.2019.89507.
- [90] T. Arora, *et al.*, “Differences in binding and effector functions between classes of tnf antagonists”, *Cytokine* **45**, 124 (2009). DOI: 10.1016/J.CYTO.2008.11.008.
- [91] W. J. Sandborn, *et al.*, “Etanercept for active crohn’s disease: A randomized, double-blind, placebo-controlled trial”, *Gastroenterology* **121**, 1088 (2001). DOI: 10.1053/GAST.2001.28674.
- [92] P. Gogesch, S. Dudek, G. van Zandbergen, Z. Waibler, M. Anzaghe, “The role of fc receptors on the effectiveness of therapeutic monoclonal antibodies”, *International Journal of Molecular Sciences* **22** (2021). DOI: 10.3390/ijms22168947.
- [93] T. S. Raju, “Terminal sugars of fc glycans influence antibody effector functions of iggs”, *Current Opinion in Immunology* **20**, 471 (2008). DOI: 10.1016/J.COI.2008.06.007.
- [94] D. Reusch, M. L. Tejada, “Fc glycans of therapeutic antibodies as critical quality attributes”, *Glycobiology* **25**, 1325 (2015). DOI: 10.1093/glycob/cwv065.
- [95] S. Kim, *et al.*, “Drifts in adcc-related quality attributes of herceptin®: Impact on development of a trastuzumab biosimilar”, *mAbs* **9**, 704 (2017). DOI: 10.1080/19420862.2017.1305530.
- [96] Y. D. Liu, G. C. Flynn, “Effect of high mannose glycan pairing on igg antibody clearance”, *Biologicals* **44**, 163 (2016). DOI: 10.1016/j.biologicals.2016.02.003.
- [97] M. Yu, *et al.*, “Production, characterization and pharmacokinetic properties of antibodies with n-linked mannose-5 glycans”, <https://doi.org/10.4161/mabs.20737> **4**, 475 (2012). DOI: 10.4161/MABS.20737.
- [98] Z. Althanoon, I. M. Faisal, A. A. Ahmad, M. M. Merkhani, M. M. M. Pharmacology, “Pharmacological aspects of statins are relevant to their structural and physico-chemical properties”, *Systematic Reviews in Pharmacy* **11**, 167 (2020).
- [99] C. Dreyer, *et al.*, “The similarity of selected statins-a comparative analysis”, *Bio-Algorithms and Med-Systems* **14** (2018). DOI: 10.1515/BAMS-2018-0034/PDF.
- [100] C. Murphy, E. Deplazes, C. G. Cranfield, A. Garcia, “The role of structure and biophysical properties in the pleiotropic effects of statins”, *International Journal of Molecular Sciences* **21**, 1 (2020). DOI: 10.3390/IJMS21228745.

- [101] F. Chilton, R. A. Collett, “Treatment choices, preferences and decision-making by patients with rheumatoid arthritis”, *Musculoskeletal Care* **6**, 1 (2008). DOI: 10.1002/msc.110.
- [102] J. R. Curtis, *et al.*, “Physician preference motivates use of anti-tnf therapy independent of clinical disease activity”, *Arthritis care research* **62**, 101 (2010). DOI: 10.1002/ACR.20020.
- [103] A. Fisher, *et al.*, “Prescriber preference for a particular tumour necrosis factor antagonist drug and treatment discontinuation: population-based cohort”, *BMJ Open* **4**, e005532 (2014). DOI: 10.1136/BMJOPEN-2014-005532.
- [104] T. Mizoshita, *et al.*, “Prospective comparison of preference and efficacy of adalimumab and infliximab for treating ulcerative colitis naive to antitumor necrosis factor therapy”, *Medicine (United States)* **96** (2017). DOI: 10.1097/MD.0000000000007800.
- [105] D. Shealy, *et al.*, “Characterization of golimumab, a human monoclonal antibody specific for human tumor necrosis factor α ”, *mAbs* **2**, 428 (2010). DOI: 10.4161/MABS.2.4.12304.
- [106] Z. Kaymakcalan, *et al.*, “Comparisons of affinities, avidities, and complement activation of adalimumab, infliximab, and etanercept in binding to soluble and membrane tumor necrosis factor”, *Clinical immunology (Orlando, Fla.)* **131**, 308 (2009). DOI: 10.1016/J.CLIM.2009.01.002.
- [107] M. Benucci, *et al.*, “Correlation between hla haplotypes and the development of antidrug antibodies in a cohort of patients with rheumatic diseases”, *Biologics: Targets and Therapy* pp. 12–37 (2018). DOI: 10.2147/BTT.S145941.
- [108] M. Liu, *et al.*, “Identification of hla-drb1 association to adalimumab immunogenicity” (2018). DOI: 10.1371/journal.pone.0195325.
- [109] A. Sazonovs, *et al.*, “Hla-dqa1*05 carriage associated with development of anti-drug antibodies to infliximab and adalimumab in patients with crohn’s disease”, *Gastroenterology* **158**, 189 (2020). DOI: 10.1053/j.gastro.2019.09.041.
- [110] J. Coghlan, *et al.*, “Streamlining the characterization of disulfide bond shuffling and protein degradation in igg1 biopharmaceuticals under native and stressed conditions”, *Frontiers in Bioengineering and Biotechnology* **10** (2022). DOI: 10.3389/fbioe.2022.862456.
- [111] Y. Kanda, *et al.*, “Comparison of biological activity among nonfucosylated therapeutic igg1 antibodies with three different n-linked fc oligosaccharides: the high-mannose, hybrid, and complex types”, *Glycobiology* **17**, 104 (2007). DOI: 10.1093/GLYCOB/CWL057.

- [112] S. Matsumiya, *et al.*, “Structural comparison of fucosylated and nonfucosylated fc fragments of human immunoglobulin g1”, *Journal of Molecular Biology* **368**, 767 (2007). DOI: 10.1016/J.JMB.2007.02.034.
- [113] K. Zheng, C. Bantog, R. Bayer, “The impact of glycosylation on monoclonal antibody conformation and stability”, *mAbs* **3**, 568 (2011). DOI: 10.4161/MABS.3.6.17922.
- [114] L. K. Hmiel, K. A. Brorson, M. T. Boyne, “Post-translational structural modifications of immunoglobulin g and their effect on biological activity”, *Analytical and Bioanalytical Chemistry* **407**, 79 (2015). DOI: 10.1007/s00216-014-8108-x.
- [115] M. Thomann, K. Reckermann, D. Reusch, J. Prasser, M. L. Tejada, “Fc-galactosylation modulates antibody-dependent cellular cytotoxicity of therapeutic antibodies”, *Molecular Immunology* **73**, 69 (2016). DOI: 10.1016/J.MOLIMM.2016.03.002.
- [116] N. A. Pereira, K. F. Chan, P. C. Lin, Z. Song, “The “less-is-more” in therapeutic antibodies: Afucosylated anti-cancer antibodies with enhanced antibody-dependent cellular cytotoxicity”, *mAbs* **10**, 693 (2018). DOI: 10.1080/19420862.2018.1466767.
- [117] W. Strohl, L. Strohl, “Development issues: antibody stability, developability, immunogenicity, and comparability”, *Therapeutic Antibody Engineering - Woodhead Publishing Series in Biomedicine* pp. 377–595 (2012). DOI: 10.1533/9781908818096.377.
- [118] A. J. Cordoba, B. J. Shyong, D. Breen, R. J. Harris, “Non-enzymatic hinge region fragmentation of antibodies in solution”, *Journal of Chromatography B: Analytical Technologies in the Biomedical and Life Sciences* **818**, 115 (2005). DOI: 10.1016/j.jchromb.2004.12.033.
- [119] H. Liu, C. Chumsae, G. Gaza-Bulseco, K. Hurkmans, C. H. Radziejewski, “Ranking the susceptibility of disulfide bonds in human igg1 antibodies by reduction, differential alkylation, and lc-ms analysis”, *Analytical Chemistry* **82**, 5219 (2010). DOI: 10.1021/AC100575N/SUPPL_FILE/AC100575N_SI_002.PDF.
- [120] J. C. Lakubub, J. T. Shipman, H. Desaire, “Recent mass spectrometry-based techniques and considerations for disulfide bond characterization in proteins”, *Analytical and bioanalytical chemistry* **410**, 2467 (2018). DOI: 10.1007/S00216-017-0772-1.
- [121] D. Weinfurtner, “Chapter 1.4 analysis of disulfide bond formation in therapeutic proteins” pp. 81–98 (2018). DOI: 10.1039/9781788013253-00081.
- [122] S. Nie, T. Greer, X. Huang, X. Zheng, N. Li, “Development of a simple non-reduced peptide mapping method that prevents disulfide scrambling of mabs without affecting tryptic enzyme activity”, *Journal of Pharmaceutical and Biomedical Analysis* **209**, 114541 (2022). DOI: 10.1016/J.JPBA.2021.114541.
- [123] D. Ouellette, *et al.*, “Studies in serum support rapid formation of disulfide bond between unpaired cysteine residues in the vh domain of an immunoglobulin g1 molecule”, *Analytical Biochemistry* **397**, 37 (2010). DOI: 10.1016/j.ab.2009.09.027.

- [124] L. Liu-Shin, A. Fung, A. Malhotra, G. Ratnaswamy, “Influence of disulfide bond isoforms on drug conjugation sites in cysteine-linked igg2 antibody-drug conjugates”, *mAbs* **10**, 583 (2018). DOI: 10.1080/19420862.2018.1440165/SUPPL_FILE/KMAB_A_1440165_SM5845.ZIP.
- [125] A. Q. Dean, S. Luo, J. D. Twomey, B. Zhang, “Targeting cancer with antibody-drug conjugates: Promises and challenges”, *mAbs* **13** (2021). DOI: 10.1080/19420862.2021.1951427.
- [126] W. C. Sung, *et al.*, “Evaluation of disulfide scrambling during the enzymatic digestion of bevacizumab at various ph values using mass spectrometry”, *Biochimica et Biophysica Acta - Proteins and Proteomics* **1864**, 1188 (2016). DOI: 10.1016/j.bbapap.2016.05.011.
- [127] A. Resemann, *et al.*, “Rapid, automated characterization of disulfide bond scrambling and igg2 isoform determination”, <https://doi.org/10.1080/19420862.2018.1512328> **10**, 1200 (2018). DOI: 10.1080/19420862.2018.1512328.
- [128] Q. Dong, *et al.*, “Comprehensive analysis of tryptic peptides arising from disulfide linkages in nistmab and their use for developing a mass spectral library”, *Journal of Proteome Research* **20**, 1612 (2021). DOI: 10.1021/ACS.JPROTEOME.0C00823/SUPPL_FILE/PROC00823_SI_001.XLSX.
- [129] N. Alt, *et al.*, “Determination of critical quality attributes for monoclonal antibodies using design principles”, *Biologicals* **44**, 291 (2016). DOI: 10.1016/J.BIOLOGICALS.2016.06.005.
- [130] H. Lim, *et al.*, “Structural biology of the tnfa antagonists used in the treatment of rheumatoid arthritis”, *International Journal of Molecular Sciences* **19** (2018). DOI: 10.3390/ijms19030768.
- [131] A. Teasdale, D. Elder, R. W. Nims, “Ich quality guidelines: An implementation guide” (2018).
- [132] EMA, “Guideline on similar biological medicinal products containing biotechnology-derived proteins as active substance: quality issues (revision 1)” (2014).
- [133] E. Zhang, *et al.*, “Design-based assessment for analytical similarity of adalimumab biosimilar hlx03 to humira®”, *AAPS Journal* **22**, 1 (2020). DOI: 10.1208/S12248-020-00454-Z/FIGURES/7.
- [134] H. Shion, M. Du, Y. Q. Yu, “Automated disulfide bond mapping in comparing innovator and biosimilar mabs using unifi software | waters” (2016).
- [135] W. C. Lamanna, *et al.*, “The structure-function relationship of disulfide bonds in etanercept”, *Nature Scientific Reports* **7**, 1 (2017). DOI: 10.1038/s41598-017-04320-5.

- [136] Y. Lu, C. S. Wong, J. Xing, Z. Zhan, “Characterization of disulfide bonds in bevacizumab biosimilar using a q-tof mass spectrometer” (2020).
- [137] C. X. Cai, *et al.*, “Investigation of cysteine modifications in recombinant protein tetanus toxoid heavy chain fragment c”, *Journal of the American Society for Mass Spectrometry* **32**, 1837 (2021). DOI: 10.1021/JASMS.1C00075/SUPPL_FILE/JS1C00075_SI_001.PDF.
- [138] C. Nowak, *et al.*, “Forced degradation of recombinant monoclonal antibodies: A practical guide”, *mAbs* **9**, 1217 (2017). DOI: 10.1080/19420862.2017.1368602.
- [139] Y. Xu, *et al.*, “Structure, heterogeneity and developability assessment of therapeutic antibodies”, *mAbs* **11**, 239 (2018). DOI: 10.1080/19420862.2018.1553476.
- [140] J. Halley, *et al.*, “An industry perspective on forced degradation studies of biopharmaceuticals: Survey outcome and recommendations”, *Journal of Pharmaceutical Sciences* **109**, 6 (2020). DOI: 10.1016/J.XPHS.2019.09.018.
- [141] J. Kang, *et al.*, “Assessment of biosimilarity under native and heat-stressed conditions: rituximab, bevacizumab, and trastuzumab originators and biosimilars”, *Analytical and Bioanalytical Chemistry* **2019 412:3 412**, 763 (2019). DOI: 10.1007/S00216-019-02298-9.
- [142] S. M. Shatat, M. A. Al-Ghobashy, F. A. Fathalla, S. S. Abbas, B. M. Eltanany, “Coupling of trastuzumab chromatographic profiling with machine learning tools: A complementary approach for biosimilarity and stability assessment”, *Journal of chromatography. B, Analytical Technologies in the Biomedical and Life Sciences* **1184**, 122976 (2021). DOI: 10.1016/J.JCHROMB.2021.122976.
- [143] Y. F. K. Dyck, *et al.*, “Forced degradation testing as complementary tool for biosimilarity assessment”, *Bioengineering* **2019, Vol. 6, Page 62 6**, 62 (2019). DOI: 10.3390/BIOENGINEERING6030062.
- [144] D. Mahon, K. I. Sen, Y. J. Kil, P. Mehndiratta, “Isotope selection in label-free quantitation and its effects in biopharmaceutical characterization” (2012).
- [145] FDA, “Guidance for industry q8(r2) pharmaceutical development” (2009).
- [146] B. L. Duivelshof, *et al.*, “Glycosylation of biosimilars: Recent advances in analytical characterization and clinical implications”, *Analytica Chimica Acta* **1089**, 1 (2019). DOI: 10.1016/j.aca.2019.08.044.
- [147] N. D. Haan, *et al.*, “Developments and perspectives in high-throughput protein glycomics: enabling the analysis of thousands of samples”, *Glycobiology* **32**, 651 (2022). DOI: 10.1093/glycob/cwac026.
- [148] S. K. Singh, K. H. Lee, “Characterization of monoclonal antibody glycan heterogeneity using hydrophilic interaction liquid chromatography-mass spectrometry”, *Frontiers in Bioengineering and Biotechnology* **9** (2022). DOI: 10.3389/fbioe.2021.805788.

- [149] M. L. A. D. Leoz, *et al.*, “Nist interlaboratory study on glycosylation analysis of monoclonal antibodies: Comparison of results from diverse analytical methods **”, *Molecular Cellular Proteomics* **19**, 11 (2020). DOI: 10.1074/MCP.RA119.001677.
- [150] C. for Drug Evaluation, Research, “Bsufa iii regulatory research pilot program: Research roadmap” (2023).
- [151] J. M. Prien, *et al.*, *Chapter 4 Orthogonal Technologies for NISTmAb N-Glycan Structure Elucidation and Quantitation* (2015).
- [152] J. Zhao, W. Peng, X. Dong, Y. Mechref, “Analysis of nist monoclonal antibody reference material glycosylation using the lc-ms/ms-based glycoproteomic approach”, *Journal of Proteome Research* **20**, 818 (2021). DOI: 10.1021/acs.jproteome.0c00659.
- [153] M. Hilliard, *et al.*, “Glycan characterization of the nist rm monoclonal antibody using a total analytical solution: From sample preparation to data analysis”, *mAbs* **9**, 1349 (2017). DOI: 10.1080/19420862.2017.1377381.
- [154] C.-H. Chen, *et al.*, “Intact nist monoclonal antibody characterization—proteoforms, glycoforms—using ce-ms and ce-lif”, *Cogent Chemistry* **4**, 1480455 (2018). DOI: 10.1080/23312009.2018.1480455.
- [155] G. Grampp, S. Ramanan, “The diversity of biosimilar design and development: Implications for policies and stakeholders”, *BioDrugs* **29**, 365 (2015). DOI: 10.1007/s40259-015-0147-0.
- [156] T. Kaur, B. N. Shukla, V. K. Yadav, M. J. Kulkarni, A. Rao, “Comparison of glycoprofiles of rituximab versions licensed for sale in india and an analytical approach for quality assessment”, *Journal of Proteomics* **244** (2021). DOI: 10.1016/j.jprot.2021.104267.
- [157] I. S.-D. Melo, *et al.*, “N-glycosylation profile analysis of trastuzumab biosimilar candidates by normal phase liquid chromatography and maldi-tof ms approaches”, *Journal of Proteomics* **127**, 225 (2015). DOI: 10.1016/j.jprot.2015.04.012.
- [158] C. for Medicinal Products for Human Use, “Ogivri assessment report” (2018).
- [159] C. for Medicinal Products for Human Use, “Kanjinti assessment report” (2018).
- [160] T. Scientific, “Orbitrap astral mass spectrometer” (2023).